Role of microglia in neurotropic viral infections

Ph. D. thesis

Rebeka Fekete

Semmelweis University

János Szentágothai Doctoral School of Neurosciences

Supervisors: Dr. Dénes Ádám, Ph.D, Dr. Környei Zsuzsanna, Ph.D

Official reviewers: Dr. Kékesi Adrienna Katalin, Ph.D

Dr. Jakus Zoltán, Ph.D

Head of the Final Examination Comittee: Dr. Falus András, Ph.D, D.sc

Members of the Final Examination Comittee: Dr. Kardos József, Ph.D

Dr. Alpár Alán, Ph.D, D.sc

Budapest

2019

Table of contents

List of Abbreviations

- AD Alzheimer's disease
- ASP Antisense promoter
- ATP Adenosine Tri-Posphate
- BBB Blood-brain barrier
- BCSFB Blood-CSF barrier
- BDG Bartha DupGreen
- BDNF Brain Derived Neurotrophic Factor
- BDR BarthaDup Red
- CCL2,19 Chemokine (C-C motif) ligand
- CD200/CD200R OX-2 type I membrane glycoprotein
- CMV Cytomegalovirus
- CNS Central Nervous System
- CSF Cerebrospinal fluid
- CSF1-R Colony Stimulating Factor 1 Receptor
- CXCL9/10 Chemokine (C-X-C motif) ligand
- Cx3cl1 Chemokine (C-X3-C motif) ligand 1/fractalkine
- Cx3cr1 CX3C Chemokine receptor 1/ fractalkine receptor
- C1q Complement component 1q
- C3 Complement 3
- DAMP Danger Associated Molecular Pattern
- DAP12 DNAX activation protein 12
- DNA Deoxyribonucleic acid
- DTR Diphtheria toxin receptor
- EMP Erythromieloid precursor cell
- FFPE Formalin-fixed paraffin embeded
- GFAP Glial Fibrillary Acidic Protein
- GFP Green Fluorescent Protein

- GWAS Genome Wide Associated Study
- HMGB1 High Mobility Group Box 1
- HIV-1 Human Immunodeficiency Virus-1
- HSV Herpes Simplex virus
- HSVE-1 Herpes Simplex type 1 encephalitis
- HSVTK Herpes Simplex viral thymidine kinase
- IFN-1 Interferon 1
- IGF-1 Insulin-like Growth Factor 1
- IgG Immunoglobulin G
- IL-1 Interleukin 1
- IL-6 Interleukin 6
- IL-12 Interleukin 12
- IL-34 Interleukin 34
- Irf8 Interferon regulatory factor 8
- MGM Meningeal macropohage
- MHV Mouse hepatitis virus
- MIP-1 Macrophage Inflammatory Proteins
- MV Measles virus
- NLRs Nod-like resptors
- NTPDase Nucleoside Triphosphate Diphosphohydrolase
- NVU Neurovascular unit
- PAMP Pathogen Associated Molecular Pattern
- PD Parkinson’s disease
- PNS Peripheral Nervous System
- PRR Pattern Recognition Receptors
- PRV Pseudorabies Virus
- Pu.1 Transcription factor PU.1
- PV Poliovirus
- PVM Perivascular macrophage
- RABV Rabies virus
- RNA Ribonucleic acid
- RLRs Rig-like receptors

- SVZ Subventricular zone
- TBI Traumatic Brain Injury
- TGFß Transforming Growth Factor ß
- TNFα Tumor Necrosis Factor α
- TLRs Toll like resptors
- TLR3 Toll-like receptor 3
- TREM-2 Triggering Receptor Expressed on Myeloid cells 2
- VZV Varicella Zooster virus
- WNV West Nile virus

"Inflammatory processes of any nature are soon to be manifested in the reaction of microglia. In cases of meningitis and meningoencephalitis the microglia of the affected areas undergoes changes corresponding to the early stages of mobilization and phagocytic intervention." Pio del Rio-Hortega 1932.

1. Introduction

1.1. Barriers in the brain and regulation of immune cell trafficking

While the weight of the brain accounts for only 2% of the total body weight, it consumes 20% of the total cardiac output. This requires constant energy balance and strictly controlled blood flow (autoregulation), as well as rapid adjustment of local perfusion needs to change in neuronal activity (functional hyperemia). In addition, for the proper functioning of neurons, the brain requires tight metabolic regulation and ion gradients that largely differ from the composition of the blood. Vascular injury or brain damage results in the dysregulation of proper brain circulation and metabolism, that may lead to irreversible neuronal injury. Therefore, the brain is protected by special barriers that allow isolation of the brain microenvironment from the peripheral circulation and circulating immune cells.

The vascular network of the central nervous system (CNS) has evolved to maintain proper homeostatic balance inside the parenchyma. Vascular permeability, immune cell trafficking, blood flow and vascular tone that are critical for the proper function of CNS is precisely controlled (Hanisch and Kettenmann 2007; Daneman 2012). To this end, the blood-brain barrier (BBB) is formed by unique blood vessels in the CNS that regulate the movement of molecules, ions and immune cells between the blood and neural tissue. The BBB also protects the CNS from injury and infection by limiting the entry of pathogens and immune cells (Engelhardt & Liebner, 2014). BBB function between the blood and the CNS parenchyma is maintained by specialized capillary endothelial cells with low pinocytotic activity, fused together by complex tight junctions (Engelhardt and Sorokin 2009; Tietz and Engelhardt 2015). The endothelial cells regulate paracellular transport in both directions, but transcellular transport is regulated by special pumps and receptors (Archer, Pitelka, & Hammond, 2004). The basal lamina of endothelial cells is surrounded by astrocyte endfeet, which contributes to the barrier function by limiting the trafficking of macromolecules and immune cells. The blood-CSF barrier (BCSFB) is the second interphase that protects the CNS, formed by the choroid plexus epithelium which produces and regulates the composition of CSF (Prinz, Priller, Sisodia, & Ransohoff, 2011). The barrier function in the choroid plexus is provided by tight junctions between epithelial cells (Engelhardt & Sorokin, 2009). The blood-CSF interface is also an important site for immune cell entry into the CNS, where low numbers of different immune cell populations are seen under physiological conditions, while their turnover is far slower than that seen in peripheral tissues (Prinz, Erny,

& Hagemeyer, 2017). In homeostatic conditions, peripheral immune cells also patrol in specialized CNS compartments located outside the brain parenchyma. Immune cells can also gain access to the CNS via the non-fenestrated vascularized stroma of the blood-CSF barrier that is surrounded by the choroid plexus epithelial cells, the perivascular space (Virchow-Robin space; (Ousman and Kubes 2012; Muoio, Persson, and Sendeski 2014). There are also specialized regions of the brain that allow direct communication between the brain and the vascular system. In the circumventricular organs, located around the third and fourth ventricles, the BBB is more permeable, containing fenestrations and discontinous tight junctions (Bauer, Krizbai, Bauer, & Traweger, 2014) and these areas are important to regulate neuro-immune interactions in health and disease. Recent research revealed that similar to the drainage of extracellular fluid in peripheral tissues, the brain also has its clearance routes, called the glymphatic system (glial-lymphatic system, (see Figure 1.). This is provided by a unique system of perivascular channels formed by astrocytes that promote efficient elimination of soluble proteins and metabolites from the CNS. It mainly operates as a waste clearance system and its role in brain inflammation and neurological diseases has also been suggested (Aspelund et al. 2015; Kipnis et al. 2017). In addition, lymph vessels have recently been identified in the meninges, which are emerging sites for neuro-immune interactions (Kipnis et al., 2017). At present, it is assumed that immune cells, primarily myeloid cell populations, which reside in the brain throughout life can gain access to the developing CNS in the first trimester in both mice and humans via both meningeal and vascular routes, while the role for the choroid plexus in their migration is also emerging. In adults, these areas in the CNS provide functionally important routes of entry for leukocytes during brain inflammation or diverse neuropathologies. In physiological conditions, meningeal, choroid plexus machrophages and a small amount of T cells patrol continuously in the subarachnoidal space and the ventricles (Figure 1.)(Ousman & Kubes, 2012).

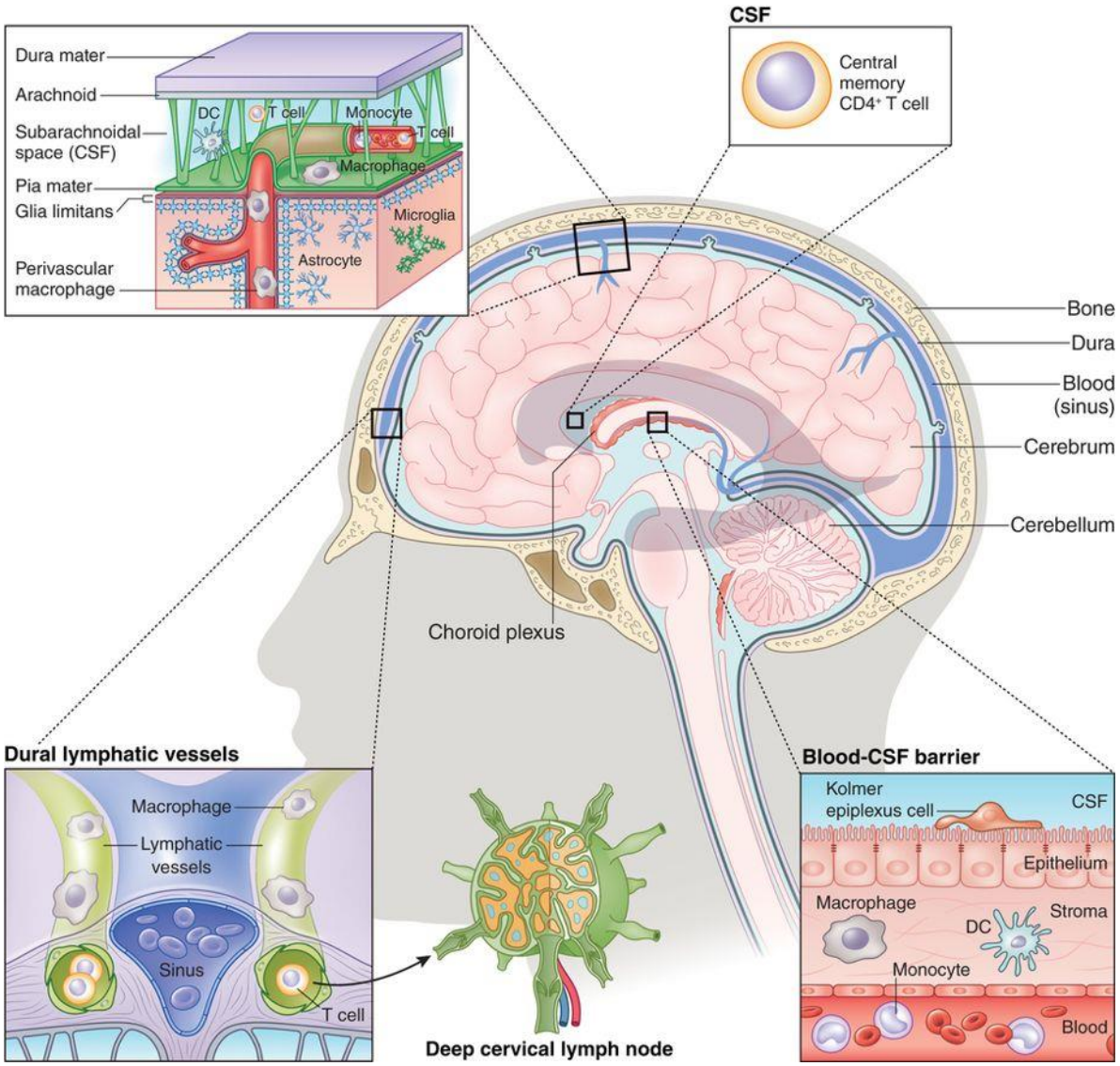

Figure 1. Barriers of the brain and immune cell trafficking in homeostatic condition. The brain is isolated and protected by the skull and three layers of meninges. The choroid plexus produces CSF which flows both in the parenchyma and in the subarachnoid area and comprises arteries and perivascular space. Thus, the CSF contains small amount of CD4+ T cells, which patrol the brain. In healthy brain tissue, leukocytes (granulocytes, monocytes, T and B cells) stay within the blood vessels. In the brain parenchyma microglial cells are the only immune cells maintaining the healty environment. In non-parenchymal areas perivascular, meningeal and choroid plexus machrophages are patrolling and protect the brain tissue (Prinz & Priller, 2017).

1.2. The neurovascular unit

The key area in the brain vasculature that regulates cerebral blood flow and immune cell trafficking is called the neurovascular unit (NVU). The NVU is formed via complex functional interactions between endothelial cells, pericytes, perivascular macrophages (PVMs), microglia, astrocytes and neurons (Figure 2.) (Wong et al., 2013). All those cell types are in an integrated relationship and they maintain homeostasis and proper function of the CNS (Thurgur & Pinteaux, 2018). The blood-brain barrier can be considered as an integral part of the NVU. The low permeability and integrity of endothelial cells is the most important feature of CNS protection from blood-borne materials (Tietz & Engelhardt, 2015). Astrocytes compose the glia limitans perivascularis, which separates the parenchyma from the blood vessels and continues as glia limitans superficialis surrounding the entire surface of the brain and spinal cord (Abbott, Rönnbäck, & Hansson, 2006). Astrocytes cover the parenchymal basement membrane, produce different growth factors for BBB maturation and maintenance and, via aquaporin channels, they can also regulate local water transport (Ransohoff & Engelhardt, 2012). Besides BBB maintenance they provide both mechanical and metabolic support for neurons (Abbott et al., 2006). Pericytes are embedded in the vascular basement membrane of microvessels. Due to their exclusive position, they have close contact with endothelial cells, astrocyte endfeet, perivascular macrophages and neurons (Rustenhoven, Jansson, Smyth, & Dragunow, 2017a). In the brain, pericytes have distinct morphologies and depending on their position in the vasculature have different functions as well. In the arteriolar end of vessels, precapillary pericytes are likely to modify vascular diameter, and true-capillary pericytes contribute more to BBB maintenance (Rustenhoven et al. 2017; Engelhardt 2008).

The main immunocompetent cell types in the NVU are microglia and perivascular macrophages. Since in this thesis the inflammatory- and immune mechanisms discussed in the context of neurotropic virus infection primarily concern microglial cells, the chapters below will focus on the origin, maintenance and effector functions of brain myeloid cell types, primarily microglia.

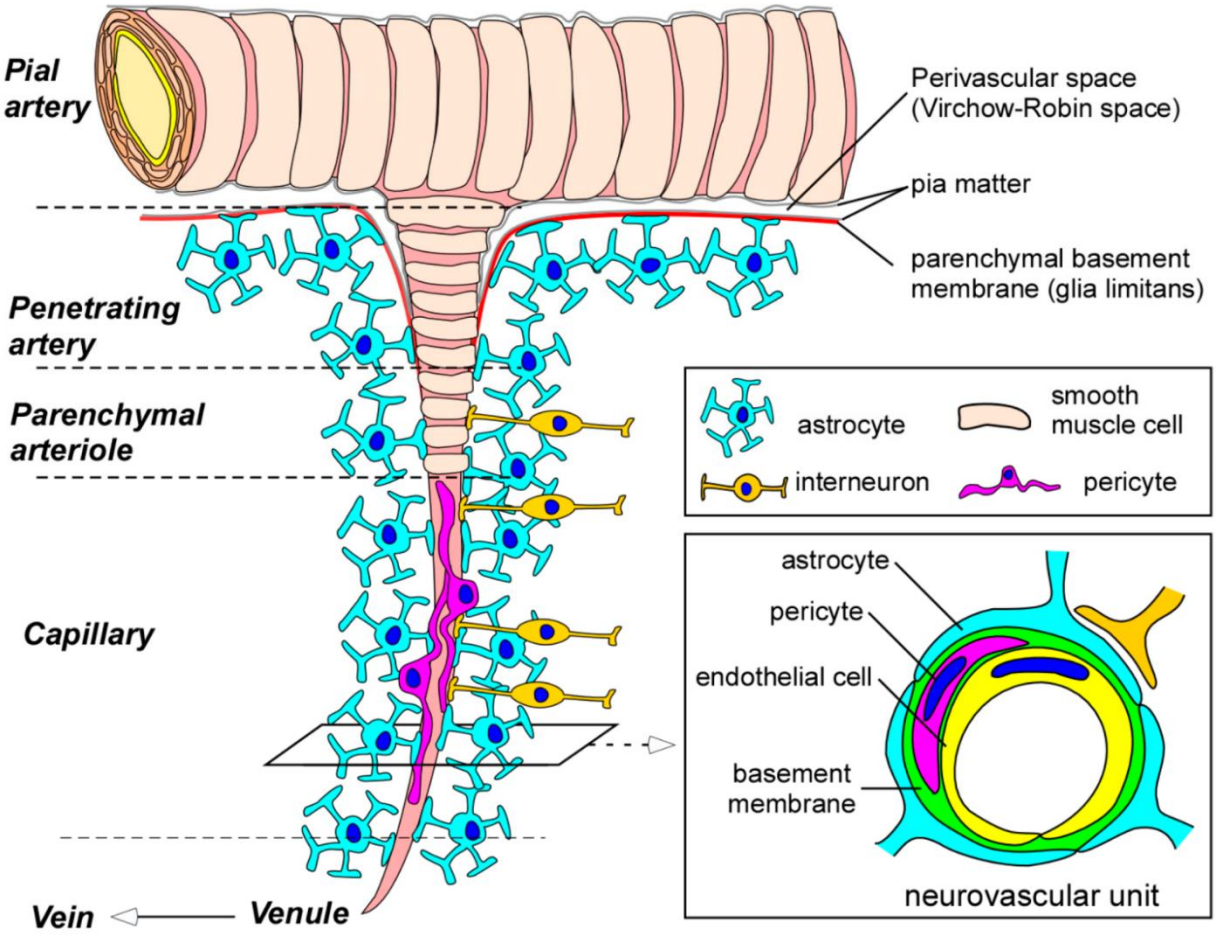

Figure 2. Structure of the blood-brain barrier (BBB) and neurovascular unit (NVU). Pial arteries branch out into smaller arteries, called penetrating arteries. They go down into the parenchyma, branching further into arterioles and capillaries. Pial and penetrating arteries are covered by vascular smooth mucle cells and are separated from the brain parenchyma by the glia limitans. Endothelial cells form the blood-brain barrier, which are in close contact with other cell types (pericytes, astrocytes, perivascular macrophages and interneurons) composing the neurovascular unit (Yamazaki and Kanekiyo 2017).

1.3. Origin of myeloid cells in the CNS

Myeloid cells in the CNS represent a heterogeneous class of innate immune cells that contribute to the maintenance of tissue homeostasis differentially during development and adulthood. Myeloid cell types in the adult CNS include microglia, perivascular macrophages as well as meningeal and choroid plexus macrophages (Li and Barres 2018; Prinz, Erny, and Hagemeyer 2017). The origin and differentiation of CNS macrophages is still under intense discussion. However, novel transgenic mouse models and fate mapping studies have shed light on the origin of parenchymal microglia and other myeloid cell types. These studies have shown that microglia are derived exclusively from prenatal hematopoietic progenitor cells that reside in the yolk sac (Ginhoux et al., 2010). Microglia and most myeloid cell types in the CNS have self-renewing populations through the whole life (Li & Barres, 2018).

Microglia are the main immune cell type of the brain. Unlike ectodermal macroglial cells such as astrocytes and oligodendrocytes, microglia originate from the yolk sac, an extraembryonic mesodermal tissue, which is the first place for early hematopoiesis during development. It has been found that microglia arise from an uncommitted CD31+c-kit+ erythromyeloid precursor (EMP) cell located in the yolk sac, which further develops via the macrophage ancestor population A1 (CD45+CX3CR1loF4/80lo) into the A2 (CD45+CX3CR1hiF4/80hi) progenitor population. Microglial progenitors migrate from the yolk sac during development to the nervous tissue in two waves (Prinz & Priller, 2014b). In humans, migration happens during the first two trimesters, in rodents in between embryonic days 10 and 19. The second population of microglial cells invades the parenchyma during early postnatal days (Hanisch & Kettenmann, 2007). During fetal development, microglial progenitors enter the CNS via blood vessels, the ventricles and the meninges (Prinz & Mildner, 2011). After their entry into the brain tissue, they migrate first tangentially and radially in a Pu.1 and Irf8 dependent manner, then undergo proliferation and apoptosis (Pósfai et al. 2018; Nikodemova et al. 2015). For healthy development and maintenance microglia need specific receptor and ligand toolkits such as CSF-1R CSF-1 axis, IL-34, Pu.1, and TGFß1 which is uniquely expressed by only microglial cells in the CNS (Erblich, Zhu, Etgen, Dobrenis, & Pollard, 2011).

Perivascular macrophages (PVM) are a distinct population of resident brain macrophages located in the perivascular (Virchow-Robin space) compartment (Figure 2.) surrounding arteries and veins. They migrate from the yolk sac into the brain during early development, like microglia. Both macrophage populations are self-renewing cells that are not replaced by

bone marrow-derived progenitors thorughout life under normal conditions (Faraco, Park, Anrather, & Iadecola, 2017). They can influence vascular permeability via restricting the movement of solutes, pathogens and immune cell entry from the periphery (Goldmann et al., 2016). Besides PVMs, there are two other non- parenchymal macrophage populations in different CNS compartments, namely the meningeal macrophages (MGM) and choroid plexus macrophages. MGMs patrol between the pia mater and surface of the brain and originate from the same yolk sac progenitors like PVM and microglia. Choroid plexus macrophages however, can be found in ventricles and have both embryonic and adult hematopoietic origins (Kierdorf and Prinz 2017; Goldmann et al,. 2016).

1.4. The role of microglia during development and in normal brain function

1.4.1. Developmental role of microglia

Due to their partially common origin with other tissue macrophage populations, it is difficult to define the precise contribution of microglia to CNS development. However, increasing evidence indicates that the absence or dysfunction of microglia results in severely impaired neuronal network development (Stevens & Schafer, 2018). Microglia are known to contribute to normal brain development via diverse functions, including phagocytosis of dead cells, guiding sprouting blood vessels in the parenchyma, maintanance and elimination of synapses or supporting neuronal network organization (Figure 3.). In fact, during development, the first microglial progenitors appear in the CNS when functional neuronal networks are formed and contact neurons and their processes. The importance of microglial presence was proved by a very rare case, when a child was born with CSF-1R mutation, which resulted in the complete absence of microglia in his brain. The absence of microglia led to largely deformed ventricles, undeveloped corpus callosum, serious functional deficits in general brain functions and eventually early death (Zhang, 2019). Gain-of-function and loss-of-functions studies also indicate that microglia are required for the normal development of the brain vasculature, ventricles and neuronal networks. Similarly to the human case, in CSF-1R deficient mouse model, the absence of microglia, exhibit severe defects in brain maturation with marked structural abnormalities, including olfactory bulb atrophy, expansion of lateral ventricles and dramatic thinning of the neocortex (Prinz & Priller, 2017). During development, microglia contribute to the maintenance of neuronal networks via activity-dependent synapse elimination, which is called synaptic pruning.

During this process, unwanted synapses are tagged with the complement protein C1q and phagocytosed by microglia (Schafer et al. 2012; Pósfai et al. 2018). In C1q knock out mice, increased number of axonal boutons of layer V pyramidal cells has been shown, which resulted in epileptic neuronal network activity (Rubino et al., 2018). Besides the complement system, the Cx3cl1-Cx3cr1 axis is also an essential contributor in synaptic pruning, axonal growth, and normal network formation. Cx3cr1, which is a chemokine, also known as fractalkine. The deficiency of this Cx3cr1 receptor on microglial cells results in decreased survival of neurons in layer V of the neocortex, and also results in impaired network maturation (Prinz & Priller, 2017). Apart from phagocytosing synaptic elements and apoptotic neurons, microglia also support and promote neuronal survival and migration via secreting neurotrophic factors, such as BDNF or IGF-1 (Stevens & Schafer, 2018).

1.4.2. The role of microglia in adulthood

Microglia are distributed over the whole CNS parenchyma. Fate-mapping studies have revealed that microglial cells are unique in the sense that they are self-renewing throughout life. In the adult brain, microglia occupy distinct non-overlapping territories and constantly scan their environment (Davalos et al. 2005; Tremblay et al. 2011). The fine processes of microglia continuously contact neurons, axons and dendritic spines to monitor their functional status. Microglia are known to sense changes in neuronal activity via altered extracellular ion gradients, CX3CL1-CX3CR1 or CD200-CD200R interactions, purinergic signaling and other mechanisms that shape synaptic connectivity and neuronal networks under physiological and pathological conditions (Kettenmann, Kirchhoff, & Verkhratsky, 2013). Microglial process motility can change dramatically in response to extracellular stimuli, including neuronal activity and exposure to neurotransmitters (Salter & Stevens, 2017). Recent evidence suggests that the motility of microglia is controlled in part, by Thik1 potassium channel on the microglial membrane (Madry et al., 2018) and various purinergic receptors (Dissing-Olesen et al. 2014; Eyo et al. 2015). Several studies have noted that ATP released by dying cells or actively pumped out of intact cells via connexin or pannexin hemichannels, as an inflammatory amplifier induces rapid microglial responses (Färber & Kettenmann, 2006). A key feature of microglia in the postnatal brain is the rapid identification of dying cells, followed by migration and clearance of apoptotic debris (Wolf, Boddeke, and Kettenmann 2017; Peri and Nüsslein-Volhard 2008). Although it is not entirely clear how microglia detect apoptotic cells under physiological conditions, studies

have identified that purinergic receptors, such as metabotropic P2Y12 as a trigger of microglial chemotaxis and phagocytosis in response to neuronal injury (Koizumi, Ohsawa, Inoue, & Kohsaka, 2013). Besides eliminating dying cells, microglia regulate the brain microenvironment via elimination of excess synaptic elements as well, directed by chemotactic signals (e.g. ATP) or phagocytic signals like C1q, and induce apoptosis without provoking inflammation (Stevens & Schafer, 2018).

Several studies are focussing on a large variety of microglial functions during either early postnatal phase or adulthood. Analyzing the exact contribution of microglia in controlling synaptic plasticity, regulating synaptic properties, especially during learning and circuit maturation have been the target of great interest. In order to study these roles, the recent development of new tools and approaches have become available. These tools include both pharmacological and genetically modified mice to deplete microglia. Pharmacological approaches include the administration of clodronate-containing liposomes (Buiting and Rooijen 1994) and the inhibition of the Csf1 signaling pathway, which is crucial for microglial survival (Elmore et al. 2014; Squarzoni et al. 2014). Genetic depletion is achieved either by removing factors indispensable for microglial maturation and survival such as CSF1R, IL-34 and PU.1 or through the expression of 'suicidal genes', such as diphtheria toxin receptor (DTR) or viral thymidine kinase (HSVTK) under the control of specific microglial promoters, like CD11b or Cx3cr1 (Paolicelli and Ferretti 2017). However, each of these models has been essential for deepening our knowledge of microglial function, each system has its own set of drawbacks.

Elimination of microglia in adulthood via inhibition with small molecules or blocking microglia produced brain-derived neurotrophic factor (BDNF), which is a key signaling molecule important in synaptic plasticity, has to lead to impaired learning and memory and synaptic plasticity (Parkhurst et al. 2013). Those results indicate that microglia serve important physiological functions in learning and memory by promoting learning-related synapse formation through BDNF signaling (Parkhurst et al. 2013). Depletion of microglia, by using Cx3cr1-CreERT2 specific mice, which express diphtheria toxin receptor (DTR) on microglia and macrophages followed by timed injection of diphtheria toxin to eliminate receptor expressing cells, also revealed that microglia are involved in the elimination and formation of dendritic spines in the cortex both during development. Interestingly depletion of microglia during adulthood in the same model, induced only reduced synapse formation but not elimination (Paolicelli and Ferretti 2017). Such a function of microglia contributes to learning dependent motor activity. Although, it seems that Cx3cr1-CreER model has its

own drawbacks since specific microglia depletion via diphtheria toxin administration resulted in only 80% elimination of microglial cells. From the remaining surviving population they were quickly recuperated by hyper-proliferation (Bruttger et al., 2015). Administration of liposome-encapsulated clodronate drug also resulted in microglia depletion in ex vivo organotypic hippocampal slices. Similarly to the previous diphtheria toxin-induced model, microglia depletion resulted in increased frequency of postsynaptic currents, which is consistent with a higher density of synapses (Frieler et al., 2015). Replenishment of microglia in the slices restored normal synaptic currents. These results indicate that the role of microglia in synapse formation persists throughout life (Parkhurst et al., 2013a). Even though ex vivo administration of clodronate works, in vivo injection into the parenchymal tissue might induce unwanted inflammatory effects (Han et al., 2019).

The seemingly efficient microglia depletion model was the development of mice expressing the herpes-simplex virus-encoded suicide-gene thymidine kinase (HSVTK) under the CD11b-promoter (Heppner et al., 2005). Administration of i.c.v. ganciclovir resulted in up to 95% depletion of microglia (Lund, Pieber, & Harris, 2017), however, after extended delivery, the drug administration became toxic, thereby limiting this approach to a period of 4 weeks. Thus, in subsequent studies, it was demonstrated that ganciclovir delivery resulted in a complete exchange of the microglial pool by peripheral myeloid cells (Varvel et al. 2012; Prokop et al., 2015). Furthermore, BBB damage was also reported upon long-term administration of ganciclovir, resulting in the infiltration of peripheral immune cell subsets (Lund et al., 2017).

Accumulating evidence from fate-mapping and genomic studies indicates that microglia requires CSF1R both during development and adulthood for survival since CSF1R-/- mice completely lack microglia (Ginhoux et al. 2010; Elmore et al. 2014). Microglia can use both ligands of CSF1R for their survival (CSF1 and IL-34) since mice mutant for either cytokine display reduction but not complete loss of microglia (Waisman et al. 2015; Waisman et al. 2015). Pharmacological inhibition of CSF1R yields complete ablation (>99%) of microglia within 21 days. This approach is practical because it requires no mouse breeding and microglial depletion can be maintained as long as the drug is administered. Surprisingly, microglia depletion via CSF1R inhibitor PLX3397 in adult mice up to 3 weeks did not result in major changes in synaptic properties and was not associated with cognitive deficits, however, longer administration can alter the synaptic density, cause accelerated learning and increased GFAP levels (Elmore et al. 2014; Prinz, Erny, and Hagemeyer 2017). This indicates that while the mechanisms controlling microglial regulation of synaptic plasticity

are not completely understood, it is clear that direct manipulation of microglia alters the ability of neurons to wire and function normally.

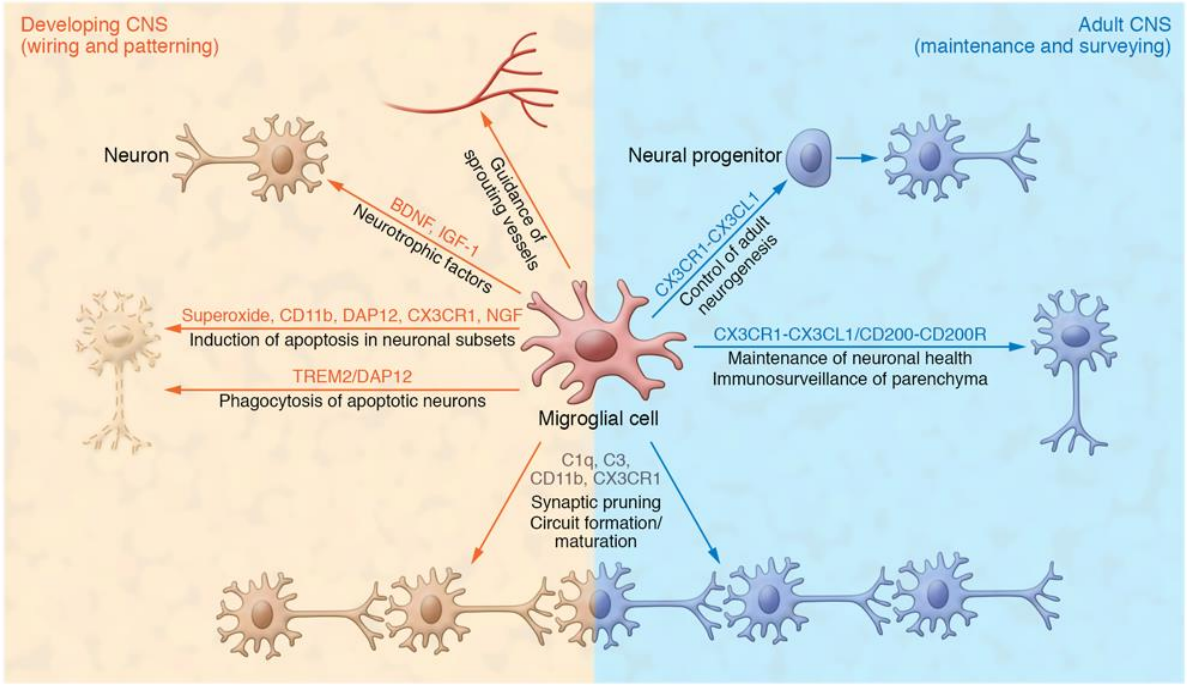

Figure 3. Microglia contribution to normal CNS functions. As resident immune cells in the CNS, microglia display many functions to maintain tissue homeostasis. Microglial cells modulate wiring and patterning during development by regulating neuron populations via phagocytosing excess synapses, releasing neurotrophic factors and guiding sprouting vessels. During postnatal development and adulhood microglia contribute to activity-dependent circuit formation, maturation of neuronal networks, regulation of adult neurogenesis and maintaining neuronal health (Kierdorf & Prinz, 2017).

1.5. The role of microglia in brain inflammation and injury

Besides contributing to the development and maintenance of the central nervous system, microglia function as the primary immune cells of the CNS. They provide the first line of defense against invading pathogens, and via the constant interaction with neurons, they often are the first to detect critical changes in neuronal activity and health status (Prinz & Mildner, 2011). Upon detection of danger associated molecular patterns (DAMPs, ATP, heat shock proteins, DNA, HMGB1), released by stressed or injured neurons, microglia initiate a series of responses triggered by a plethora of surface receptors, such as Toll-like receptors (TLRs), purinergic receptors, scavenger receptors, and cytokine and chemokine receptors (Salter & Stevens, 2017). Their activation results in phagocytosis of pathogens and dying cells and the release of soluble factors involved in neuronal damage, tissue repair, and remodeling as well as recruitment of other immune cells from the blood (Stevens & Schafer, 2018). In recent years, multiple studies have indicated that microglia function as a double-edged sword, playing a protective or a detrimental role depending on the given conditions during different brain pathophysiologies (Shemer, Erny, Jung, & Prinz, 2015). Depending on the nature of the stimulus, microglia can take a number of activation states, which correspond to altered microglia morphology, gene expression, and function. For example, it has been reported that upon acute injury such as traumatic brain injury (TBI), early microglial responses may contribute to the restoration of brain homeostasis (Donat, Scott, Gentleman, & Sastre, 2017). Selective elimination of microglia was found to exacerbate brain injury after experimental stroke (Szalay et al., 2016). On the other hand, prolonged microglial activation or the release of pro-inflammatory cytokines (IL-1, IL-6, TNFa) and chemokines (CCL2, CX3CL1, MIP-1), may result in augmented tissue damage and this may potentially contribute to neurodegeneration.

Uncontrolled synapse loss might indicate microglial dysfunction, which eventually can lead to reduced neuroprotection and neuronal repair, and increased neurodegeneration associated with chronic neuroinflammation (Salter & Stevens, 2017). For example, microglial dysfunction contributes to neurodegeneration in experimental models Alzheimer's disease (AD) and Parkinson's disease (PD) (Ransohoff, 2016). Selective elimination of microglia reduces cognitive deficits in experimental AD models (Najafi et al., 2018), which is similar to that seen after blockade of complement-mediated synapse elimination (Salter & Stevens, 2017). Furthermore, large-scale genome-wide association studies (GWAS) have revealed that several CNS disorders that are considered as a primary microgliopathy whereby

microglial dysfunction is considered to be a primary disease mechanism, providing a direct link between microglia and neurodegeneration (Prinz et al. 2011; Arcuri et al. 2017). A good example is Nasu-Hakola disease, an autosomal recessive disorder characterized by progressive dementia and bone cystic lesions (Kaneko, Sano, Nakayama, & Amano, 2010), showing that microglia may act as a primary contributor to the disease. This rare genetic disease is caused by mutations in the DNAX activation protein 12 (DAP12) or triggering receptor expressed on myeloid cells 2 (TREM-2) in microglial cells (Paloneva et al., 2002), which results in impaired phagocytic activity and excessive pro-inflammatory microglial activation. Other studies have uncovered, that similar mutations on DAP12 and TREM-2 could be strongly linked to the progression of AD and frontotemporal dementia (Salter and Stevens 2017; Kleinberger et al. 2017). Several other CNS disorders have been considered to be caused by genetic mutations resulting in microglial dysfunction, including Rett syndrome, Fragile X syndrome and Phelan-Mc Dermic syndrome (Arcuri et al., 2017). Thus, depending on their phenotype and role in given physiological processes, microglia may also play diverse roles in differrent brain diseases. Therefore, understanding the mechanisms through which microglia recognize and respond to injury or infection and interact with other cell types in the brain may lead to the identification of novel therapeutic targets. Among many brain conditions, infections induce strong microglial reaction and experimental models of infection are valuable to study microglial responses and function.

1.6. Neurotropic viruses

Neurotropic viruses, which are capable of infecting nerve cells, are among both DNA and RNA viruses of different families. Their infection inside the CNS leads to serious clinical syndromes of meningitis, encephalitis or meningoencephalitis. Despite the presence of the blood-brain barrier and blood-CSF barrier, as it was discussed in detail in previous chapters, viruses have evolved to find their way into the CNS (Miller, Schnell, & Rall, 2016). Three major routes of viral entry into the brain have been identified, as outlined in Figure 4.: direct infection of the cells that comprise the blood-brain barrier (BBB) and blood-cerebrospinal fluid barrier; infection of cells that are able to cross these barriers; and transneuronal migration across synapses from the peripheral nervous system (PNS) into the CNS (Koyuncu, Hogue, & Enquist, 2013).

Alternatively, neurotropic RNA viruses including poliovirus (PV), measles virus (MV), or some members of the Flavivirus family, like West-Nile virus infect endothelial or epithelial cells of the BBB and can act through the engagement of Toll-like receptor 3 (TLR3) to induce pro-inflammatory cytokines by circulating antigen presenting cells. As a result, BBB integrity becomes compromised by loosening its tight junctions, allowing viral particle migration into the brain tissue. Viruses may also passively access resident CNS cells by infecting lymphocytes or monocytes that can be transported across the blood-brain barrier. This strategy is often referred to as the 'Trojan horse' approach because viral particles are released once the blood-borne leukocytes gain access to the parenchyma. A classic example of this mode of invasion is provided by the human immunodeficiency virus type 1 (HIV-1): CD16+ monocytes, permissive for HIV-1, traffic across the BBB and release virions that can then infect CNS microglia (McGavern & Kang, 2011). The third mode of CNS entry is transneuronal migration, a strategy adopted by rabies virus (RABV) herpesviruses (HSVs), and pseudorabies virus (PRV). Intracellular trafficking in PNS neurons, which is necessary to shuttle cellular components to and from the synapse, can be commandeered to facilitate viral travel within and among synaptically connected neurons. The best-characterized examples of this type of spread are provided by herpesvirus family members such as Herpes simplex type 1 (HSV-1) and the closely related PRV (Koyuncu et al., 2013). After infection of epithelial cells in the oral mucosa, HSV-1 spreads to sensory and autonomic ganglia, establishing lifelong latency (Pomeranz, Reynolds, & Hengartner, 2005). Inside infected epithelial cells, these viruses become non-lytic within PNS neurons. During latency, only a few viral transcripts are synthesized, which do not encode functional proteins but prevent neuronal apoptosis via inhibition of caspase activity and disruption of both innate and adaptive immune signaling (Getts, Chastain, Terry, & Miller, 2013). However, in response to decreasing to immune monitoring, stress or other infections the virus can reactivate from its latent phase, which leads to an active infection of PNS neurons. Newly replicated viral particles can traffic along via microtubule tracks along the axons of sensory neurons, which have a pseudo-unipolar morphology. This way one axon is in contact with epithelial cells and the other synapses are in contact with CNS neurons (Kramer & Enquist, 2013). Such viral strains can reactivate long after the initial viral exposure, contributing to several neurodegenerative disorders.

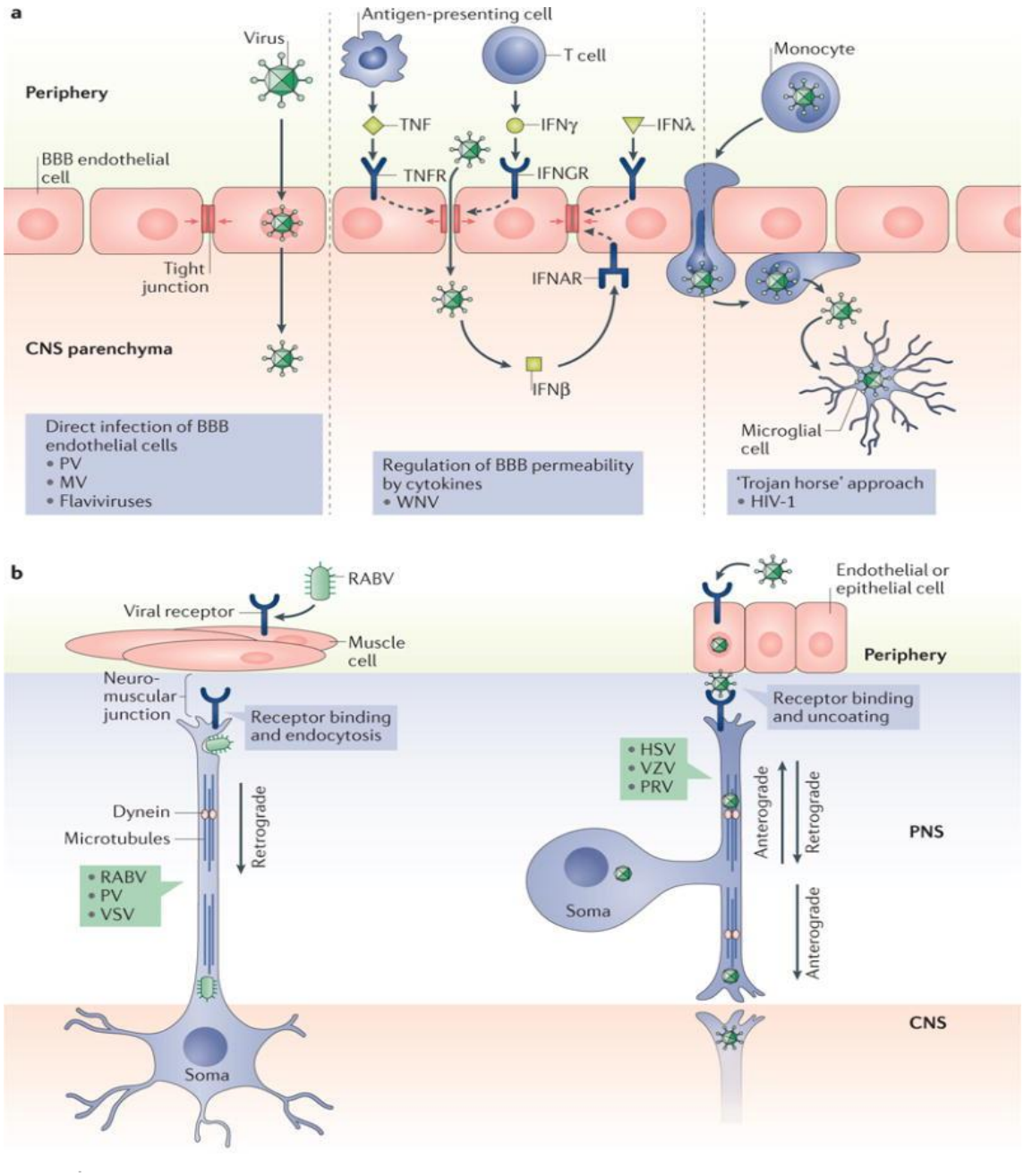

Figure 4. Different routes of viral entry into the CNS. a, Direct infection of BBB endothelial cells, followed by release of viral particles into the parenchyma (left panel). Some viruses can diffuse across permeable regions of the BBB, by influencing the release of pro- and anti-inflammatory cytokines or various interferons (IFNß, IFNγ, IFNλ), which can loosen barrier integrity (middle panel). With the 'Trojan horse' approach (right panel), viruses can infect lymphocytes, monocytes or macrophages which traffic across the BBB or blood-CSF barrier, releasing virus particles once in the brain parenchyma. **b,** Transsynaptic spread of viral particles involves the transport of viral genomes and associated proteins via microtubules and molecular motor proteins. Rabies virus (RABV) moves from muscle, across the neuromuscular juction via dinein-mediated retrograde transport into the CNS (left panel). Herpes simplex virus (HSV), Pseudorabies virus (PRV) and Varicella zooster virus (VZV) traffic across the endothelial-neuron junction. Inside neurons retrograde transport brings virions to the neuronal soma, and anterograde transport delivers them to the PNS-CNS synaptic junctions (right panel) (Miller et al., 2016).

1.6.1. Pseudorabies virus

Pseudorabies virus (PRV) belongs to the same family, Alphaherpesviridae, as the human pathogen Herpes Simplex Virus (HSV) and Varicella Zoster Virus. The natural host of the virus is the pig, in which viral infection leads to Aujenszky's disease (Schmidt, Hagemoser, & Kluge, 1992) with similar symptoms to that caused by rabies infection. PRV has a wide range of hosts, infecting all mammals except for higher primates (McFarland, Hill, & Tabatabai, 1987), probably due to circulating autoantibodies. Among other virus strains (vesicular somatitis virus, rabies virus, mouse hepatitis virus) pseudorabies virus have the unique ability to spread between exclusively synaptically connected chains of neurons. Such neuronal spread requires direct virus entry into the neuron (first-order neuron) and replication. The encapsulated viral genome is then transported at sites of synaptic contact to a second order of neuron where replication takes place again. This self-amplificating property allows the first order neuron as intensly labeled as the second or third order neurons (Pomeranz et al., 2005). Tracing studies using this feature of PRV have been successfully employed in a number of different animal models: pigs (the natural host), lambs and sheep, dogs, cats, chicken embryos, ferrets, and other rodents such as rats, mole rats, mice, gerbils, and hamsters (J. P. Card 1998; J. Card et al. 2018). Transsynaptic spread, self-amplification and broad host range made PRV an ideal tool in an extensive number of neuroanatomical studies seeking to define the architecture of multisynaptic pathways (Kramer & Enquist, 2013). Transsynaptic spread of PRV was proved by detailed electron microscopic studies which support the view that PRV spreads in the CNS primarily by direct cell-cell contact, rather than diffusion of virions through the extracellular space or via non-neuronal cells. Analysis of infected nervous tissue by electron microscopy revealed viral capsids and structural proteins localised at the synapses of infected neurons (Pomeranz et al., 2005). This feature of the virus was well described via the analysis of different neuronal pathways between the ventral musculature of the stomach to the brainstem and higher order structures of the CNS (Pomeranz et al., 2005). PRV spread in the nervous system also requires synaptically connected intact neuronal circuit. This was tested by direct injection of PRV into brain ventricles, which result only in the infection of nearby neurons, astrocytes and ependymal cells which line the walls of ventricles, but the virus did not spread futher (Rinaman, Card, & Enquist, 1993). Even tough, PRV is able to infect non-neuronal cells in the brain, such as epitehelial cells and astrocytes, non-synaptic spread is severly limited. Astrocytes are susceptible to PRV infection but not permissive for viral replication, they do

not contribute to trans-neuronal spread of the virus (Card, J. P., 2001). Rather, the infection of astroglia is tought to represent an effort of local intrinsic and innate immune defense to contain the infection (Card, J. et al., 2018). According to previous studies, microglial cells are the only cell type which can not be affected by PRV, althoug the exact reason is still unclear (Rinaman et al., 1993). When injected directly into the brain parenchyma, PRV virions diffuse very little, producing only focal infection site (Pomeranz et al., 2005). In order to effectively infect neurons, replicate and produce infectious progeny, and spread through synapses the virus needs several essential elements, including envelope proteins, which help viral capsids to interact with the extracellular matrix and gain access to permissive neurons (Figure 5.a,). PRV uses a common adhesion molecule, nectin to invade neurons through a receptor-mediated fusion of the viral envelope and plasma membrane of the target cell (Brittle, Reynolds, & Enquist, 2004). As a result, tegument protein associated viral capsids, containing the genome are released inside the host neuron, where they are transported along microtubules to the soma. The genome of virus enters the nucleus along with tegument proteins which initiate the expression of immediate early genes and initiates a transcription cascade which generates all necessary proteins for new virions (Brittle et al., 2004). During the lytic cycle viral genes (immediate-early, early and late) are expressed in a certain timeline. After achieving the right amount of copies, virus DNA is packed into capsids and exit the nucleus. Before leaving the host cell, naked capsids require envelopment, then they get transported into vesicles (Figure 5. c,) (Koyuncu et al., 2013).

The attenuated vaccine strain of PRV (PRV-Bartha) which have reduced virulence has been successfully used as a self-amplifying neural tracer after peripheral injection for its reduced neurotoxicity and prominently retrograde spread. Mutant PRV-Bartha strains are favored for tracing studies because they penetrate further into neuronal circuits due to increased host survival time. Since Bartha strains lack glicoprotein E, once introduced into the nervous system, PRV-Bartha spreads only in retrograde direction inside a circuit, while wild type strains, such as PRV-Becker and PRV-Kaplan, spread in both anterograde and retrograde directions (Pomeranz et al., 2005). Since Bartha strain is able to infect PNS neurons projecting to CNS neurons and invade specific brain regions by retrograde transport, the strain has been widely used for defining CNS ciruits that modulate the autonominc and somatic peripheral outflows (Pomeranz et al., 2005). The detailed retrograde spreading of PRV-Bartha has been effectively characterized in rats and hamsters, by injecting the virus intraocularly (Card, J. P., 1998). As different genetically modified PRV-Bartha strains have become popular tracing tools, more research has propelled the search for new techniques to

further enhance this powerful tool. Major autononmic pathways were defined during stress situations via dual tracing, employing ß-galactosidase (product of lacZ) expressing PRV-Bartha strain kombined with PRV-Kaplan strain (Jansen, Van Nguyen, Karpitskiy, Mettenleiter, & Loewy, 1995). Since then this dual tracing approach was used to map multiple autonomic connections in the CNS. Besides ß-galactosidase enzime, different fluorophores were inserted into PRV derivatives as well, such as EGFP or DSRed. In a model of cultured rat dorsal root ganglia the same fluorescent strains were used to uncover collateralized pathways (Miranda-Saksena, Boadle, Armati, & Cunningham, 2002). Genetically modified viral tracers, such as PRV, HSV or rabies only recently started to become powerful tools to study viral infections and immune responses in the CNS.

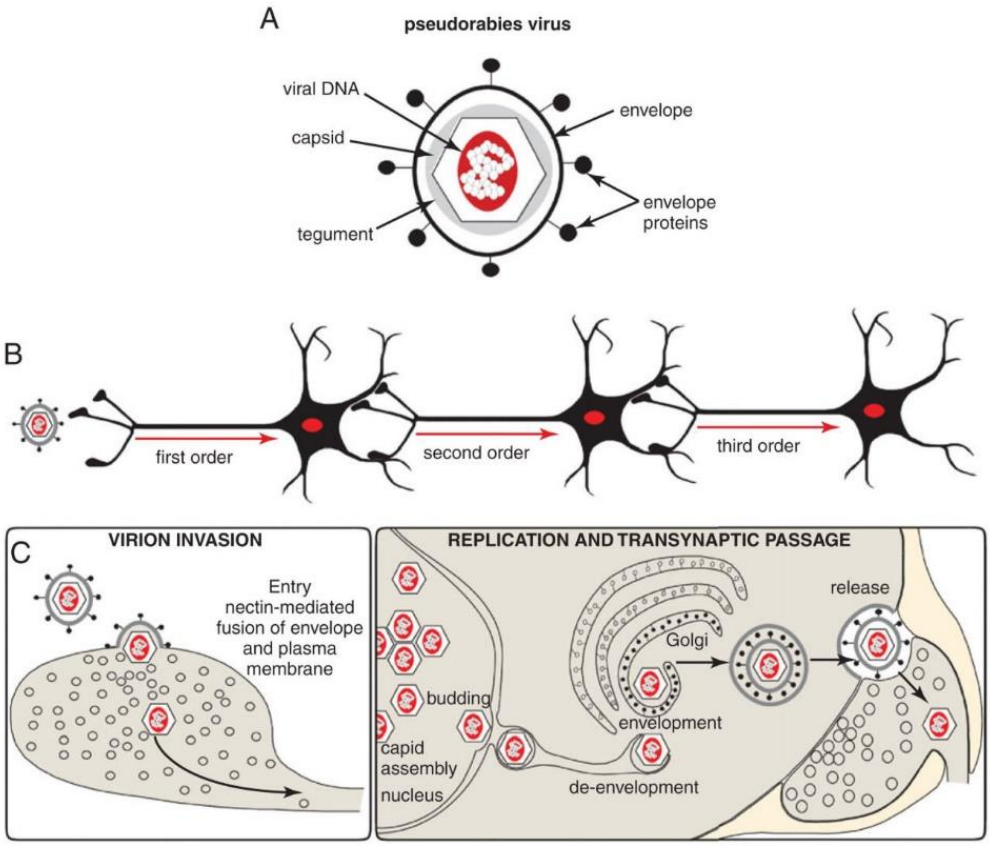

Figure 5. Structure and spreading mechanism of Pseudorabies virus. a, The structure of alphaherpes virus virions compose of several capsid and tegument proteins that are contained within the virus envelope which is acquired from the host cell. The envelope contains a second set of virally encoded proteins that are crucial for target recognition, attachment and fusion that lead to the release of the capsid into permissive neurons. **b,** Mutant strains of PRV spread selectively in the retrograde direction through exclusively synaptically linked neural circuits. **c,** Multiplication of virions is a multistep process which lead to assembly of mature virions in the cell soma. Virions are trafficked through the soma and denrites of infected neurons by vesicular motor proteins and released in the vicinity of synapses (Koyuncu et al., 2013).

1.7. Infection-induced inflammation and anti-viral immunity in the brain

Invasion of pathogens, such as viruses, bacteria or parasites into the brain results in chronic, often lethal diseases, which are associated with severe blood-brain injury, impaired neuronal communication, innate myeloid cell activation, and leukocyte infiltration. Unlike other cell types of the CNS, neurons are generally non-renewable, thus the cytolytic and inflammatory strategies that are effective in the periphery could be damaging if deployed in the brain (Getts et al., 2013). Upon infection-induced inflammation, the immune response of the brain aims to maintain neuronal network integrity while eliminate invading pathogens and the terminally injured cells.

As discussed above, the brain is shielded from external threats at both macro- and microscopic levels: it is enveloped in bone, to prevent physical injury, and separated from peripheral tissues and blood via highly specialized barriers. To overcome this, viruses have developed sophisticated strategies to enter the CNS either via transcellular and paracellular pathways across the BBB or anterograde/ retrograde trafficking along neurites from peripheral neurons (Miller et al., 2016). If occurring via parenchymal routes, pathogen invasion into the brain is sensed immediately by specialized innate immune cells, which include microglia, perivascular macrophages, and meningeal or choroid plexus macrophages. As first responders to tissue injury and pathogen invasion, brain myeloid cells are equipped to launch an immune response (Prinz et al., 2011). In case the reaction of CNS cells to infection or tissue injury extend a certain limit, vascular activation and production of chemokines may initiate the recruitment of immune cells from the periphery. Thus, regulation of the central immune response is crucial in protecting the brain from further tissue damage due to immunopathology, and lingering inflammation that can sometimes augment BBB injury, neuronal loss and hinder the tissue repair process (Russo & McGavern, 2015).

Although immune cell migration into the CNS is tightly regulated due to the blood-brain barrier (BBB), several routes exist for peripheral leukocytes to enter the CSF, the choroid plexus (CP), the meninges, perivascular spaces and eventually the parenchymal tissue (Prinz et al., 2017). Following infection by different neurotropic viruses, both innate (monocytes, neutrophil granulocytes) and adaptive immune cells ($CD8^+$ T cells, $CD4^+$ T cells and B cells) are recruited, to participate in pathogen elimination and clearance. Upon pathogen entry into the CNS, most immune responses begin with pattern recognition receptors (PRRs) sensing pathogen-associated molecular patterns (PAMPs) via Toll-like receptors, RIG-like receptors

(RLRs), or Nod-like receptors (NLRs) expressed by neurons, astrocytes, and microglia (Klein & Hunter, 2017). At the BBB, in response to TLR and PRR activation endothelial cells and astrocytes become strongly activated, and try to control viral entry (Rinaman et al., 1993). Endothelial cells respond to these cues via modulating barrier integrity through altered expression of CAMs and Rho GTPases, while activated astrocytes produce proinflammatory cytokines such as Il-1, IL-6, TNFa, and IFNγ. These proinflammatory cytokines aid in viral clearance through recruitment of mononuclear cells but may also be detrimental long-term to neuronal function and regeneration. Among the infiltrating immune cells, T cells are the first to enter the CNS during viral infection, with the production of T cell-derived cytokines, such as IFN-γ, which is critically involved in viral clearance and the amplification of immune cell infiltration through upregulation of chemokines. Recent studies have highlighted the importance of T cell recruitment and their reactivation in multiple infection models. In an HSV-1 induced encephalitis model inhibition of T cells via the downregulation of CXCL9 T cell attractant chemokine lead to increased mortality during HSV-1 infection. Direct injection of CXCL9 into the CNS infection site enhanced HSV-1 specific $CD8^+$ T cell accumulation, leading to marked improvements in the survival of infected mice (Koyanagi et al., 2017). In a clinical study of blood donors testing positive for West-Nile virus (WNV), T regs were found to expand after infection, and asymptomatic patients had higher levels of T reg cells compared to symptomatic patients, suggesting that T regulatory cells (T regs) control of antiviral responses may influence the severity of clinical disease. Similar results could be detected in a mouse WNV infection model, in which animals depleted of T regs showed more severe symptoms and had significantly higher mortality rate than control mice (Lanteri et al., 2009). Importantly, the specific chemokine milieu in the infected brain appears to influence T cell activity and antiviral response as well. Cytokines expressed by T cells, also have a major role in the antiviral response, such as IFN-γ which control infectious virus replication in the periphery but clears the virus from the CNS, without affecting acute viral replication (Baxter VK. et al., 2016). Animals that lack IFN-γ or the ability to signal through its receptor IFNγR, exhibit decreased B cell recruitment (Klein & Hunter, 2017). B cell functions, including antiviral humoral immune responses, are critical for control of viral dissemination in the periphery and neuroinvasion during neurotropic viral infections (reviewed in (Kyle Austin & Dowd, 2014). Early infiltrating B cells express multiple cytokines (such, as CXCL9, CXCL10, CCL19) which are upregulated within the CNS during viral infections. Although classically considered part of the adaptive immune response, B cells are activated soon after infection by several viruses prior to the

generation of specific immunoglobulin G (IgG) (Rojas, Narváez, Greenberg, Angel, & Franco, 2008). B cell responses to viruses are often initiated antigen recognition via their surface immunoglobulin receptors, such as IgG and IgM. Their activation and proliferation are also affected by T cell chemokine expression, although a recent study of neurotropic coronavirus infection suggest that activated B cells can respond to viral infection independently from CD8+ T cells (Phares, Marques, Stohlman, Hinton, & Bergmann, 2011). Their crucial role in viral infection was also proved by an infection model induced by the neurotropic strain JHMV of mouse hepatitis virus, in which the absence of B cells resulted in uncontrolled, persistent CNS infection despite viral reduction by T cells (Phares et al., 2011). As described above, PRR detection of viral nucleic acids induces expression of chemoattractants that promote the parenchymal entry of mononuclear cells, including blood-borne monocytes, which differentiate into tissue macrophages at sites of infection or injury. Upon neurotropic viral infections, it is still an uncleared question whether these cells aid in viral clearance and recovery or mediate continuing damaging inflammation in the CNS (Klein et al. 2019.). Macrophages can produce anti-inflammatory mediators, scavenge the infected area, phagocytose cell debris and regulate extracellular matrix and glial scar surrounding the damaged area (London, Cohen, & Schwartz, 2013). However, these cells have also been shown to have potent effector functions, including antigen presentation, T cell stimulation, and production of multiple proinflammatory mediators and reactive oxygen species (Terry et al., 2012). Monocyte recruitment can be affected by depletion of CCL2 and CCL7 proinflammatory cytokines resulting in increased viral burden and mortality (Bardina et al., 2015). Upon subsequent restoration of CCL7 by exogenous administration increased monocyte and neutrophil recruitment and improved survival.

Microglia are thought to protect CNS from viral infection via multiple mechanisms, including the production of antiviral cytokines, phagocytosis of virus-infected and dying neurons, and the induction of neuronal repair and homeostasis (Prinz et al. 2011; Ransohoff and Engelhardt 2012). In addition to restricting viral replication, microglia are suggested to orchestrate peripheral immune response against invading pathogens in the CNS. In the healthy brain, microglia do not express MHC, however, when activated by pathological conditions, they upregulate these molecules (Tsai et al., 2016). However, assessing specific immune contributions of microglia during infections has been challenging for multiple reasons, which would be discussed below.

1.8. The role of microglia in neurotrop viral infections of the CNS

As the main resident immune cell type of the brain parenchyma, microglia are known to shape CNS immune responses to viral infections that occur in the brain. However, for multiple reasons, the functional contribution of microglia to neurotropic viral infections has been described inadequately. Previous studies have stated, that microglia coordinate CNS immune responses via pro-inflammatory cytokine or chemokine secretion, and possibly via presenting antigen to T cells that are recruited into the brain (Zhang, Liu, & Wei, 2017). In response to a pathogen invasion microglia increase the expression of toll-like receptors (TLRs) which are critical in generating innate immune reactions. Others have indicated that in the case of HSV infection microglial TLR2 and TLR9 signaling have a pivotal role in the production of proinflammatory cytokines and chemokines (J. Card et al. 2018; Rinaman, Card, and Enquist 1993). As an anti-viral response, IFN-I production by microglia and phagocytosis of infected cells have been previously observed (Dénes, Boldogkoi, Hornyák, Palkovits, & Kovács, 2006). Rapid induction of microglia was also noticed in response to the immediate release of normally intracellular proteins and/or high-energy purine nucleotides (such as ATP, ADP, and UTP) from injured neurons (Davalos et al., 2005a). As it was previously described by others (Wolf, Boddeke, and Kettenmann 2017; Davalos et al. 2005) massive release of purines occurs after metabolic stress or trauma that might trigger microglial activation through P2 type receptor-mediated mechanisms (Dénes et al., 2006). However, it remains unknown if these mechanisms are involved in the activation and recruitment of microglia during virus infections. In spite of this information, studying microglial responses during viral infections in vivo has been quite difficult. As previous studies have described (J. P. Card 2001; Boldogköi et al. 2004; Dénes et al. 2006), it is clear that PRV and HSV infection of the brain produces a complex cascade of innate responses that are not limited to microglia (Rinaman et al., 1993). Virulent and attenuated strains of HSV and PRV have been shown to induce neuropathological changes and ultimately lead to reactive astrogliosis, activation and recruitment of brain macrophages and different CD45-positive blood-born immune cell populations to sites of infection (Dénes et al., 2006). Using the more virulent Becker strain of PRV, trafficking, and appearance of cells positive for CD45 leukocyte common antigen as well as $CD8^+$ cytotoxic- and $CD4^+$ lymphocytes at the sites of infections were reported. However, activated microglia also express CD45, therefore the distinction between infiltrated CD45-positive leukocytes and resident microglia remained challenging (Rassnick, Enquist, Sved, & Card, 1998).

Note, that in this complex inflammatory cascade it has been very difficult to isolate immediate microglial immune responses. Discrimination of microglia from infiltrated monocytes and macrophages is difficult due to the phenotypic transformation of activated microglia rendering them morphologically similar to infiltrating mononuclear phagocytic cells. According to previous researches (Rassnick et al. 1998; Enquist and Leib 2016) it is becoming increasingly clear that multiple glial cells participate in the immune response to neurotropic viral infections by isolating afflicted neurons and thereby facilitating transsynaptic spread of the virus (Rinaman, Card, and Enquist 1993; Boldogköi et al. 2004). Previous research proved that highly GFAP-positive astrocytes have the ability to isolate infected neurons, by wrapping afflicted cells and their synaptic contacts with processes that separate them from uninfected cells (Rinaman et al., 1993). Also, TLR3 was shown in astrocytes to sense HSV-2 infection immediately after entry into the CNS, possibly preventing HSV from spreading beyond the neurons mediating entry into the CNS (Reinert et al., 2012). However, it is likely that astrocytes do not have the ability to phagocytose compromised neurons, unlike microglia and macrophages. By using genetically modified strains of the „Bartha-Dup" strains of PRV (Boldogköi et al., 2004). Dénes et al., 2006 have described, that microglia are able to respond rapidly to early infection and isolate compromised neurons even while the infected neuronal membrane is still intact. Even though the exact molecular mechanisms of microglial responses to early infection need to be further investigated. By using the same highly specific, retrograde, transsynaptically spreading „Bartha-Dup" PRV strain and highly selective microglia elimination tool we were able to uncover some of these precise microglial mechanisms in response to virus infections.

2. Objectives

Microglia are the main immunocompetent cell type of the CNS that play a role in multiple physiological and pathological processes. The importance of microglial actions in acute brain injury, such as brain trauma or stroke and in chronic neurodegenerative diseases, like Alzheimer's is widely recognised. However, the role of microglia in anti-viral immunity of the brain is less studied. Notably, the mechanisms through which microglia recognize signs of infection at the cellular level and how infected cells are discriminated are still unclear. Therefore, the main goal of my work was to investigate inflammatory processes in the central nervous system during neurotropic virus infection, focusing on the following three main topics:

1) To study central inflammatory processes and the functional role of microglia in a mouse model of neurotropic virus infection.

2) To identify the role of microglial P2Y12 receptor in neurotropic virus infection.

3) To study inflammation and microglial responses in human post-mortem brain tissues after herpes simplex encephalitis.

3. Materials and methods

3.1. Processing of human samples

Post-mortem human brain tissues

Formalin fixed, paraffin embedded (FFPE) post-mortem tissue sections from patients (n=5) with known HSV-encephalitis (age between 42-66 years) were used. Tissue samples from two additional patients with no known neurological disease were used as controls. Control samples were perfusion-fixed with Zamboni fixative (4% PFA, 15 % PIC) and postfixed overnight in the same solution. All performed procedures were approved by the Regional and Institutional Committe of Science and Research Ethics of the Scientific Council of Health (ETT-TUKEB 62031/2015/EKU, 34/2016 and 31443/20116EKU (518/pi/11)).

Immunohistochemistry and immunofluorescence on post-mortem human brain tissues

To investigate microglia recruitment in response to neurotropic virus infection in the human brain, 4-6μm thick brain sections were cut and samples were mounted on gelatine-coated slides. After deparaffination, HIER (Novocastra Epitope Retrieval Solution pH9, Leica Biosystems) and peroxidase blocking (in 1% H2O2 solution) was carried out. Sections were blocked with 2.5% Normal Horse serum (#S-2012, Vector Laboratories) and were incubated with microglia and immune cell specific primary antibodies, see in Table 1. For signal amplification ImmPRESS anti-rabbit HRP Kit (#MP-7401, Vector Laboratories) and for visualisation either ImmPACT NovaRED HRP substrate (for detection of HSV I) or DAB-Ni HRP substrate (for detection of other markers, #SK-4805, Vector Laboratories) was used. Representative pictures were taken on 20x magnification using a Nikon Ni-E C2+ microscope. To assess the proportion of P2Y12-positive microglia, P2Y12 and Iba1 double immunofluorescence has been performed on 50 μm thick free-floating brain sections. Images were captured using a Nikon Eclipse Ti-E inverted microscope (Nikon Instruments Europe B.V., Amsterdam, The Netherlands), with a CFI Plan Apochromat VC 60X water immersion objective (NA: 1.2) and an A1R laser confocal system.

Table 1. All primary antibodies used for human microglia and infiltrated immune cell labeling.

Antigen	Host species	Target species	Dilution	Catalogue number
HSV I	rabbit	human	1:200	#361A-14, Cell Marque
HSV II	rabbit	human	1:200	#362A-14, Cell Marque
P2Y12	rabbit	human	1:100	#AS-55043A, AnaSpec, Inc.
Tmem119	rabbit	human	1:250	#ab185333, Abcam
CD68	mouse	human	1:50	#NCL-L-CD68, Leica
CD45	mouse	human	1:50	#NCL-L-LCA_1 ml, Leica
CD3	mouse	human	1:100	#NCL-L-CD3-565, Leica
CD20	mouse	human	1:100	#NCL-L-CD20-L26, Leica
CD15	mouse	human	prediluted	#PM 073 AA, Biocare Medical

Table 2. Patient characteristics and tissue processing information for post-mortem human brain tissues.

	Nr.	Age(y)	Sex	HSVE survival	Assessed region	Co-pathology	Cause of death	Post-mortem delay	Fixation time
cases	1	35	female	21 years	temporal lobe	none	bronchopneumonia	<24 h	8 weeks
	2	66	female	16 days	temporal lobe	none	acute encephalitis/ brain/ edema/herniation	<24 h	8 weeks
	3	65	female	9 day	temporal lobe	none	acute encephalitis/ brain/ edema/herniation	<24 h	3 weeks
	4	41	female	24 months	temporal lobe	none	bronchopneumonia	<24 h	4 weeks
	5	24	male	10 days	temporal lobe	none	acute encephalitis/ brain/ edema/herniation	62 h	3 weeks
controls	Sko13	60	female	N.A.	temporal lobe	chronic bronchitis	respiratory arrest	<24 h	2-3h perfusion and overnight post-fixation
	Sko16	72	male	N.A.	temporal lobe	acute bronchitis	respiratory arrest	<24 h	2-3h perfusion and overnight post-fixation

3.2. In vivo mouse expreiments

Animal housing and treatment

Experiments were carried out on 12-18 weeks old C57BL/6J, P2Y12$^{-/-}$, P2X7$^{-/-}$, Cx3Cr1$^{GFP/+}$ and Cx3Cr1$^{GFP/+}$ P2Y12$^{-/-}$ mice. Mice were maintained at 12 h light/dark cycle with food and water avaliable ad libitum in the Medical Gene Technology Unit of the IEM. All experimental procedures were performed according to the ethical guidelines set by the European Communities Council Directive (86/609 EEC) and the Hungarian Act of Animal Care and Experimentation (1998; XXVIII, Sect. 243/1998), approved by the Animal Care and Use Committee of the Institute of Experimental Medicine of the Hungarian Academy of Sciences.

Selective elimination of microglia in the brain

Mice were fed a chow diet containing the CSF1R-inhibitor PLX5622 (Plexxikon Inc. Berkeley, USA; 1200 mg PLX5622 in 1 kg chow) for three weeks to eliminate microglia from the brain. We could not observe any sign of physiological illness (alterations in food intake, weight, physical appearance) or behavioural changes (social interactions, exploration) during the diet period, in accordance with other studies (Szalay et al., 2016).

Neurotropic herpesvirus infection

For all experiments genetically modified recombinant strains of PRV-Bartha derivatives, PRV-Bartha-Dup-Green (BDG) or a parent viral strain expressing red fluorescent protein, PRV-Bartha-DupDsRed (BDR) were used (Boldogköi et al., 2002). To study the recruitment of microglia to infected neurons, we used the ability of the virus to induce retrograde transsynaptic infection in the brain after injected into peripheral target organs (Card, J. P., 2001). The neuro-invasiveness of BDG was modified by insertion of a GFP gene expression cassette to the putative antisense promoter (ASP) located at the repeated invert region of the virus. This construct also allows time-mapping the spread of infection in individual cells (Boldogköi et al., 2004). The activity of the strong immediate-early promoter/enhancer of the human cytomegalovirus is independent from the viral protein, enabling very early stages of infection to be detected by GFP expression. PRV genes encoding structural proteins are driven by late promoters, resulting in the appearance of the virus proteins in the late stage of the infection. Mice were injected either intraperitoneally or directly into the epididimal adipose white tissue. In a series of studies, where mice were fed a PLX5622 diet to achieve selective microglia depletion, BDG was

injected on 16th day of the diet to assess the effect of the infection whitin microglia depleted environment (see Fig2. c,). For in vivo two-photon imaging, $Cx3Cr1^{+/GFP}$ mice were infected with BDR, allowing us to examine viral infection and microglial actions at the same time. After the viral injection, we allowed mice to survive for 5-7 days depending on the study design and regularly monitored them for neuropathological symptomes and behavioral changes.

In vivo two-photon imaging

Virus injection and cranial window surgery: To assess microglia recruitment to infected neurons in the mouse brain in real-time, $Cx3Cr1^{GFP/+}$ mice were i.p. injected with 10µl of the BDR virus ($1,5x10^{10}$ PFU/ml). 7 days after virus injection, cranial window surgery was performed on anaesthetized (3% isoflurane for induction, 1.5-2% during surgery) mice and a circular craniotomy (3 mm diameter) was made above motor cortex (Bregma – 0,82); on the right hemisphere. A custom-made aluminium head plate was fixed to the skull using Cyanoacrylate glue. During skull opening the place of craniotomy was washed continuously with cold Ringer solution. The craniotomy was covered with a circular cover glass and dura mater remained intact under the glass to ensure that microglial activation is not induced by the surgical procedure (Szalay et al., 2016). The cover glass was fixed with Paladur mixed with Cyanoacrylate.

Two-photon imaging: Measurements were performed by using a Femto2D-DualScanhead microscope (Femtonics Ltd., Hungary) coupled with a Chameleon Ultra II laser (Coherent, Santa Clara, USA) (Chiovini et al., 2014). The wavelength of the laser was set to 980nm to measure DsRed and GFP signal simultaneously. Excitation was delivered to the sample, and the fluorescent signal was collected using a CFI75 LWD 16XW/0.8 lens (Nikon, 16x, NA 0.8) and then separated using a dichroic mirror (700dcxru) before the two channel detector unit, which was sitting on the objective arm (travelling detector system) as described in detail earlier (Katona et al., 2012). The dichroic mirror and emission filters (490-550 nm for the green and 570-640 nm for the red channel) was purchased from Chroma Technology Corp. (Vermont, USA). Data acquisition was performed by MES softver (Femtonics Ltd.) A Z-stack from of 32 images (800x800 pixel, field-of-view=210x210 µ, Z stack contained 12 image planes with 4.6

μm step size (range= 80-135 μm from pial surface) was made at every 3 minutes. Two-photon image sequences were exported from MES and analysed using ImageJ.

Tissue processing and immunostaining on mouse brain samples

Under deep anaesthesia with intraperitoneal injection with Fentanyl (0.25 mg/kg) mice were transcardially perfused with 0.9% saline for 2 minutes, followed by 4% paraformaldehyde (PFA) in 0.1 M phosphate buffer (PB, Ph= 7.4) for 20 minutes. After fixation, the brains were carefully removed from the skull, and were postfixed in 10% sucrose 4% PFA solution for 24 hour. After that the solution was changed to 10% sucrose PBS for cryoprotection and to remove the fixative. The brains were then sectioned at 25 μm thickness using a Leica sledge microtome (Leica Biosystems). Free-floating brain sections were used for immunostaining throughout the study. Brain sections were blocked with 2% normal donkey serum and incubated with a mixture of primary antibodies in Table 3. overnight at 4^{o}C. The following day after several washing steps all slices were labelled with the appropriate fluorescent secondary antibodies (Table 3.). Images were captured with a Nikon Ni-E C2+ confocal microscope, and image processing was done using the NIS Elements Viewer 4.20 software. Quantitative analysis was performed on 3 randomly selected fields within the region of interest for each brain section, on 3-3 serial coronal sections for given brain areas.

Immunohistochemical labeling for NTPDase1

After the fixative was washed out, the coronal brain sections were incubated in blocking solution (5% normal goat serum and 1 mg/ml BSA) for 1 h at 22 ˚C. Incubation in the solution of the polyclonal NTPDase1 antibody, was performed overnight at 4 ^{o}C. Following three, 10 min washes in PBS, the sections were incubated with biotinylated secondary antibody for 2 h. The staining was performed with Vectastain ABC Elite kit using DAB as the chromogen. After washing thoroughly with distilled water, sections were postfixed in 1% OsO4, dehydrated in ethanol, stained with 1% uranyl acetate in 50% ethanol for 30 min, and embedded in Taab 812. Negative control experiments were performed using the same protocol but substituting pre-immune serum for the primary antibody. Ultrathin sections were cut using a Leica UCT ultramicrotome (Leica Microsystems, Milton Keynes, UK) and examined using a Hitachi 7100 transmission electron microscope (Hitachi; Tokyo, Japan).

Table 3. Primary and secondary antibodies used in this study.

Antigen	Host species	Target species	Dilution	Catalogue number	Secondary anibodies
Iba1	donkey	goat	1:500	#NB100-1028, Novusbio	donkey-anti-goat Alexa594
P2Y12	rabbit	mouse	1:500	#55043A, Anaspec	donkey anti-rabbit Alexa647
CD45	rat	mouse	1:250	#MCA1388, AbD Serotec	doneky anti-rat Alexa594
anti-PRV	rabbit	PRV	1:500	custom made (from Lynn Enquist)	donkey anti-rabbit Alexa647
anti-GFP	donkey	chicken	1:1000	#A10262, Invitrogen	donkey anti-chicken Alexa488
CD68	rat	mouse	1:250	#NCL-L-CD68, Leica	donkey anti-rat Alexa594
tomato lectin	biotinylated	----------	1:100	#L0651-1MG, Sigma	steptavidin Marina Blue
ICAM	donkey	goat	1:500	#AF796, R&D Systems	donkey anti-goat Alexa594
NDTPase	rabbit	donkey	1:500	custom made (from Jean Sévigny)	donkey anti-rabbit Alexa647

Immuno-electron microscopy

Fixation of the tissues: The brains were fixed by the standard protocol. . Following fixation, phosphate buffer (PB) was perfused to remove extra fixative from the tissue. Brains were removed from the skull and 50 μm thick free-floating sections prepared by using a Leica vibrotome (Leica Biosystems).

Immunohistochemistry: Brain sections were incubated in 30% sucrose overnight for cryoprtection. To unmask antigens in the tissue and help the penetration of the antibodies, slices were frozen in liquid nitrogen 3 times and then washed in TBS buffer. After combined immunogold-immunoperoxidase stainings, sections were treated with osmium tetroxide, dehydrated in ascending ethanol series and acetonitrile, and embedded in epoxy resin. During dehydration, sections, were treated with uranyl acetate. After polymerization, 70 nm thick sections were cut on an ultramicrotome, picked up on formvar-coated single-slot copper grids, and sections were examined using a Hitachi H-7100 electron microscope.

Correlated confocal laser-scanning microscopy, electron microscopy and electron tomography

Fluorescent labeling for confocal microscopy: Before immunofluorescent labeling 50 μm thick brain sections from BDG-injected $Cx3Cr1^{+/GFP}$ mice were washed in PB, treated with 0,5 % sodiumborohydride for 5 minutes, and further washed in PB and TBS. This was followed by blocking for 1 hour in 1% human serum albumin (HSA). After this, sections were incubated in mixtures of primary antibodies: chicken anti-GFP, rat-anti-mouse CD68 and rabbit anti-PRV. To eliminate non-specific binding, the anti-PRV antibody solution was incubated with control brain sections for one day before use. After repeated washes in TBS, sections were treated with blocking solution containing 0.5% cold water fish skin gelatine and 0.5% HSA in TBS for 1 h. After incubation, sections were washed in TBS, and incubated overnight at 4 °C in the mixture of biotinylated goat-anti-chicken, Alexa 594 conjugated donkey-anti-rat and Alexa 647 conjugated donkey-anti-rabbit diluted in GelB. Secondary antibody incubation was followed by washes in TBS and PB. Sections were mounted in PB, coverslipped and coverslips sealed with nailpolish. Immunofluorescence was analysed using a Nikon Eclipse Ti-E inverted microscope (Nikon Instruments Europe B.V., Amsterdam, The Netherlands), with a CFI Plan Apochromat VC 60X water immersion objective (NA: 1.2) and

an A1R laser confocal system. We used 488, 561 and 642 nm lasers, and scanning was done in line serial mode. Image stacks were obtained with NIS-Elements AR software with a pixel size of 50x50 nm in X-Y, and 150 nm Z-steps. Stacks were deconvolved using Huygens Professional software (www.svi.nl), and 3D-reconstruction was performed using the IMOD software package.

Electron microscopy: After imaging, sections were washed 0.1 M PB, TBS and incubated in ABC (1:300, Vectastain Elite ABC HRP Kit, #PK-6100. Vector Laboratories) diluted in TBS. Sections were washed in TBS, and tris-buffer (TB) pH 7.6, and the immunoperoxidase reaction was developed using 3,3-diaminobenzidine as chromogen. After subsequent washes, sections were treated with 0.5 % osmiumtetroxide in PB for 20 minutes. Then sections were dehydrated in ascending ethanol series and acetonitrile, and embedded in epoxy resin. During dehydration sections were treated with 1% uranylacetate in 70% ethanol for 20 minutes. After polymerization, 70 or 150 nm thick sections were cut on an ultramicrotome, and picked up on formvar-coated single-slot copper grids. The sections were examined using a Hitachi H-7100 electron microscope and a side-mounted Veleta CCD camera.

Electron tomography: For the electron tomographic investigation, we used the 150 nm thick sections. Grids were put on drops of 10% HSA in TBS for 10 minutes, dipped in distilled water (DW), put on drops of 10 nm gold conjugated Protein-A (#AC-10-05-05, Cytodiagnostics) in DW (1:3), and washed in DW. Finally, we deposited 5-5 nm thick layers of carbon on both sides of the grids. Electron tomography was performed using a Tecnai T12 BioTwin electron microscope equipped with a computer-controlled precision stage and an Eagle™ 2k CCD 4 megapixel TEM CCD camera. Acquisition was controlled via the Xplore3D software (FEI). Regions of interest were pre-illuminated for 4-6 minutes to prevent further shrinkage. Tilt series were collected at 2 degree increment steps between -65 and +65 degrees at 120 kV acceleration voltage and 23000x magnification with -1.6 – -2 μm objective lens defocus. Reconstruction was performed using the IMOD software package. Isotropic voxel size was 0.49 nm in the reconstructed volumes. Segmentation has been performed on the virtual sections using the 3Dmod software.

Super-resolution (STORM) microscopy

Free-floating brain sections were blocked with 2% normal donkey serum followed by immunostaining with rabbit anti-mouse P2Y12 antibody for microglia, donkey anti-chicken GFP for viral immediate-early GFP signal, and rabbit anti-PRV for virus protein labeling were used. For secondary antibody labelings donkey anti-rabbit Alexa 647, donkey anti-chicken Alexa 488 were used (in dilution described in Table2.). Sections were mounted onto 1.5 thick borocilicate coverslips and covered with imaging medium immediately before imaging.

3.3. In vitro mouse experiments

Primary cell cultures

Neuronal cultures: Primary cultures of embryonic cortical cells were prepared from CD1 mice on embryonic day 16 (Czöndör et al., 2009) . Cells were seeded onto poly-L-lysine–coated (#P1524, Sigma-Aldrich) 24-well tissue culture plates at 3×10^5 cells/well density and grown in NeuroBasal medium (#21103-049, ThermoFisher Scientific) supplemented with 5% foetal bovine serum (FBS, #F7524, Sigma), B27 (#17504-044, ThermoFisher Scientific), Glutamax (#35050061, ThermoFisher Scientific), gentamicin (40 μg/ml, Sandoz), amphotericin B (2.5 μg/ml, #A2411, Sigma-Aldrich). Cytosine-arabinofuranoside (CAR, 5 μM, #C6645, Sigma-Aldrich) was added to the cultures 48-72 h after plating to limit glia growth, and then one third of the culture medium was changed to NeuroBasal medium supplemented with B27 without FBS every 3–4 day thereafter. Cells were cultivated for 6-8 days at 37°C in 5% CO_2, 95% air atmosphere until further measurements.

Astroglia and microglia cultures: Astroglia/microglia mixed cell cultures were prepared from the whole brains of CD1, C57BL/6J, CX3CR1$^{GFP/+}$, P2X7$^{-/-}$ or P2Y12$^{-/-}$ newborn (P0-P1) mouse pups, as described earlier (Környei et al., 2005). In brief, meninges were removed and the tissue pieces were subjected to enzymatic dissociation, using 0.05% w/v trypsin (#T4549, Sigma Aldrich) and 0.05% w/v DNase (#DN-25, Sigma-Aldrich) for 10 minutes at room temperature. The cells were plated onto poly-L-lysine (#P1524, Sigma-Aldrich) coated plastic surfaces and were grown in Minimal Essential Medium (#M2279, Sigma-Aldrich) supplemented with 10% FBS (#10500, Gibco), 4 mM glutamine (#G3126, Sigma-Aldrich), 40 μg/ml gentamycin (Sandoz) and amphotericin B (2.5 μg/ml, #A2411, Sigma-Aldrich) in humidified air atmosphere containing 5% CO2, at 37^{o}C. The culture medium was changed on the first two days and every third day afterwards. Cultures reaching confluency at ~DIV7 were

harvested by trypsinization and re-plated onto PLL coated glass coverslips or into petri dishes, according to the actual experimental design. Secondary astrocytic cultures reaching confluency and displaying mosaic-like pattern were infected with PRV strains, as it follows. Microglial cells were isolated from 21-28 day old mixed cultures either by shaking or by mild trypsinization (Saura, Tusell, & Serratosa, 2003).

Neurotropic herpesvirus infection of primary neuronal and astroglial cultures

The neuronal or astroglia cultures were infected with either PRV-Bartha-Dup-Green (BDG) virus or PRV-Bartha-DupLac (BDL) at a final titter of $2.5x10^5$ PFU/ml, as described earlier (Gönci et al., 2010b). The multiplicity of infection (MOI) was ~0,17 PFU/cell. The cells were incubated with the virus containing medium for 1h, at room temperature. In order to remove infective virus particles from the culture medium we washed the cultures at least three times after the 1h viral exposure.

Establishment of neuron/microglia and astroglia/microglia co-cultures

In cultures used for time-lapse recordings microglial cells isolated from mixed glial cultures were seeded on top of astrocytic or neuronal cell cultures in 10 000 cell/cm^2 density, immediately after the infection and the subsequent washing steps. If not $CX3CR1^{+/GFP}$ microglia were used, the cells were subjected to staining with the orange or red vital CellTracker dyes CMTMR/CMTPX (#C2927, #C34552, ThermoFisher Scientific) prior co-culture establishment (30min, 37ºC).

Time-lapse microscopy

Time-lapse recordings were performed on a computer-controlled Leica DM IRB inverted fluorescent microscope equipped with a Marzhauser SCAN-IM powered stage and a 10x N-PLAN objective with 0.25 numerical aperture and 5.8 mm working distance. The microscope was coupled to an Olympus DP70 colour CCD camera and a Zeiss Colibri LED epifluorescent illumination system. Cell cultures were kept at 37°C in humidified 5% CO_2 atmosphere in tissue culture grade Petri dishes in a stage-top incubator mounted on the powered stage of the microscope. Stage positioning, focusing, illumination and image collection were controlled by a custom-made experiment manager software on a PC. Phase contrast and epifluorescent images were collected consecutively every 10 minutes from several microscopic fields for durations up to 48 hours. Images were edited using NIH ImageJ software.

Cell motility data analysis

Cell tracking: Images were analysed individually with the help of custom-made cell-tracking programs (G-track and Wintrack) enabling manual marking of individual cells and recording their position parameters into data files. At the magnification applied, the precision of this tracking procedure is estimated to be 10 μm, comparable to the average cell diameter (10-50 μm). In the following, the position of the i^{th} cell at time t is denoted by $x_i(t)$.

Trajectories: Cell positions, $x_i(t)$, from several microscopic fields were recorded over 24 hours and each cell's trajectory was plotted. Subsequently, the starting positions of trajectories were aligned to the origin (x=0, y=0) and consecutive relative cell positions were plotted and superposed yielding groups of centered trajectories enabling the comparison of cell migration directionality. Trajectories in the monolayer cell cultures studied indicate a persistent random walk behaviour with different velocity and directional persistence.

Displacement: The motion of individual cells is often evaluated in terms of average cell displacement, d, over a time period t as:

$$d^2(t) = \left\langle \left(X_i(t + t_0) - X_i(t_0) \right)^2 \right\rangle_i$$

where $X_i(t)$ denoting the center of cell i at time t, $\langle \cdot \rangle_i$ is an average over all possible cells, and t_0 is an arbitrary reference frame of the image sequence analysed. The empirical $d(t)$ curves indicate a persistent random walk behaviour in monolayer cell cultures studied.

Average velocity: Average cell velocity was, calculated directly from cell displacements in consecutive steps of cell tracking. The velocity, $v_i(t)$, of a given cell i at time t was calculated as

$$v_i(t) = |x_i(t + \Delta t) - x_i(t)| / \Delta t$$

where Δt is the difference of two consecutive steps of cell tracking and thus the time resolution data acquisition. To characterize the motility of an ensemble of cells, time-dependent average velocity $v(t)$ was calculated as

$$v(t) = \frac{1}{N(t)} \sum_{i=1}^{N(t)} v_i(t)$$

where the summation goes over each $N(t)$ cell being in the cell population. Average velocity, v, was calculated by averaging $v(t)$ over all time steps of cell tracking as

$$v = \frac{1}{K} \sum_{t=\Delta t}^{K \cdot \Delta t} v(t)$$

where K is the number of time steps of tracking.

Cytokine measurement from media of primary cell cultures

Concentrations of IL-1α, IL-1β, TNF-α, IL-6, MCP-1, RANTES (CCL5), G-CSF and KC (CXCL1) were measured from conditioned media of primary neuronal, astroglial and microglial cell cultures by using cytometric bead array (CBA) Flex Sets (all from BD Biosciences, #560157, #560232, #558299, #558301, #558342, #558345, #560152, #558340, respectively). Measurements were performed on a BD FACSVerse machine and data were analysed using an FCAP Array software (BD Biosciences) as described earlier (Denes A., et al. 2015). The cytokine levels of conditional media were corrected for total protein concentrations of the samples measured by Bradford Protein Assay Kit (#50000201, Bio-Rad Laboratories).

Total RNA isolation and quantitative RT-PCR

For total RNA isolation, cell culture samples were homogenized in 500 µl TRI Reagent and isolation was performed using Tissue Total RNA Mini Kit according to the manufacturer's instructions. To eliminate genomic DNA contamination, DNase I treatment was introduced (1 U/reaction, reaction volume: 50 µl). Sample quality control and the quantitative analysis were carried out by NanoDrop. cDNA synthesis was performed with the High Capacity cDNA Reverse Transcription Kit according to the manufacturer's instructions. The chosen primer sequences used for the comparative C_T experiments were verified with the Primer Express 3.0 and Primer-BLAST software. The sequences were as follows:

Table 4. All primers used for quantitative PCR measurements.

GAPDH	fw TGA CGT GCC GCC TGG AGA AA, rev AGT GTA GCC CAA GAT GCC CTT CAG
IL-1α	fw CCA TAA CCC ATG ATC TGG AAG AG, rev GCT TCA TCA GTT TGT ATC TCA AAT CAC
TNF-α	fw CAG CCG ATG GGT TGT ACC TT, rev GGC AGC CTT GTG CCT TGA
MCP-1	fw CCAGCACCAGCACCAGCCAA, rev TGGATGCTCCAGCCGGCAAC
RANTES	fw CAGCAGCAAGTGCTCCAATCTT, rev TTCTTGAACCCACTTCTTCTCTGG
IL-6	fw CTCTGCAAGAGACTTCCATCC, rev AGTCTCCTCTCCGGACTTGT
G-CSF	fw TGCCCAGAGGCGCATGAAGC, rev GGGGAACGGCCTCTCGTCCT

The primers (purchased from Invitrogen) were used in real-time PCR reaction with Fast EvaGreen qPCR Master Mix (Biotium, USA) on a StepOnePlus (Applied Biosystems) instrument. The gene expression was analysed by using the StepOne 2.3 program (Applied Biosystems). Amplicons were tested by Melt Curve Analysis on StepOnePlus instrument. Experiments were normalized to *gapdh* expression.

Quantification of nucleotides and adenosine

For quantification of ATP derivatives released by or retained in control vs. infected cells, embryonic (E16) primary cortical neuronal cultures were used. The cells were infected at DIV9. 16 hours post-infection GFP expression was visible in most cells, while the cell membrane integrity was not compromised and the overall viability was not reduced based on MTT cell viability tests. The cell culture media and the cell fractions were collected 15 min after media change, as it is described below. The adenine nucleotides (ATP, ADP, AMP) and adenosine (Ado) were determined in extracts from cells and culture media by using HPLC method. The medium (400 µl) was separated into a cold Eppendorf tube which contained 50 µl of homogenization solution. The cell layer was frozen with liquid nitrogen and extracted in 100 µl volume of ice-cold homogenization solution. The homogenization solution was 0.1 M perchloric acid that contained theophylline (as an internal standard) at 10 µM concentration. The cell extract was centrifuged at 3510 g for 10 min at 0-4^{o}C and the pellet was saved for protein measurement. Perchloric anion from the supernatant was precipitated by 1 M

potassium hydroxide, the precipitate was then removed by centrifugation. The culture media after the acid extraction was centrifuged as described above. The extracted purines were kept at -20^{o}C until analysis. The adenine nucleotides and adenosine in extracts from cells and culture media were determined by online column switching separation using Discovery HS C18 50 x 2-mm and 150 x2-mm columns. The flow rate of the mobile phases ["A" 10 mM potassium phosphate, 0.25 mM EDTA "B" with 0.45 mM octane sulphonyl acid sodium salt, 8 % acetonitrile (v/v), 2 % methanol (v/v), pH 5.2] was 350 or 450 µl/min, respectively in a step gradient application. The enrichment and stripping flow rate of buffer [10 mM potassium phosphate, pH 5.2] was during 4 min and the total runtime was 55 min. The HPLC system used was a Shimadzu LC-20 AD Analytical & Measuring Instruments System, with an Agilent 1100 Series Variable Wavelength Detector set at 253nm. Concentrations were calculated by a two-point calibration curve using internal standard method. The data are expressed as pmol per mg protein or pmol per mL.

Enzyme histochemistry for detection of ecto-ATPase activity

A cerium precipitation method was used for electron microscopic investigation of ecto-ATPase activity (Kittel, 1999). Briefly, thoroughly washed sections were incubated in a medium containing 1 mM ATP as substrate, 3 mM CeCl3 (precipitating agent for the liberated phosphate), 1 mM levamisole (inhibitor of alkaline phosphatases, Amersham, Poole, UK), 1 mM ouabain (Na+, K+-ATPase inhibitor; Merck, Darmstadt, Germany), 50 mM αβ-methylene ADP (5'-nucleotidase inhibitor) and 5 mM KCl in 70 mM Tris–maleate buffer (pH 7.4) for 30 min at room temperature. Incubation was followed by three rinses in Tris–maleate buffer and washing with distilled water. The tissue blocks were then postfixed, dehydrated and treated and embedded into Taab 812 resin for ultrathin sectioning and microscopic examination as described above. Control reactions were performed without adding the ATP substrate.

Flow cytometric analysis of brain, spleen and blood samples

Cells were isolated from mouse brains by enzymatic digestion with the mixture of DNase I (10µg/ml, #11284932001, Roche) and Collagenase/Dispase (0,5mg/ml, #11088866001, Roche) in 10% FCS/DMEM, followed by several centrifugation steps with Percoll (40% and 70%) and washing in 10% FCS/DMEM. Spleen cells were isolated by mechanical homogenization of the spleen and red blood cells were removed by centrifugation. Brain and spleen cells were diluted with FACS buffer (PBS containing 0.1% Tween 20) before acquisition. Venous blood was collected from the heart before transcardial perfusion using 3.8% sodiumcitrate as an anticoagulant. For flow cytometric analysis, Fc receptor blockade was performed (anti-mouse CD16/CD32, 1:100, #16-0161-85, eBioScience), followed by labelling blood cells, splenic leukocytes or brain cells with cocktails of selected antibodies (Table 5.). Cells were acquired on a BD FACSVerse flow cytometer and data were analysed using FACSuite software (BD Biosciences). Total blood cell counts were calculated by using 15 µm polystyrene microbeads (#18328-5, Polysciences).

Table 5. Antibodies used for flow cytometry.

Antigen	Host species	Dilution	Catalogue number
CD8a-PE	anti-mouse	1:400	#12-0081-82 eBioScience
CD3e-APC	anti-mouse	1:200	#17-0032-80, eBioScience
CD11b-PE	anti-mouse	1:200	#101207, BioLegend
Ly6C-PECy7	anti-mouse	1:400	#25-5932-80, eBioScience
CD115-APC	anti-mouse	1:100	# 17-1152-80, eBioScience
F4/80-like receptor-BV421	anti-mouse	1:200	#563900, BD Biosciences
CD39-PE	anti-mouse	1:100	#143803, BioLegend
CD45-PercyP5.5	anti-mouse	1:200	#103131, BioLegend
Zombie Violet	none	1:200	#423113, BioLegend

Statistical analysis

All quantitative measurements and analysis were performed in a blinded manner in accordance with STAIR and ARRIVE guidelines. Data were analysed using the GraphPad Prism 7.0 software. For comparing two experimental groups Student's *t* test with Welch's correction or Mann–Whitney U test, for comparing three or more groups one-way or two-way ANOVA followed by Tukey's, Sidak's and Dunnett's post hoc comparison was used. $P < 0.05$ was considered statistically significant.

4. Results

4.1. Microglia are essential for anti-viral immunity in the central nervous system

4.1.1. Microglia control the spread of viral infection in the brain

First we wanted to test whether microglia respond to signals originating from virus infected neurons in their vicinity. For this purpose, we made use of the Bartha-DupGreen recombinant strain of Bartha-PRV derivative, which displays precisely controlled, retrograde transsynaptic spread to central autonomic nuclei after uptake by peripheral nerve endings (Fig.1.a,) (Boldogköi et al., 2004). Similar to that seen in previous studies, viral infection reached the hypothalamus across synaptically linked neurons via the sympathetic ganglia, the spinal cord and the medulla (Dénes et al., 2006) 6 days after intraperitoneal (i.p.) virus administration. In line with the appearance of infected neurons in the hypothalamic paraventricular nucleus (PVN), Iba1 positive microglia were recruited around infected neurons (Fig.1.b, c,).

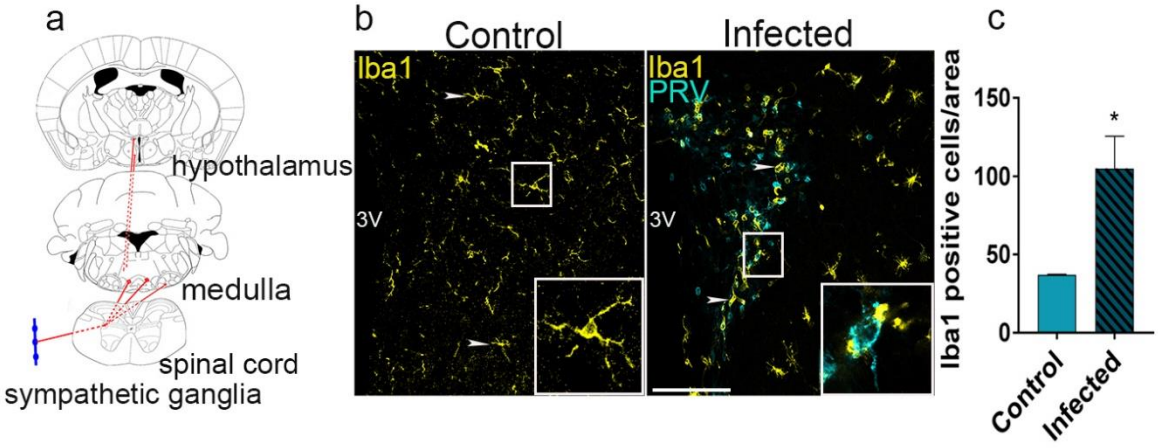

Figure 1. Microglia are recruited to infected neurons in the CNS. a, Retrograde trans-synaptic spread of PRV-Bartha-DupGreen (BDG) to the hypothalamic paraventricular nucleus (PVN) 6 days after injection. **b**, Infected neurons (PRV: cyan blue) induce the recruitment of microglia (Iba1: yellow) in the PVN. **c,** Number of recruited microglia significantly increases at sites of virus-infection, area: 0.2 mm^2 c, *p<0.05 n=4-5 mice/group, Mann-Whitney test. Scale bar on b, 50 µm (Fekete et al. 2018).

4.1.2. Selective elimination of microglia results in uncontrolled viral spread and neurobehavioral pathologies

To investigate the role of microglia in controlling viral infection, we performed selective microglia depletion, by feeding mice a chow diet containing PLX5622, a CSF1 receptor antagonist, as described in previous studies (Szalay et al., 2016). After three weeks of depletion, 96% of microglia were eliminated from the CNS, as shown on Fig.2.a-b.. Selective elimination of microglia led to a significant increase in the number of infected neurons in the whole brain (Fig.2.c-d,). In the absence of microglia, we noticed that the number of PRV-immunopositive neurons and disintegrating neurons also increased three-fold, compared to that seen in the microglia competent infected group (Fig.2.e,). We also observed the emergence of diverse neurological symptoms in microglia depleted infected mice, starting on the 5th day after virus injection. These symptoms included heavy breathing and drooling, seizure-like episodes or muscle spasms, which were completely absent in control mice (Fig.2.f,). This also suggested the importance of microglial control of neurotropic viral infection.

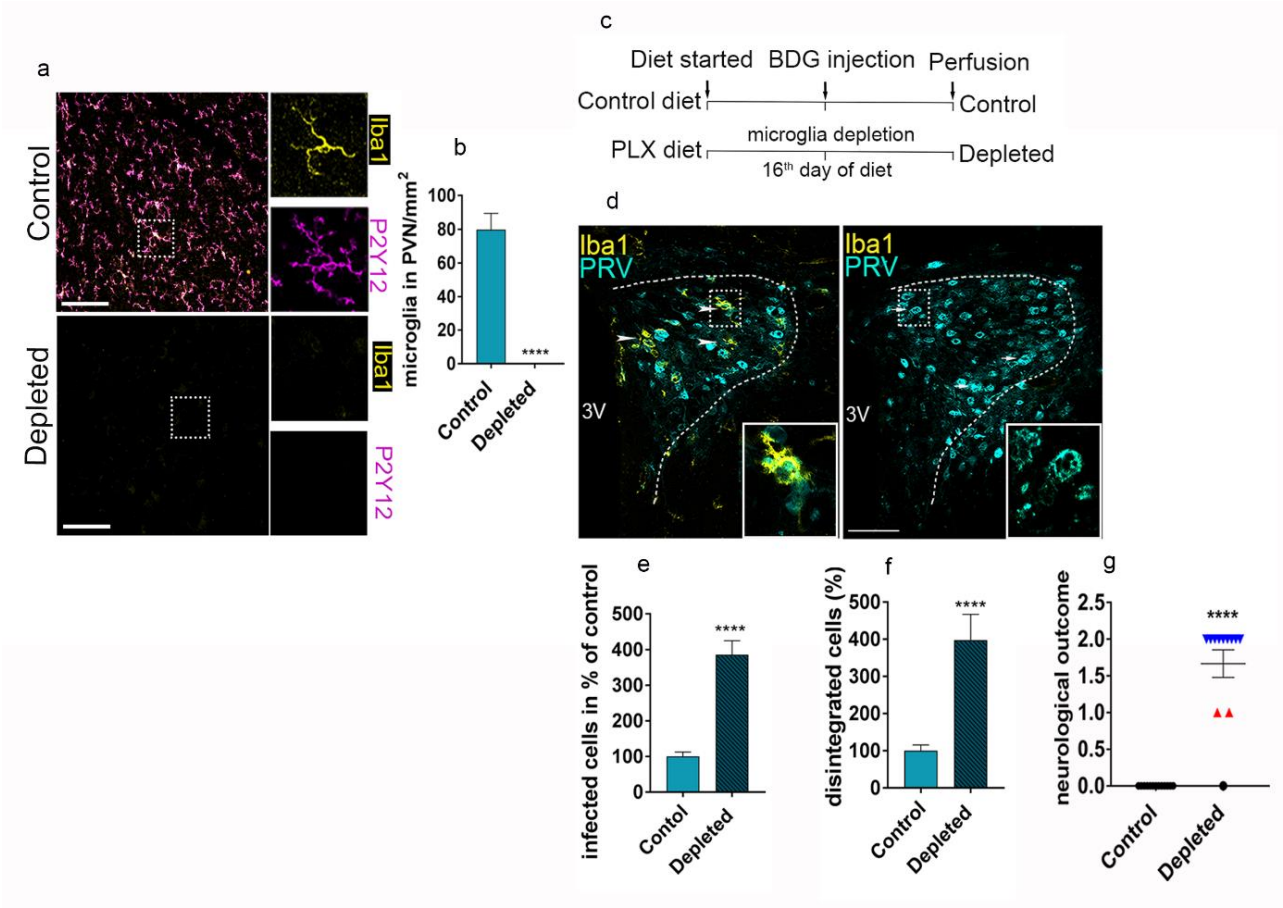

Figure 2. Microglia elimination results in uncontrolled viral infection and pathological behavioural changes. a, Selective depletion of microglia by PLX5622 for 3 weeks (Iba1: yellow; P2Y12: magenta). **b,** The depletion resulted in 96% elimination of microglia. **c,** An absence of microglia results in profound increases in virus-infected neurons in the brain. Control and microglia depleted mice were injected intraperitoneally with BDG on the 16th day of the diet and allowed to survive for 5 days to allow transsynaptic spread of PRV into the hypothalamus. **d,** The number of infected neurons in the PVN increases over twofold in microglia depleted mice 5 days after virus injection. Note that the numerous infected neurons outside the PVN are indicating increases in non-synaptic (contact) infection in the absence of microglia **e,** Absence of microglia leads to the increase of infected neurons in the PVN. **f,** Absence of microglia leads to increased number of disintegrated neurons in the PVN. **g,** Elimination of microglia results in rapidly appearing neurological symptoms 5 days after virus injection. (0: no symptoms, 1: heavy breathing and drooling, 2: muscle spasms and seizures). **b,** ****p <0.0001 unpaired t-test n=6 mice/group, **e, f,** ****p<0.0001 Mann-Whitney test n=10-11 mice/group **g, ****p<0.0001 Mann-Whitney test n=10-11 mice/group. Scale bars: a, 50 µm, d, 100 µm (Fekete et al. 2018).

To test whether the role of microglia in controlling viral infection would depend on the site of virus injection, we injected the viral construct into control and microglia depleted mice intraperitoneally or into the white adipose tissue of the epididymis (an organ receiving primarily sympathetic innervation). The results showed that both after injecting the virus into the epididymal white apidose tissue and i.p., the number of infected neurons were markedly higher in the absence of microglia. (Fig.3.). In these mice, retrograde infection even reached several sensory and motor cortical areas, which were not affected when microglia were present in the brain (Fig.3. left panel).

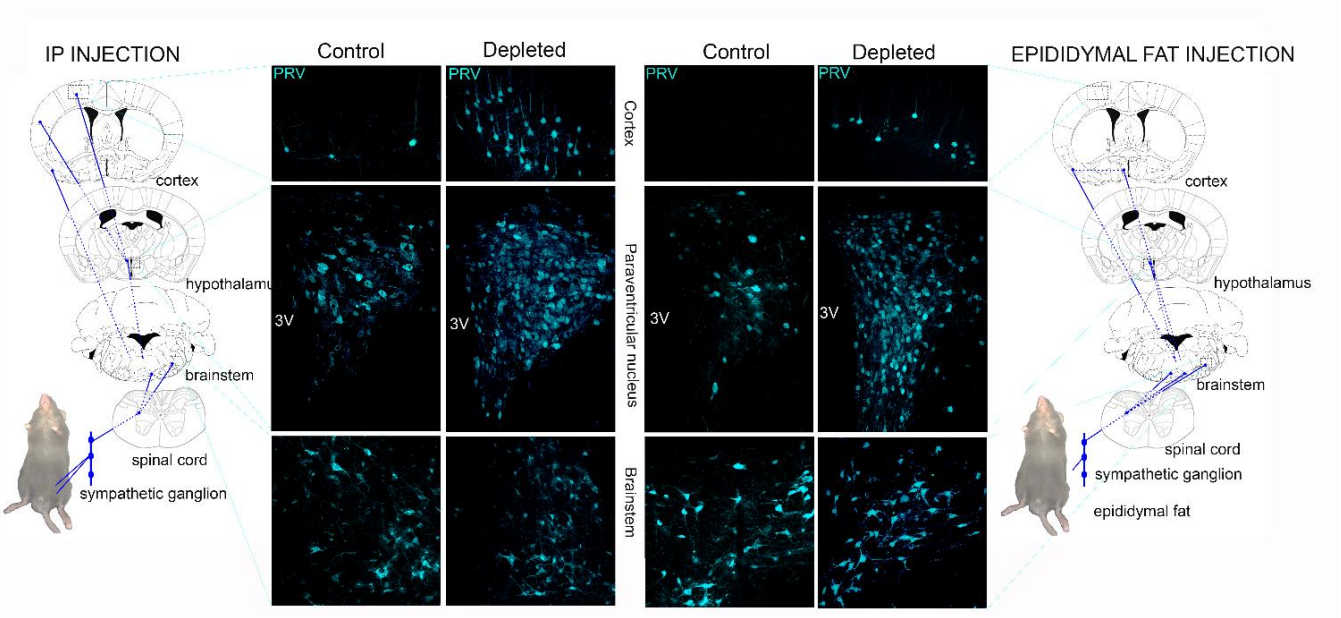

Figure 3. The effect of microglia depletion on the spread of virus infection in the brain. Bartha-DupGreen (BDG) injection into control and microglia depleted mice intraperitoneally (i.p.) (left side) or into the epididymal white adipose tissue (right side) results in infection in similar central autonomic brain areas. In microglia depleted animals number of infected neurons were significantly higher both with i.p. or after epididymal injection. The increased number of infected cells in higher cortical regions indicate that in the absence of microglia infection would not exclusively spread in a transsynaptic manner, but possibly also via released virus capsids leading to contact infection of nearby neurons. Maximum Intensity Projection from confocal Z stack of 5 steps were made with 3,38 µm (cortex), 0,83 µm (PVN), 4,05 µm (brainstem) step size. Scale bars: 50 µm. 3V- third ventricle (Fekete el al. 2018).

4.1.3. Microglia phagocytose infected neurons but are resistant to productive viral infection

To investigate the nanoscale interaction between microglia and infected neurons, we turned to super-resolution microscopy, using the stochastic optical reconstruction microscopy (STORM) technology. To visualize viral proteins phagocytosed by microglia, cell were identified by the microglial phagosome/lysosome marker CD68 (Fig.4.a-b,). In control mice, recruited microglia surrounded the soma of infected neurons tightly and the already phagocytosed neuronal parts containing viral particles were present inside the phagosomes (Fig.4, a, insert). The absence of microglia resulted in increased extracellular viral protein level and PRV-immunopositive cell debris (Fig.4.b,). These results were confirmed with electron microscopy as well, which revealed the direct contact between microglial processes and the membrane of infected neurons, as well as the phagocytosed parts of infected neurons (Fig.4. c-d,). In contrast with control (microglia competent) mice, in microglia-depleted animals we observed disintegrated neuronal membranes and extracellular immunogold labelled viral proteins (Fig.4.e-g,). In line with this, we could not detect any immediate early GFP signal, which is expressed by BDG or any PRV-immunopositive viral capsids neither in the cytoplasm, nor in the nucleus of microglia (Fig.4.h,j,). Thus, while in some cases neurotropic viruses can cause productive infection in myeloid cells (Wheeler, Sariol, Meyerholz, & Perlman, 2018a), we show that the attenuated PRV strains used in this study do not develop productive infection in microglia.

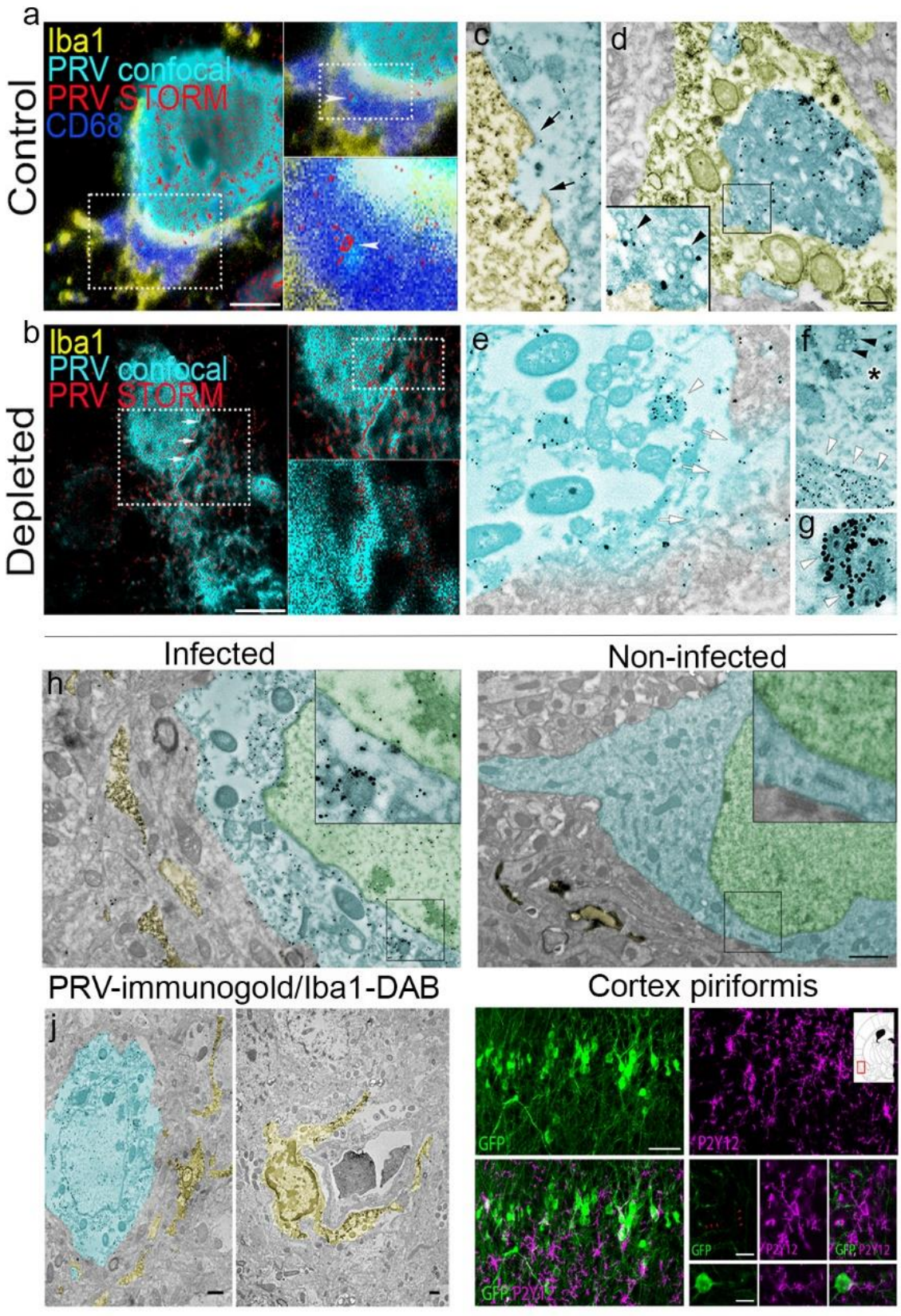
a
Control
Iba1
PRV confocal
PRV STORM
CD68
c
d
b
Depleted
Iba1
PRV confocal
PRV STORM
e
f
*
g
Infected
Non-infected
h
PRV-immunogold/Iba1-DAB
j
Cortex piriformis
GFP
P2Y12
GFP,P2Y12

Figure 4. The presence of extracellular viral structural proteins increases in the absence of microglia. a, STORM super-resolution microscopy reveals co-localisation of phagocytosed infected neuronal debris with CD68-positive phagosomes (dark blue) inside recruited Iba1 positive (yellow) microglia. **b,** Microglia depletion leads to massive increase in extracellular virus proteins around infected and disintegrated neurons. **c,** Microglial process (yellow pseudocolor) tightly surrounds infected neuronal cell membrane (cyan pseudocolor). **d,** Infected neuronal debris containing viral capsids labelled with PRV-immunogold (black arrows on insert) completely phagocytosed by microglia. **e,** In the absence of microglia anti-PRV immunogold labelled virus capsids invade the extracellular space from disintegrating neurons. **f,** Infected neuron containing virus capsids (black arrowheads; black asterisk marks the nucleus), white arrowheads mark mature virions labelled with strong PRV-immunogold in the cytoplasm. **g,** PRV-virions are visualized at higher magnifications. **h,** Transmission electron microscopic (TEM) pictures show the presence of PRV-immunolabelling inside an infected cell and the complete absence in control tissue. Microglial processes (yellow pseudocolour) can be seen close to the neuron (cytoplasm: blue, nucleus: green pseudocolour). In the infected neuron high level of PRV-immunogold (black grains) can be seen, which are linked to viral capsids and mature virions (insert). In control neuron no PRV-labelling could be detected, which confirms the specificity of the antibody. **j,** TEM pictures show that DAB-positive microglia (yellow pseudocolour) show the complete absence of viral capsids, and anti-PRV immunogold labelling. This was further confirmed with confocal microscopy (second panel), where, contrary to infected neurons, immediate-early GFP signal is absent in microglia (magenta). Scale bars: a, b, 100 μm, d, e, f, 400 nm, g, 175 nm, h-j, 1 μm, on confocal panels: 50 μm and 10 μm (Fekete et al. 2018).

4.2. Microglia recruitment is initiated rapidly to virus-infected neurons in the brain

4.2.1. Microglia are recruited to infected neurons within hours as suggested by differential expression of viral immediate-early and structural proteins

After showing that microglia are instrumental for the control of neurotropic viral infection in the CNS, we aimed to investigate whether microglial recruitment occurs early enough to allow the isolation of infected neurons before the breakdown of neuronal cell membranes. For this purpose we used the immediate-early GFP marker, which is expressed by infected neurons prior to the production of viral proteins (Fig.5. a, b,). This feature of the virus allowed us to time-map the different infection phases at single neuron level (Boldogkői et al. 2004; Dénes et al. 2006). Early infected cells are only GFP-positive, then parallel with the decrease of immediate-early GFP signal, viral structural proteins start to accumulate in the cytoplasm of the infected neurons. This transition occurs in a few hours based on our earlier studies (Boldogkői et al. 2004; Dénes et al. 2006). In fact, neurons expressing only GFP (Phase I) were only occasionally surrounded by microglia, while cells with low levels of GFP and detectable levels of viral structural (PRV) proteins were already surrounded by microglia (Fig 5. a, Phase II). In Phase III cells, only viral protein signal could be detected in neuronal

cytoplasm, which paralleled increases in the number of microglia around them, resulting in an average of 1-3 microglial cells contacting the soma of infected neurons (Fig 5. a, Phase III).

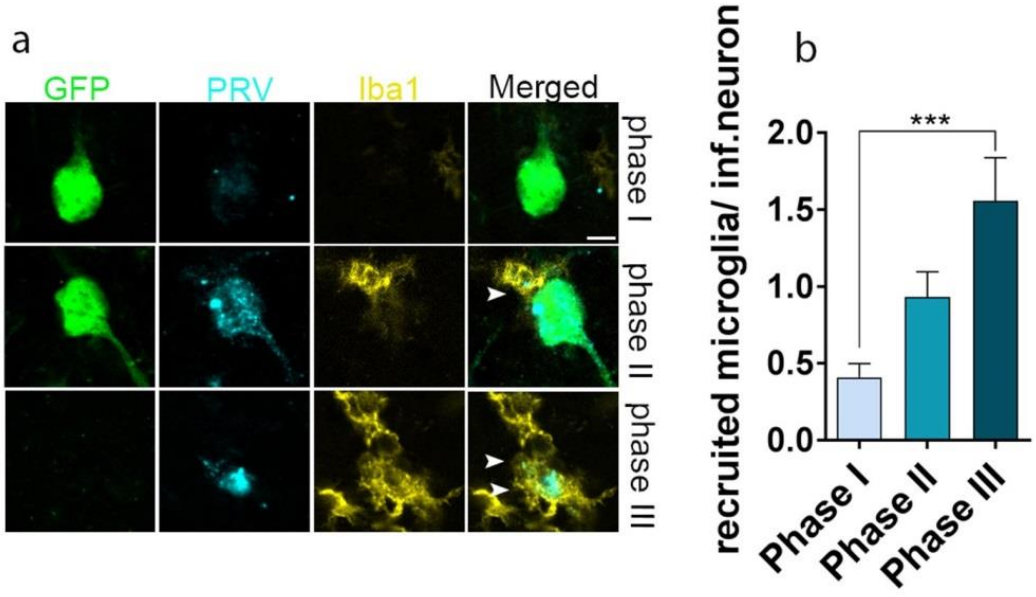

Figure 5. Microglia rapidly isolate virus-infected neurons in the brain. a, Iba1 positive microglia (yellow) recruited to PRV-infected neurons that express GFP with immediate-early kinetics (BDG) in the hypothalamic paraventricular nucleus (PVN). Note that microglia recruitment starts after the expression of immediate-early marker GFP (phase I), when low levels of viral structural proteins become detectable (phase II). High levels of viral structural proteins indicate a late stage of viral infection (phase III), which is associated with higher number of microglia recruited to infected cells **b,** Parallel with the propagation of virus infection number of recruited microglia increases significantly. Data are expressed as mean **±** s.e.m. **b,** ***p<0.001 one-way ANOVA, n=8 infected neurons/group Scale bar: a, 10 µm (Fekete et al. 2018).

4.2.2. Imaging microglia recruitment with in vivo two-photon microscopy in real-time

To be able to observe microglia recruitment in real-time, we used *in vivo* two-photon microscopy. Since microglia are very sensitive to any disturbances in the brain (Davalos et al., 2005a), we first optimized our surgical procedure to avoid the activation of microglia due to cranial window preparation. To this end, prior to two-photon imaging we thinned the skull bone of $Cx3Cr1^{+/GFP}$ reporter mice, and the following day we imaged microglial processes (Fig6. a,). We found that in case the dura mater remains intact upon craniotomy, microglial processes remain in normal homeostatic condition, comparable to that seen when imaging through thinned skull bone, which did not allow appropriate resolution and depth to be achieved. In response to injury to the dura, microglia activated rapidly, leading to thickening

and withdrawal of their motile processes (Fig6.a, right panel). Thus, during the in vivo imaging studies the dura mater was always kept intact and the removed skull bone was replaced by glass coverslip to achieve appropriate resolution at the level of layer 2/3 neurons and to monitor microglial processes in real-time. To co-detect viral infected neurons with microglia, we used PRV-Bartha-DupDSRed (BDR) virus, allowing us to recognize early phases of the infection based on the production of the red fluorescent protein DSRed (Boldogkői et al., 2009). To investigate microglia recruitment, $Cx3Cr1^{+/GFP}$ microglia reporter mice were infected with BDR and were allowed to survive for 7 days, resulting in virus infection in upper layers of the cerebral cortex. With *in vivo* two-photon imaging, we were able to see the recruitment of GFP+ microglial processes, in parallel with the increase of DSRed signal in infected neurons within 3 hours (Fig.6.b,). 3D reconstructions of *in vivo* imaging revealed that microglial processes form a barrier-like structure, establishing several direct contact points with the infected neuronal soma (Fig.6.c,). Recruited microglia also showed increased velocity of process motility in response to local signals induced by infected neurons (Fig.6.d,).

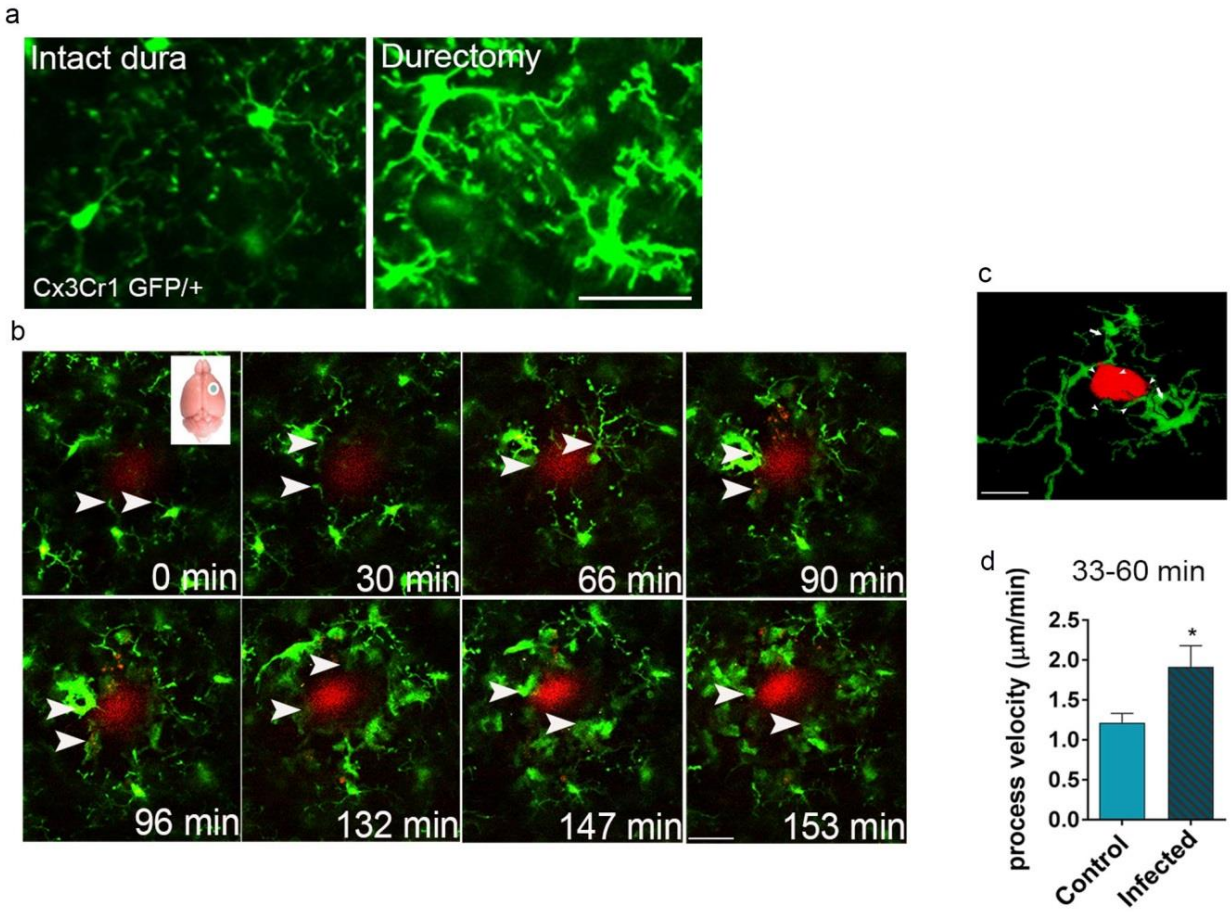

Figure 6. Microglia form barrier around infected neuron. a, Thinned skull bone with intact dura mater revealed ramified microglia with *in vivo* two-photon imaging, however following durectomy microglia activated rapidly (images from, Szalaey et al. 2016). **b,** *In vivo* two-photon imaging reveals microglial (green) recruitment to virus-infected neuron (red) in real time. Retrograde, transsynaptic infection was induced by BDR-injection in Cx3Cr1 $^{+/GFP}$ microglia reporter mice, 7 days prior to imaging. The infected neuron could be visualized in cerebral cortex via immediate-early DSRed expression. **c,** Merged Z-planes of microglial cells around PRV-DSRed-positive neuron and recruited microglial cells (white arrows indicate recruited microglia, arrowheads show contact sites of microglial processes on the infected neuron soma). **d,** The velocity of recruited microglial processes increases significantly in response to viral infection compared to control microglia. d, *p<0.05, unpaired t test, n=10 microglia. Scale bars: a, 50 µm, b-c, 20 µm. (Szalay et al. 2016 ; Fekete et al.2018).

4.2.3. Neurons are directly contacted by microglia at the early phase of virus infection

To further explore, whether microglia form direct contact with infected neurons in early phases of infection, we performed a correlated study using confocal microscopy, electron microscopy and electron tomography. For this purpose, we made use of $Cx3Cr1^{+/GFP}$ microglia reporter mice, and visualized microglia-neuron contact with confocal microscopy. 3D reconstruction of confocal Z stacks revealed microglial contact formation with infected neuronal soma and main dendrites prior to the appearance of mature virions in the cytoplasm (Fig.7.a,). The surrounding processes of microglia showed CD68-immunopositivity, indicating phagocytic activity (Fig.7.a,). It is important to note that we did not detect any viral capsids outside of phagosomes in microglial cytoplasm in any phase of viral infection (Fig.4.d; Fig.7.b-c,). Correlated electron tomography revealed the formation of specific membrane-to-membrane interactions between microglial processes and infected neuronal soma suggesting the early recognition and contact with the intact cell membranes (Fig.7.d,). We also showed on transmission electron microscopic pictures that in early phase of infection neuronal membranes are still intact with normal chromatin structure (Fig.7.e,). From these data we can conclude that microglial processes are able to sense even the early phase of infection in these neurons, and form direct contact with them (Fig.7.e, middle and last panels).

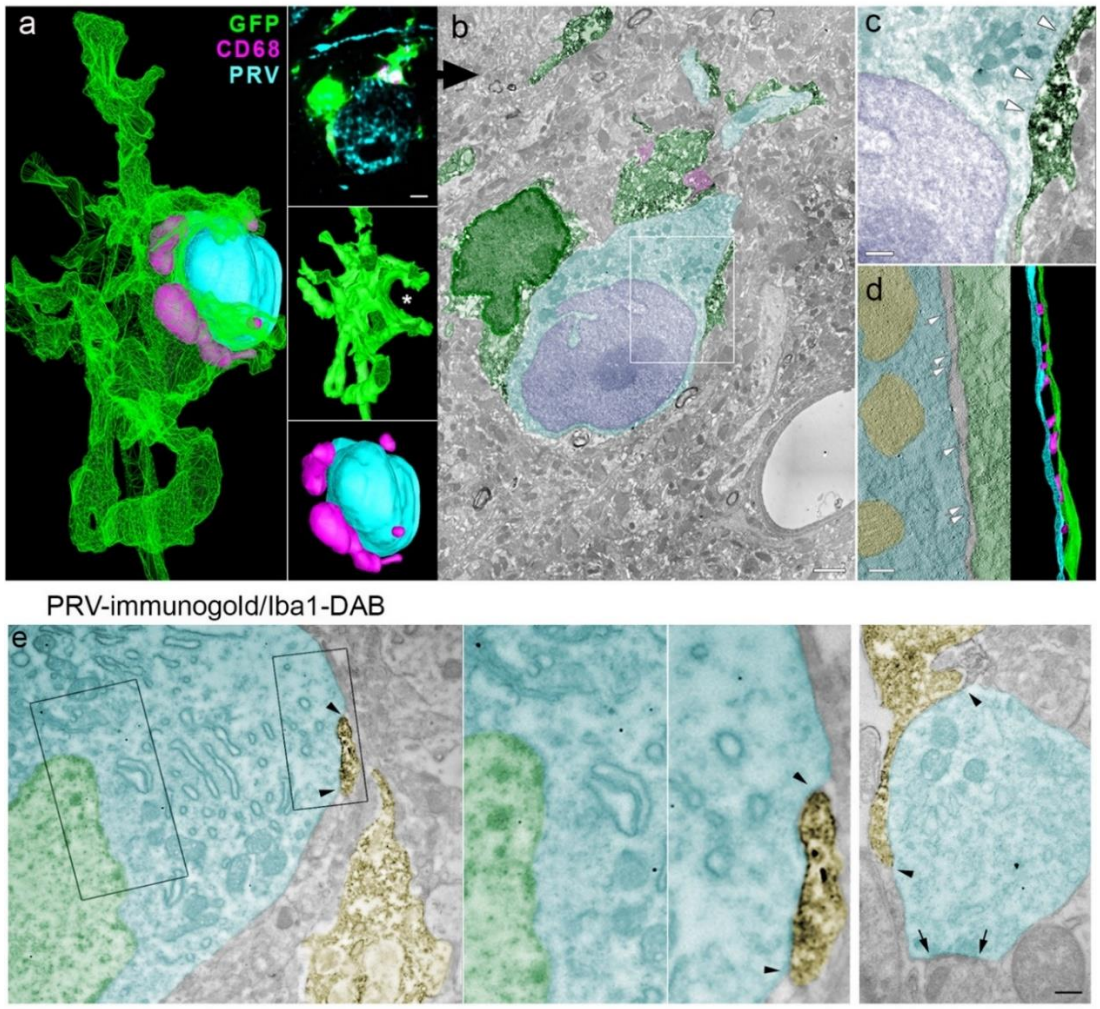

Figure 7. Correlated study confirms direct microglia-neuron contact in the early phase of virus infection. a, 3D reconstruction made from deconvolved confocal Z stack uncovers CD68-positive (magenta) phagosomes inside recruited microglia (green) engulfing PRV-positive infected neuronal soma (cyan). **Upper insert:** single image plane of the same confocal stack. **Middle insert:** 3D reconstruction of the same microglial cell, rotated 180^{o} around vertical axis. White asterisk labels the place of phagocytosed soma of infected neuron. **Lower insert:** 3D reconstruction of PRV-positive infected neuronal cell body surrounded with phagosomes located inside microglia. **b,** Transmission electron micrograph shows the same cells on an ultrathin section matching the confocal image plane in the upper insert in a,. **c,** Enlarged insert from panel b, (white box). Intact neuronal membrane is confirming the early phase of infection. Note that the nucleus is loaded with viral capsids. **d,** Electron tomographic image of a 3nm thick section and corresponding 3D reconstruction show direct membrane contact points between microglia (green pseudocolour) and infected neuronal cell membrane (cyan pseudocolor). White arrowheads point to putative contact sites, where the distance of the two membranes are the smallest and several filament-like structures can be observed connecting the two cells. **e,** TEM images show that microglial processes (dark DAB-precipitate, yellow pseudocolour) find and contact infected neurons even at the early phase of the infection, when only low levels of anti-PRV immunogold labelling can be detected (cytoplasm: cyan pseudocolour, nucleus: green pesudocolour). Black arrowheads point to microglial process contacting infected neuronal membrane. Black arrows point to a synapse of an infected neuronal dendrite. Scale bars: a, 2 µm, b, 1 µm, c, 400 nm, d, 100 nm, e, 50 µm (Fekete et al. 2018).

4.3. Virus infection triggers the recruitment and phagocytic activity of microglia *in vitro*

4.3.1. Microglial responses to infection in vitro

We aimed to uncover the mechanisms of microglia recruitment to sites of virus infection, so we established *in vitro* co-cultures of neurons and GFP^{+} microglia from Cx3Cr1$^{+/GFP}$ mice and performed 48 hour long time-lapse imaging. In control cultures, microglia scanned and frequently contacted the cell body and main dendrites of healthy neurons, but did not cause any injury or showed phagocytic activity (Fig.8.a, upper panel). Opposing this, microglia added to virus infected neuronal cultures displayed rapid recruitment and phagocytic activity (Fig.8.a, lower panel).

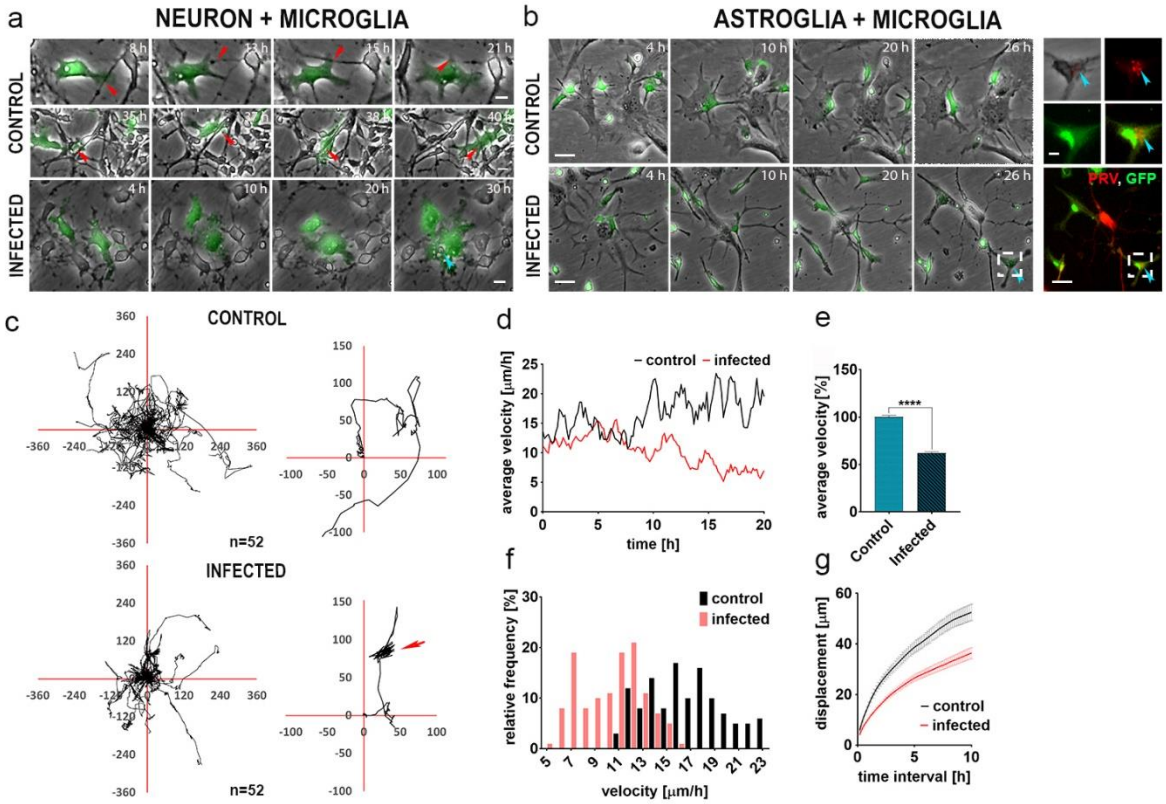

Figure 8. Microglia are recruited rapidly and phagocytose virus-infected cells *in vitro*. a, $Cx3Cr1^{+/GFP}$ microglia (green) frequently scan non-infected neuronal processes and cell bodies without hindering process outgrowth or affecting network stability. Red arrowhead points to an uninterruptedly growing neurite (upper panel), and microglia scanning and slipping under dense neuronal network (middle panel). In PRV-infected neuronal cultures microglia acquire an amoeboid shape and phagocytose compromised cells (bottom panel, cyan blue arrow). **b,** $Cx3Cr1^{+/GFP}$ microglia (green) move freely and monitor healthy astrocytes contacting them regularly (upper panel). In virus infected cultures microglia recruit rapidly to infected astrocytes and display phagocytic activity (lower panel). Satellite images: PRV-immunopositive cell particles (red) eaten up by a $Cx3Cr1^{+/GFP}$ microglial cell (green) **c,** Individual trajectories of randomly selected microglial cells are displayed after 24 hours in control and infected astroglial cultures. Individual cell trajectories were positioned to start from the origo and superimposed for better comparison of migration directionality. Insets show control, random walk behaviour (upper inset), and shorter, targeted directionality (red arrow) of phagocytic microglia (lower inset). **d,** Microglial average time-dependent velocity in control and infected astroglial cultures. **e,** Average velocity of microglia decreases markedly in infected cell cultures over 24 hours. **f,** Frequency distribution of time-dependent average velocities of microglia cells in control and infected astroglial cultures. **g,** Average displacement of microglia in various time intervals of migration in control and infected astroglial cultures. Error stripes correspond to s.e.m. Scale bars: a, 10µm; b, 25µm and 10µm, respectively. Data are expressed as mean± s.e.m. **e,** g=121 cells, unpaired t-test, ****$p<0.0001$. (Fekete et al. 2018).

4.3.2. Microglia phagocytose infected cells in vitro

Next, we wanted to study microglial behaviour more precisely, which required more sparsely distributed cell cultures. Since this was not feasible with neuronal cultures, we took advantage of that astrocytes are also infected with PRV under *in vitro* conditions (Gönci et al., 2010). In fact, in sparse astrocyte cultures microglia migrated much longer distances on average to reach infected cells. Statistical analysis of longer cell trajectories enabled us to more effectively separate random migration from targeted movement of microglial cells to infected astrocytes, followed by localized scanning activity and phagocytosis (Fig.8.b,). As we previously detected in neuronal cultures, microglia recognised and phagocytosed infected astrocytes, which was also confirmed with immunofluorescent detection of phagocytosed cell particles (Fig.8.b, bottom panel and insert). This was also evidenced by individual microglia trajectories showing characteristic localized patterns as microglia tended to remain longer at sites of virus infected cells (Fig.8.c,), which was in sharp contrast with microglia trajectories in uninfected cultures showing random walk behaviour pattern. We associated this phenomenon with the reduction of cell velocities in infected cultures (16.6±3.2 µm/h in control and 10.3±2.6 µm/h) in infected cultures, Fig.8.d-g,) suggesting that signals from

infected cells direct microglial migration, scanning behaviour and phagocytosis. Importantly, the development of productive infection was never observed in microglia neither *in vivo nor in vitro* even after the direct exposure of cells to high viral titers or following phagocytic activity, as evidenced by the absence of the immediate-early GFP signal and PRV proteins in microglial cells outside phagosomes (Fig. 4. h, j, Fig.9.).

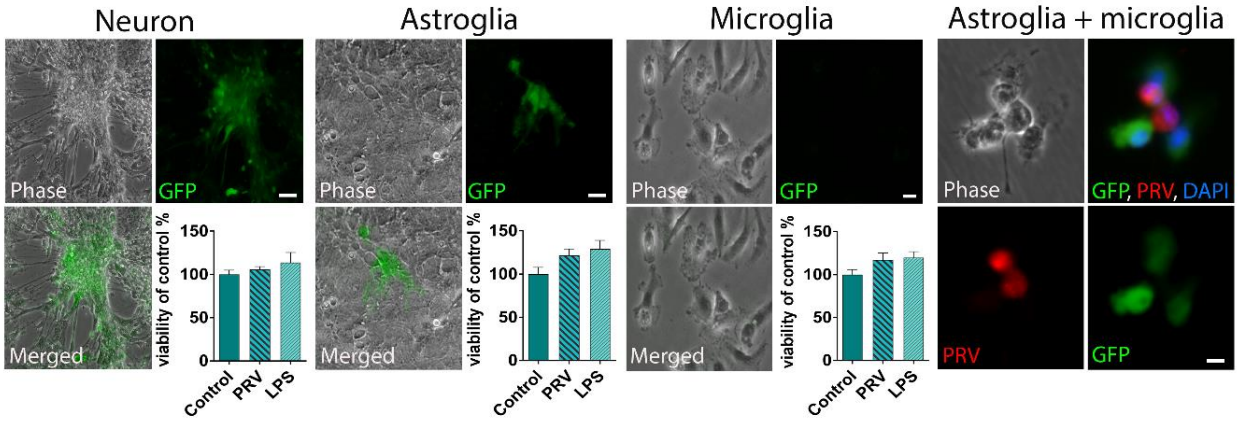

Figure 9. BDG does not induce productive infection in microglial cells *in vitro*. In primary neuronal, astroglia and microglia cultures (bottom panel) infection with Bartha-DupGreen (BDG) was induced 24 hours prior to the assessment of infection-induced GFP expression or the cell viability (MTT) assay. It is important to note that in microglia cultures productive infection could not be detected, whereas in neuronal and astrocyte cultures GFP signal was visible. The viability of microglia, astrocytes and neurons is not reduced by virus infection or treatment with lipopolysaccharide (LPS). Data are expressed as mean ± s.e.m. Scale bars: 50 μm, 15 μm (Fekete et al. 2018).

4.4. Nucleotides released from infected cells trigger microglia recruitment and phagocytosis via microglial P2Y12 receptors

4.4.1. Neurotropic virus infection induces the production of inflammatory mediators

Next, we aimed to investigate the production of inflammatory mediators induced by neurotropic virus infection, therefore we measured several inflammatory cytokines and chemokines that are commonly upregulated in response to virus infection in neuronal and astroglial cell cultures (Lokensgard, Cheeran, Hu, Gekker, & Peterson, 2002). As a positive control, we used bacterial lipopolysaccharide (LPS), which is a widely used pro-inflammatory stimulus. LPS treatment induced a robust increase of TNFα, IL-6, CXCL1, CCL5 (RANTES), G-CSF and MCP-1 in astrocytes and CCL5, MCP-1 and CXCL1 increase in neurons.

However, we noticed that PRV infection increased only CCL5 levels in both cell types at mRNA and peptide levels 24 hours after infection (Fig.10.).

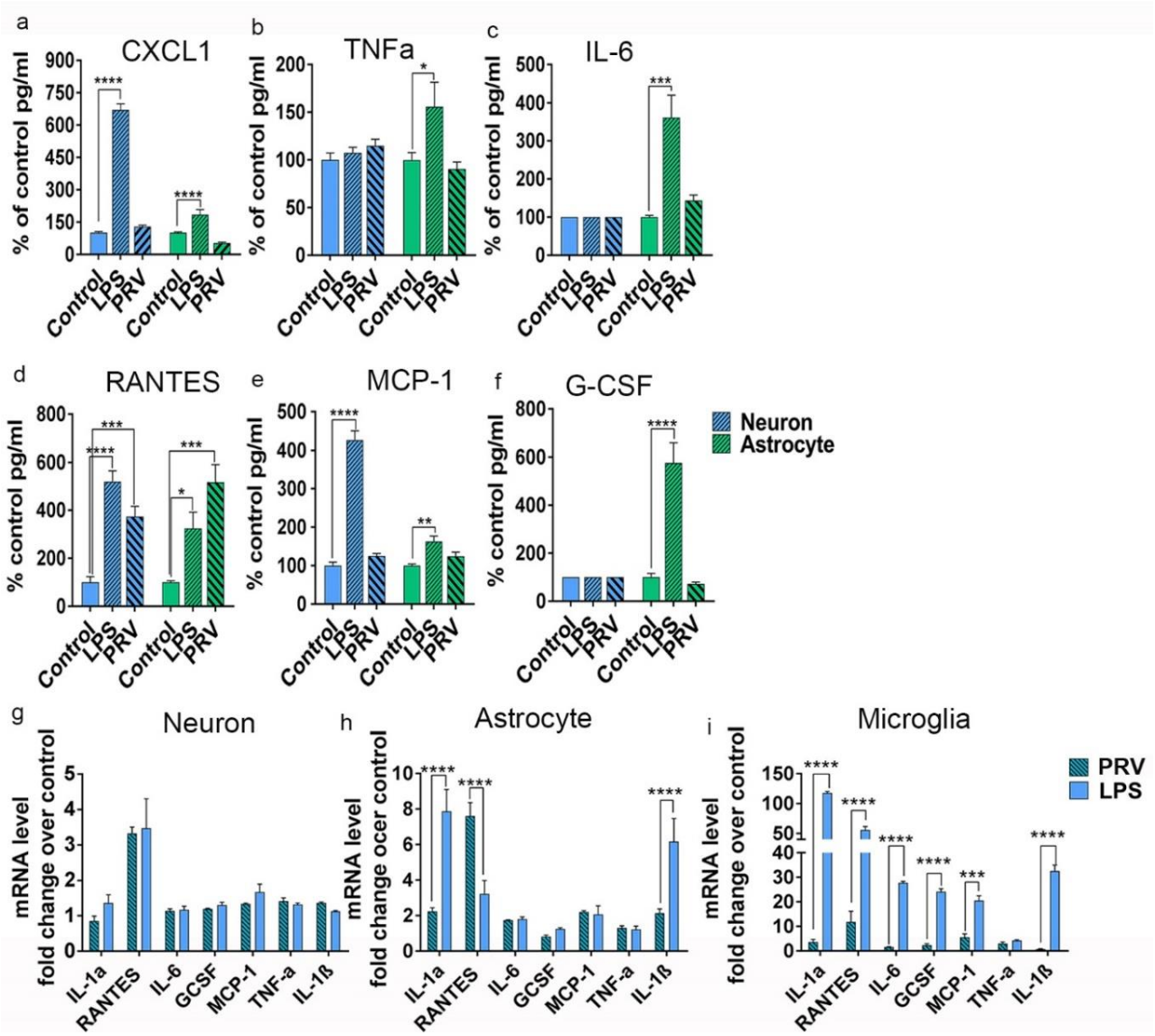

Figure 10. In response to viral infection inflammatory cytokines and chemokines are produced by astroglia, microglia and neuronal cell cultures *in vitro*. a-i, Cytokine levels were measured 24 hours after PRV infection from conditioned medium of astroglial and neuronal cultures by cytometric bead array (CBA). As a positive control, LPS treatment was induced parallel with virus infection. For qPCR measurement cell homogenates were collected as well. **a-f,** one-way ANOVA, followed by Tukey's post hoc test. **a**,****p<0.0001 Cont vs LPS; **b,** *p<0.05 Cont vs LPS; **c,** ***p<0.001 Cont vs LPS; **d,** ****p<0.0001 Cont vs LPS, ***P<0.001 Cont vs LPS, Cont vs PRV, *p<0.05 Cont vs LPS; **e,** ****p<0.0001 Cont vs LPS, **p<0.01 Cont vs LPS; **f,** ****p<0.0001 Cont vs LPS; **g-i,** two-way ANOVA followed by Sidak's multiple comparisons test; **h,** ****p<0.0001 BDG vs LPS; **i,** ****p<0.0001 BDG vs LPS, ***p<0.001 BDG vs LPS (Fekete et al. 2018).

4.4.2. <u>Release of purinergic nucleotides triggers rapid microglia activation</u>

Since synthesis and release of chemokines could last for several hours and our *in vivo* data suggested rapid microglia recruitment to sites of virus infection, we checked whether purine nucleotides such as ATP that are chemotactic for microglia could be released from infected cells at a short time scale (Davalos et al., 2005a). We found that cultured neurons released ATP after virus infection, which was associated with reduced ATP, ADP, AMP and adenosine levels in cell lysates within hours (Fig.11.a,b,) upon the expression of the immediate-early marker GFP, which precedes the expression of viral structural proteins required for productive infection (Dénes et al., 2006). The changes in purinergic metabolites were associated with increased ecto-ATPase levels in infected cells (Fig.11.c,) but were not due to apoptosis or necrosis, since at the early stages of infection neurons expressing high levels of GFP showed no uptake of propidium iodide (PI) (Fig.11.g,h,). In addition, increased ecto-ATPase levels and NTDPase1 expression were found in microglia at sites of virus infection in the brain, indicating that microglia respond to changes in the levels of purine nucleotides (Fig.11,d,e,) (Sperlágh & Illes, 2007).

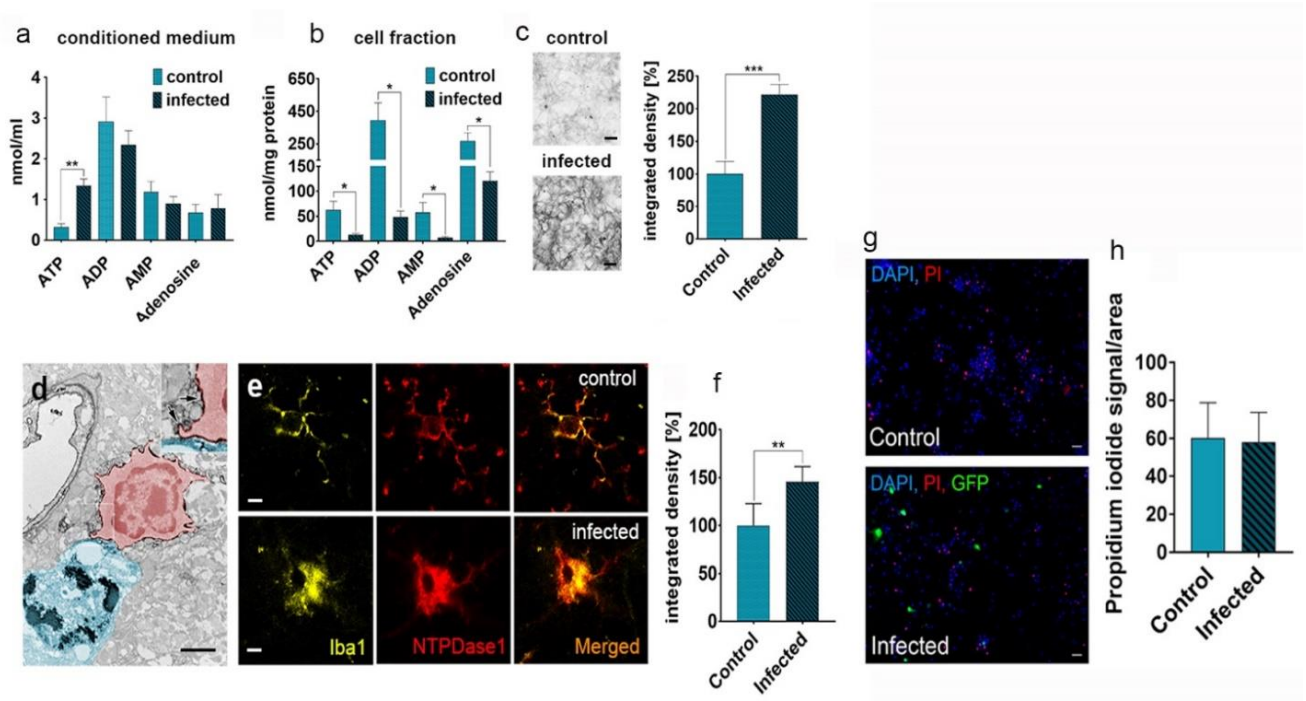

Figure 11. Microglia react to nucleotides released upon viral infection. a, and **b,** graphs show that ATP, ADP, AMP and adenosine levels were measured with HPLC analysis in the supernatant (a) and in cellular fractions (b) of control and virus-infected neuronal cell cultures . **c,** Enzyme histochemistry and densitometric analysis of ecto-ATPase show that the enzyme activity increased markedly upon infection. **d,** Electron microscopic image shows NTDPase1 expression of microglia (red) in PRV-infected brain. NTDPase1^{+} microglia is in contact with a disintegrating PRV-immunopositive neuron (blue). **e,** NTDPase1^{+} microglia in control and infected brains. **f,** Densitometric analysis of NTDPase1 enzyme, measured from control and infected mouse brains. **g, h,** Propidium iodide (PI, red), was used as viability marker to show that neuronal death in cell cultures was not increased 16 hours after infection. All data are expressed as mean ± s.e.m **a-b,** n=4 cell culture per group, unpaired t-test, *p<0.05; **p<0.001 **c,** n=6 cell culture per group, unpaired t-test, ***p≤0.001 **f,** n=7 brain slice per group, unpaired t-test, **p<0.01. Scale bars: c, 25 μm; d, 50 μm; e, 10 μm; g, 50 μm (Fekete et al. 2018).

4.4.3. Microglia recruitment to infected neurons is mediated by P2Y12 receptors in vitro

To further investigate the mechanisms mediating microglial responses to purinergic nucleotides we established co-cultures of P2X7$^{-/-}$ or P2Y12$^{-/-}$ microglia and wild type astrocytes. Similar to that seen in wild type microglia, motility of P2X7 deficient cells decreased when exposed to infected cells (Fig.8.a,b,) and trajectories showed characteristic localized pattern due to regular scanning activity, suggesting that P2X7 deficiency does not impede recognition of virus-infected cells by microglia (Fig.12.e,). In contrast, virus exposed P2Y12$^{-/-}$ deficient microglia showed marked increase in their motility (Fig.12.f-j,) with trajectories characteristic of random walk behaviour and lacking the localized pattern. (Fig.12.k,). This suggests that these cells are unable to display targeted recruitment in response to viral infection. Moreover P2Y12-deficient microglia showed very low phagocytic activity in virus exposed environment, compared to wild type and P2X7$^{-/-}$ microglia that showed marked increase in phagocytosis (Fig.12.l-n,). Thus, P2Y12 is a key contributor in recognition and phagocytosis of compromised cells by microglia *in vitro*.

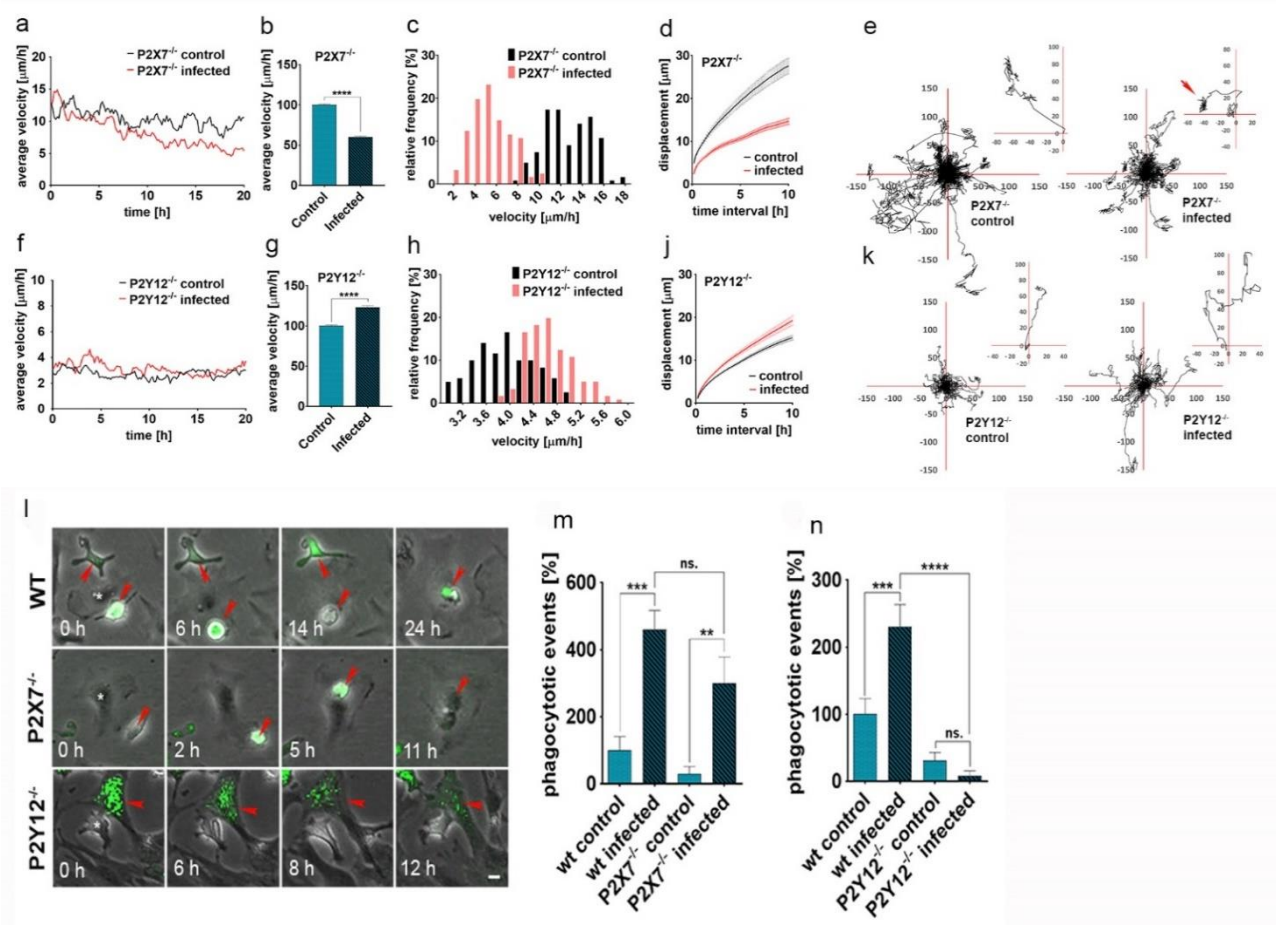

Figure 12. Microglial recruitment and phagocytosis are mediated by purinergic signalling upon virus infection. a, and f, Time-dependent average velocities of P2X7 (n_c=67, n_i=74) and P2Y12 (n_c=51, n_i=59) deficient microglial cells in control and infected astroglia cultures. Decreased velocity of $P2X7^{-/-}$ and the lack of such decrease of $P2Y12^{-/-}$ microglia cells can be detected in infected cultures**. b,** and **g,** Average velocities of $P2X7^{-/-}$ and $P2Y12^{-/-}$ microglia over 24 hours in control and infected astrocyte cultures. **c, and h,** Frequency distribution of time-dependent average velocities of $P2X7^{-/-}$ and $P2Y12^{-/-}$ microglial cells in control and infected astroglial cultures. **d, and j,** Average displacement of P2X7 and P2Y12 deficient microglia in different time intervals of migration in control and infected astroglial cell cultures. Error stripes correspond to s.e.m. **e, and k,** Individual trajectories of equal number (n=50) randomly chosen $P2X7^{-/-}$ and $P2Y12^{-/-}$ microglial cells over 24 hours in control and infected astrocyte cultures. For better comparison of migration directionality individual cell trajectories were centered to start from the origo. $P2X7^{-/-}$ microglia showed more localised migration pattern and scanning activity in infected cultures compared to the random walk behaviour under control condition. $P2Y12^{-/-}$ microglial cells showed the absence of this localised scanning behaviour in their trajectories in infected cultures. **l,** Phagocytic activity of wild type (WT), P2X7 and P2Y12 deficient microglia. Expression of immediate-early GFP marker can be seen in infected astrocytes. Red arrowheads point to phagocytosed, infected cells. **m-n,** Percentage of phagocytic events by wild type, $P2X7^{-/-}$ and $PY12^{-/-}$ microglia. Note that P2Y12 deficient microglial cells are unable to phagocytose infected cells. **b** and **g,** n=121 cell per group, unpaired t-test, ****p<0.0001. **m** and **n,** n=9 cells per group, one-way ANOVA, **p<0.001; *** p<0.0001 **** p<0.0001, ns = not significant (Fekete et al. 2018).

4.5. Microglial P2Y12 receptors mediate recruitment of microglia and elimination of virus infected cells *in vivo*

4.5.1. Microglial P2Y12 receptors form clusters when contacting the cell membranes of infected neurons

Next, we investigated whether nucleotides released from compromised neurons are involved in the recruitment of microglia *in vivo*. We found that all microglia surrounding the soma and the processes of infected neurons in either C57BL/6 or $Cx3Cr1^{+/GFP}$ mice expressed P2Y12 receptors. (Fig.13.a-c,). STORM super-resolution microscopy allowed us to monitor the changes in the localization and amount of P2Y12 receptors at 20 nm lateral resolution. We found that microglial P2Y12 receptors formed clusters at sites, where microglial processes contacted infected neuronal cell bodies directly (Fig.13.d,). Inside clusters, the number of receptors increased two-fold in response to virus infection (Fig.13.f,). However, microglial processes of the same cells, which did not come in contact with infected neurons did not show the clustering of P2Y12 receptors, neither did the receptor numbers increase within the clusters. This suggests that microglial P2Y12 clustering is contact specific around infected neurons (Fig.13.e,g,h,), which may be an integral part of microglial scanning behaviour at microglia-neuron contact sites.

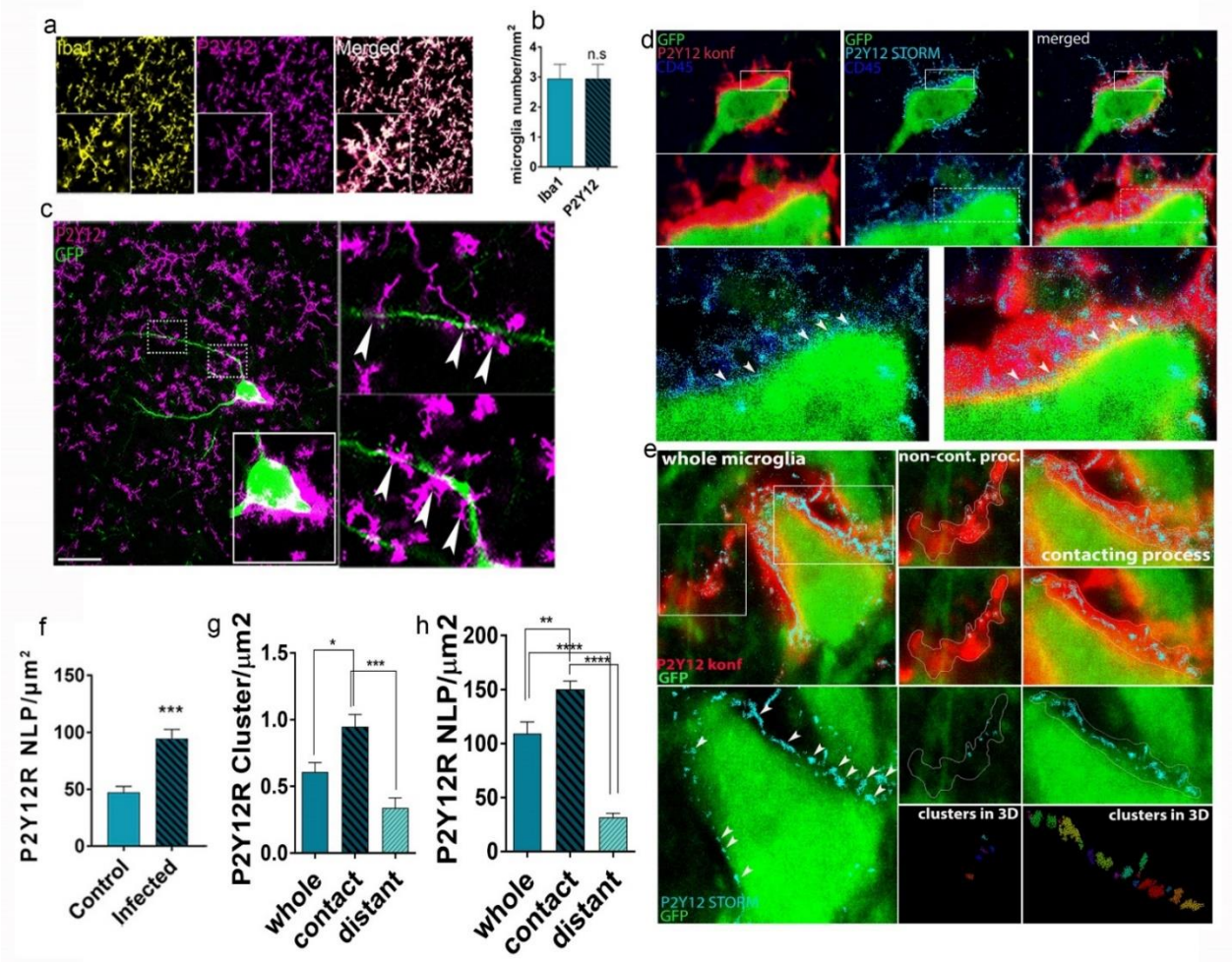

Figure 13. Microglial P2Y12 receptors form clusters when contacting the cell bodies of infected neurons. a, Fluorescent images show that P2Y12 receptors are specifically expressed by microglia in the CNS. Every microglial cell co-expresses the microglia/macrophage marker Iba1 with P2Y12. **b,** Iba1 and P2Y12 markers are expressed by all microglia. **c,** P2Y12-positive microglia are recruited to infected neurons in the brain. Recruited microglia (magenta) contact virus-infected neuronal soma and dendrites (green). **d,** STORM super-resolution images reveal P2Y12 receptors clustering (cyan blue dots) at microglial cell membrane directly contacting infected neurons. Neurons were identified by GFP expression with immediate-early kinetics, indicating early stage of virus infection. **e,** STORM images uncovered that clustering of P2Y12 receptors is associated with formation of physical microglia-neuron contact. On distant microglial processes P2Y12 receptors do not form clusters (middle panel). **f,** Based on the analysis of STORM images, P2Y12 localisation point (NLP) numbers are markedly increased at microglia-neuron contact sites, when microglia are contacting infected neurons compared with microglia touching non-infected cells. **g-h,** STORM analysis of P2Y12 clusters and localisation points (NLP) on whole, contacting and distant microglia membrane surface. All data are expressed as mean ± s.e.m. **b,** ns=not significant; **f, ***p<0.001 unpaired t-test n=7-13 cells per group; **g,** *p<0.05 one-way ANOVA, ***p<0.001 one-way ANOVA; **h,** **p<0.01, ****p<0.0001 one-way ANOVA. Scale bars: a,c, 50 µm, d, e, 100 µm (Fekete et al. 2018).

4.5.2. Microglia recruitment is impaired in the absence of P2Y12 receptors in vivo, but neurological symptoms are not augmented by P2Y12R deficiency

To investigate the contribution of P2Y12 receptor-mediated activities and purinergic signalling of microglia to the defence against viral infections *in vivo*, we induced viral infection in $P2X7^{-/-}$ and $P2Y12^{-/-}$ mice (Fig.14.a,). We found that the lack of P2Y12 resulted in an over 50% reduction of microglia recruitment (Fig.14. e,) to infected neurons in the PVN (Fig.14. b,c, $p<0.05$), whereas the absence of P2X7 receptor showed a non-significant trend in reduction (by 35 %) of recruited microglia compared to wild type mice (Fig14.d,). Similar to what we have seen in microglia-depleted mice (Fig2.d,), the number of infected neurons containing viral structural proteins increased over three-fold in $P2Y12^{-/-}$ mice. In contrast lack of P2X7 receptors did not influence the spread of virus infection in the brain (Fig.14.b,c,). Interestingly, we observed that clusters of microglia at sites of virus infection in $P2Y12^{-/-}$ mice were located in the close vicinity of disintegrated, PRV-immunopositive neurons, suggesting that P2Y12 deficiency markedly impairs microglial responses to signals released from infected neurons and comprises phagocytic responses, but does not fully block microglial migration to already disintegrated cells (Fig.14.d,e,). Despite of the increased number of infected neurons in P2Y12 receptor deficient mice, we did not observe any neurological symptoms, suggesting that the absence of microglia (Fig.2.g,), but not microglial P2Y12 could be responsible for the adverse neurological outcome in this model (Fig.14.f,).

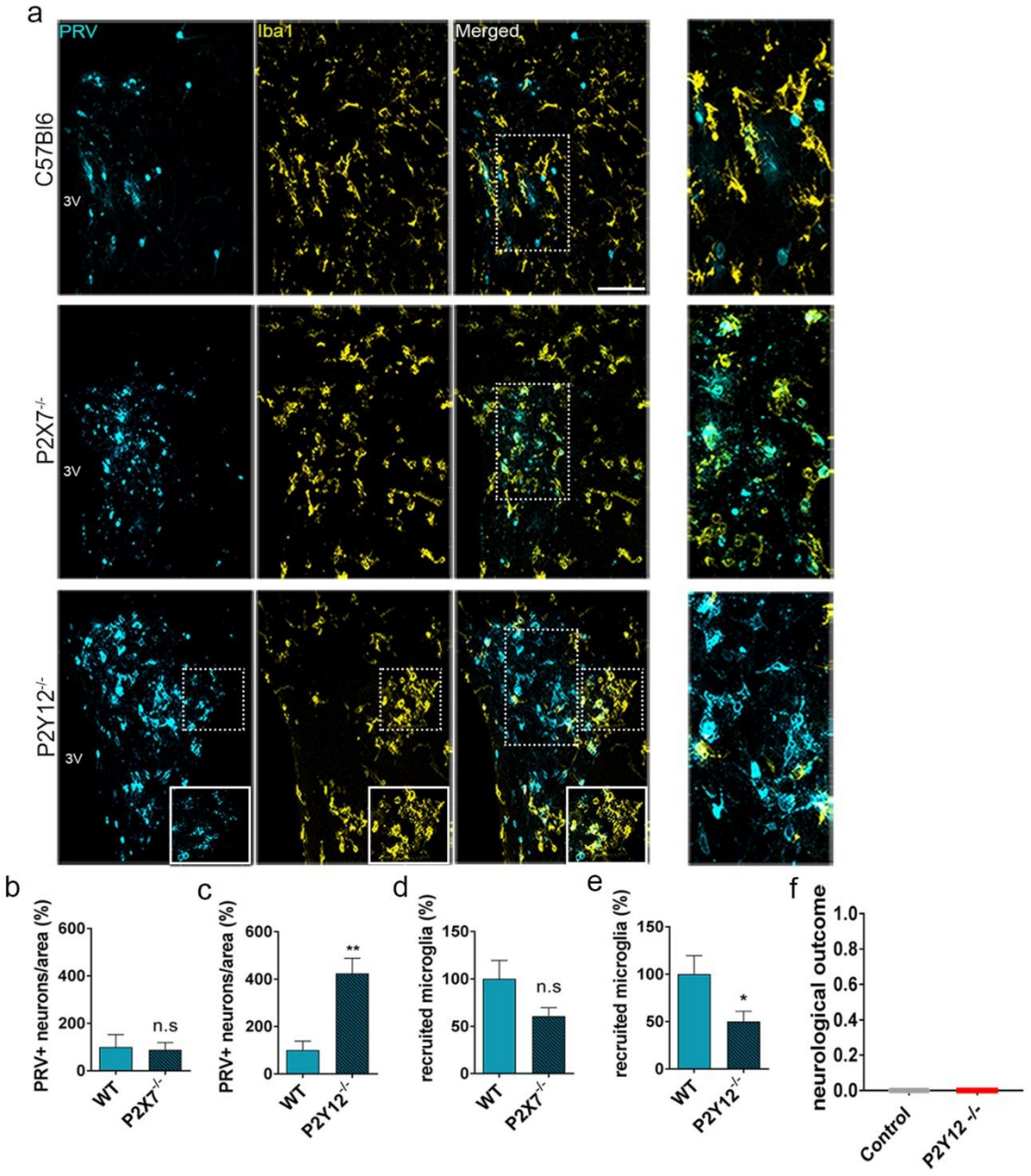

Figure 14. P2Y12 receptor mediates microglial recruitment and phagocytosis in response to virus infection *in vivo*. a, Confocal fluorescent pictures show the spread of infection in the paraventricular nucleus of the hypothalamus in wild type, P2X7$^{-/-}$ and P2Y12$^{-/-}$ mice. Immunostaining against PRV structural proteins (cyan blue) revealed neurons in the late state of the infection and recruited microglia around them, labelled with Iba1 (yellow). **b-c,** In P2Y12$^{-/-}$ animals the numbers of PRV-immunopositive neurons were markedly increased compared to that seen in wild type and P2X7 receptor deficient animals. **d-e,** In P2Y12 deficient mice significantly less microglia were recruited to infected neurons compared to wild type and P2X7 receptor deficient mice. **f,** Lack of P2Y12 receptor did not result in any neurological symptoms 6 days after virus infection. area: 0.2 mm$^{2.}$ 3V - 3rd ventricle. All data are expressed as mean ± s.e.m. **b,d**, n.s=not significant. **c, ****p<0.01 Mann-Whitney test, n=7 animals per group **e,** *p<0.05 n=7 animals per group unpaired t-test. Scale bar: a, 50 µm (Fekete et al. 2018).

To test for the possible mechanisms underlying the controversies concerning the role of microglial P2Y12 in the spread of infection, but a lack of an effect in neurological outcome compared to microglia-depleted mice, we designed a new study, which enabled direct comparison of control, $P2Y12^{-/-}$ and microglia depleted mice after virus infection. In this experiment, we could again confirm our previous results that in $P2Y12^{-/-}$ mice there is deficient recruitment of microglia to infected neurons. As we detected earlier, both the absence of P2Y12 and microglia depletion caused a significant increase in the numbers of virus infected and disintegrated neurons (Fig.15.a-c,). However, the neurological symptoms only emerged in microglia-depleted animals (Fig.15.d,). In contrast, levels of extracellular virus proteins were identical in $P2Y12^{-/-}$ and microglia-depleted mice, while markedly increased compared to control mice (Fig.15.e,f,). $P2Y12^{-/-}$ microglia showed significantly lower levels of CD68-positive phagosomes compared to that seen in control mice, indicating the lack of normal phagocytic activity in the absence of P2Y12 (Fig.15.g,h,).

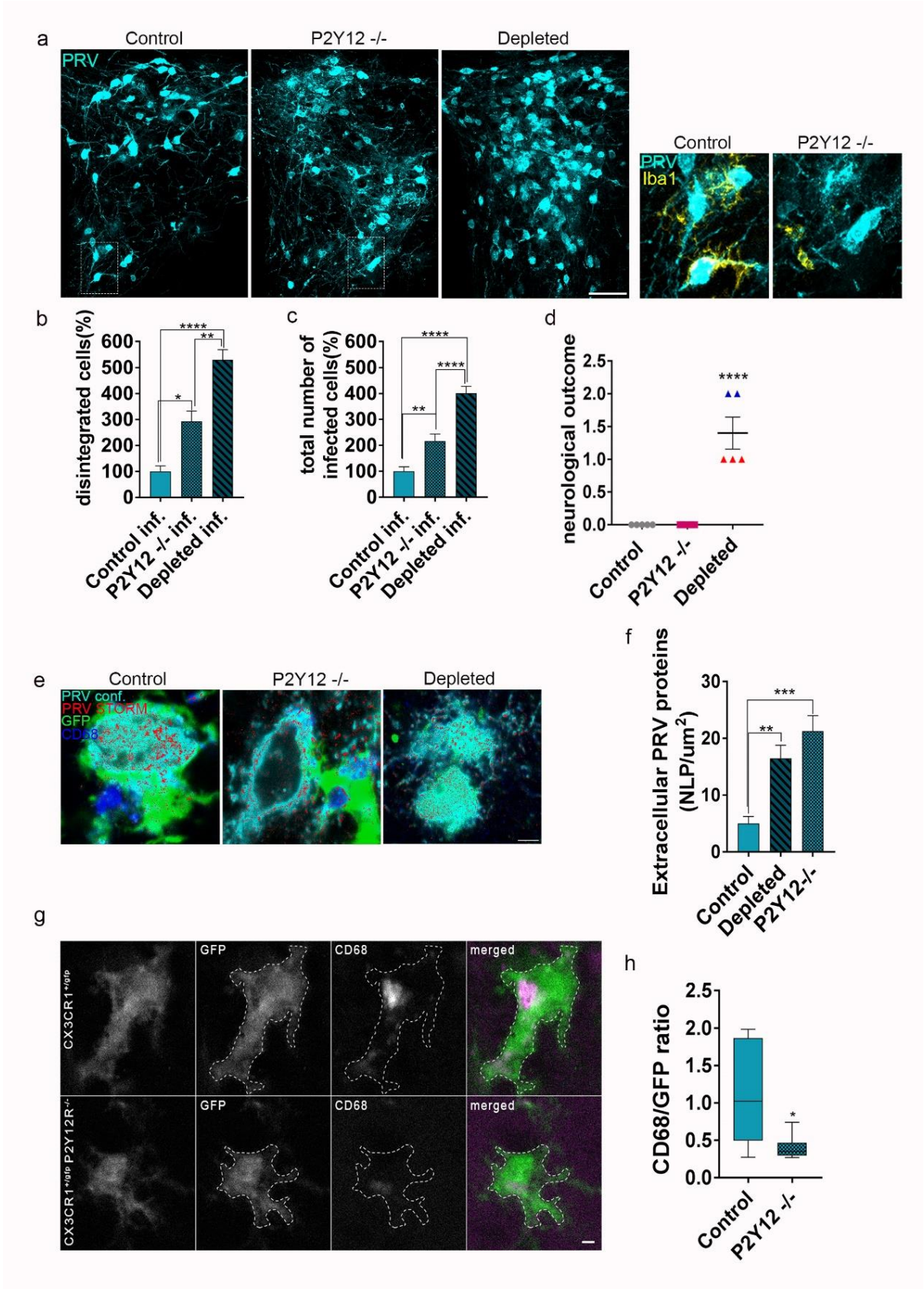
a
Control
P2Y12 -/-
Depleted
PRV
Control
P2Y12 -/-
PRV
Iba1
b
disintegrated cells(%)
600
500
400
300
200
100
0
****
**
*
Control inf.
P2Y12 -/- inf.
Depleted inf.
c
total number of infected cells(%)
600
500
400
300
200
100
0
****
****
**
Control inf.
P2Y12 -/- inf.
Depleted inf.
d
neurological outcome
2.5
2.0
1.5
1.0
0.5
0.0
****
Control
P2Y12 -/-
Depleted
e
Control
P2Y12 -/-
Depleted
PRV conf.
PRV STORM
GFP
CD68
f
Extracellular PRV proteins (NLP/um2)
30
20
10
0
***
**
Control
Depleted
P2Y12-/-
g
GFP
CD68
merged
CX3CR1+/gfp
CX3CR1+/gfp P2Y12R-/-
h
CD68/GFP ratio
2.5
2.0
1.5
1.0
0.5
0.0
*
Control
P2Y12 -/-

Figure 15. P2Y12 deficiency leads to impaired phagocytosis but does not exacerbate neurological symptoms *in vivo*. a, Parallel comparison of PRV-immunopositive neurons in control, P2Y12 deficient and microglia depleted mice. $P2Y12^{-/-}$ phenotype shows lack of microglia (yellow) recruitment to infected neurons (cyan blue) (satellite images). **b,** Highest number of disintegrated neurons were detected in microglia depleted mice, but $P2Y12^{-/-}$ mice also showed a marked increase in disintegrating cells. **c,** Total number of PRV-immunopositive neurons was markedly higher in microglia depleted and P2Y12 deficient animals compared to control group. **d,** Absence of P2Y12 does not cause any neurological symptoms 5 days after virus infection, which could be seen in microglia depleted animals (0: no symptoms, 1: drooling and heavy breathing, 2: seizures and muscle spasms). **e,** STORM super-resolution microscopy reveals elevated levels of extracellular PRV proteins in microglia depleted and P2Y12 deficient mice compared to wild type group. **f,** Quantitative analysis of extracellular level of PRV proteins on STORM images. **g,** In control $Cx3cr1^{+/GFP}$ and P2Y12 deficient ($Cx3cr1^{+/GFP}$ x $P2Y12^{-/-}$) microglia CD68-positive phagosomes (magenta) were visualized. Lack of CD68, can be seen in P2Y12 deficient microglia compared to control cell. **h,** $P2Y12^{-/-}$ microglia show significant decrease of CD68-positive phagosomes compared to wild type microglia (CD68 immunofluorescent integrated density/GFP immunofluorescent integrated density within microglial cell bodies, p=0.0322, Mann-Whitney U-test, n=35 cells/ 16 ROIs). Data on d, expressed as median and interquartile range, otherwise as mean± s.e.m. **b, c, d,** Mann-Whitney U-test, n=5-6 animals per group. Scale bars: a, 100 μm e, and g, 2 μm. All data expressed as mean± s.e.m. **b,** Control vs P2Y12 *p< 0.05; Control vs Depleted ****p<0.0001; P2Y12 vs Depleted **p<0.01, One-Way ANOVA **c,** Control vs P2Y12 **p<0.001; Control vs Depleted ****p<0.0001; P2Y12 vs Depleted ****p<0.0001 One-Way ANOVA **d,** Control vs Depleted ****p<0.0001; P2Y12 vs Depleted ****p<0.0001 One-Way ANOVA **f,** Control vs Depleted p**< 0.01; Control vs P2Y12 ***p< 0.001 One-Way ANOVA (Fekete et al. 2018).

4.6. Microglia recruit leukocytes into the brain upon virus infection independently of P2Y12-mediated signalling

4.6.1.P2Y12-mediated signalling does not affect leukocyte recruitment during viral infection

Previous studies have shown that following virus infection blood-borne cells are recruited into the brain (Rassnick et al., 1998). In light of this information, we wondered whether P2Y12-mediated actions of microglia are involved in neuroinflammatory changes in the present experimental model. As expected, numerous $CD45^{high}$ immunpositive leukocytes were recruited to sites of virus infection (Fig.16.a,). Based on the higher CD45 expression, we could clearly discriminate blood-borne infiltrated leukocytes from microglia. The absence of microglia/macrophage marker Iba1 and microglia specific P2Y12 signal further confirmed this (Fig.16.b,). Next, we investigated whether purinergic signalling via microglial P2Y12 receptors contributes to leukocyte infiltration. Using immunofluorescent labelling, we found that the number of CD45-positive blood-borne leukocytes did not change in P2Y12 deficient mice after infection (Fig.16.c,). With fluorescence-activated cell sorting (FACS) we

characterized recruited leukocyte populations. Most of the infiltrated leukocytes were CD45^{high}, Cx3Cr1^{+}, CD11b^{+}, Ly6C^{high} cells, which markers are characteristic for monocytes (Fig.16.d-e,). Although P2Y12-mediated mechanisms play a major role in controlling the spread of virus infection, we concluded that the absence of P2Y12 does not impair leukocyte infiltration in PRV infected brains (Fig.16. f-g,).

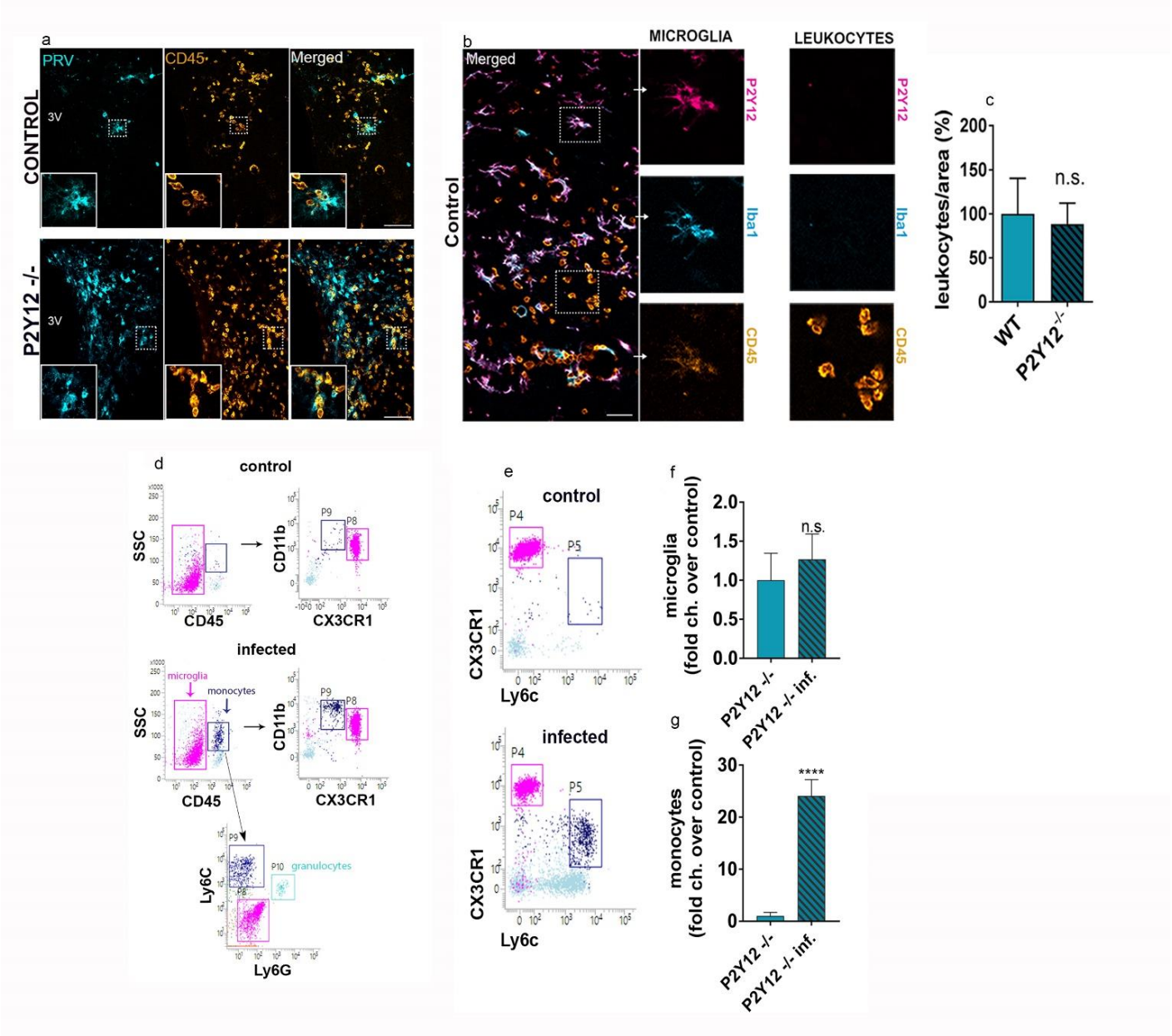

Figure 16. Leukocyte infiltration upon PRV infection is independent of P2Y12 signalling. **a,** Fluorescent pictures show CD45-positive (orange) leukocyte recruitment to PRV-immunopositive neurons in the PVN in wild type and P2Y12 deficient mice. **b,** P2Y12-expressing (magenta)microglia were clearly separated from blood-borne cells highly expressing CD45 (orange), most of which were also negative for microglia/macrophage marker Iba1 (blue). **c,** Numbers of infiltrated leukocytes show no significant difference in control and $P2Y12^{-/-}$ mice, area:0.2 mm^2. **d,** Flow cytometric dot plots show that microglia ($Cx3Cr1^{high}$, $CD45^{low}$, $Ly6C^-$, $Ly6G^-$ cells, P8) can be well characterized and clearly separated from infiltrated monocytes ($Cx3Cr1^{int}$, $CD45^{high}$, $Ly6C^{high}$, $Ly6G^-$ cells, P9) during viral infection in the brain. **e,** Flow cytometric dot plots show infiltrated monocytes (P5) in the brain. **f,** Microglial numbers do not change in response to virus infection compared to control condition. **g,** Monocytes are recruited into the brain in response to virus infection in P2Y12 receptor deficient mice. All data expressed as mean ± s.e.m. **f,** n.s.= not significant **g,** ****$p<0.0001$ n=4 brains per group unpaired t-test. Scale bars: a,b, 50 μ (Fekete et al. 2018).

4.6.2.Selective depletion of microglia influences leukocyte infiltration in virus infected brain

In contrast with our previous results in $P2Y12^{-/-}$ animals, selective elimination of microglia surprisingly resulted in a marked decrease in CD45-positive leukocytes around virus infected areas in spite of the increased number of infected neurons in the brain (Fig.17.a,). It is important to note that the lack of leukocyte infiltration in microglia-depleted animals was not due to the drug, PLX5622 itself, as it was also confirmed earlier with another CSF-1R inhibitor, PLX3397 (Szalay et al., 2016). Treatment with PLX5622 was not associated with any significant changes in circulating or splenic myeloid cell populations including granulocytes and monocytes, while lymphocytes were not affected either in microglia-depleted animals, compared to controls (Fig.20.). Using FACS analysis we uncovered that from all infiltrated CD45-positive cell populations, $CD45^{high}$, $Cx3Cr1^+$, $CD11b^+$, $Ly6C^{high}$ monocyte numbers were markedly reduced in microglia depleted, virus infected animals (Fig.17.c-e,). To further elaborate on the mechanisms through which microglia may recruit monocytes, we showed that microglia exposed to high titers of PRV *in vitro* produced CCL5 (RANTES) and MCP-1 (a chemokine to recruit monocytes/macrophages), whereas CCL5 and IL-1a were reduced markedly in hypothalamus homogenates of microglia depleted, virus infected mice (Fig.18.). Note that extensive virus infection in the brain was also associated with increased number of circulating granulocytes in microglia-depleted mice, suggesting that peripheral myeloid populations were capable of responding to central viral infection, but the recruitment to the brain was inhibited by the absence of microglia (Fig.20.). Next, we aimed to investigate the causes behind the absence of the inflammatory $Ly6C^{high}$ monocyte population. Previous studies have shown that in response to viral infections, leukocyte

infiltration is augmented by blood-brain barrier (BBB) injury (Benakis, Garcia-Bonilla, Iadecola, & Anrather, 2015). Surprisingly, we could not detect any significant difference in the integrity of BBB between microglia depleted infected and control infected animals. For further explanation, we made use of Intercellular Adhesion Molecule 1 (ICAM) to fluorescently label activated vessels in infected areas, which did not show any difference between microglia depleted infected and control infected PVN regions (Fig.19.).

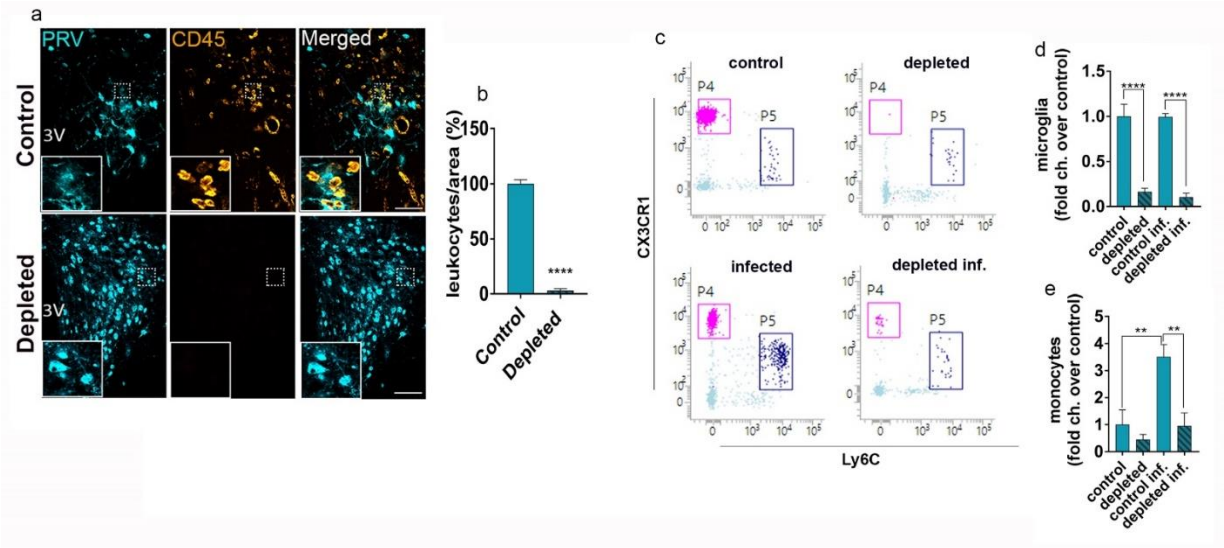

Figure 17. Recruitment of leukocytes to the brain is diminished in response to virus infection in the absence of microglia. a, Immunofluorescent pictures show that recruitment of CD45-positive leukocytes (orange) can be detected in virus infected PVN which is markedly reduced in microglia depleted, infected animals. **b,** Leukocyte numbers are significantly lower in microglia depleted animals. **c,** Flow cytometric dot plots show the almost complete absence of microglia in depleted animals (P4). Despite of the adverse virus infection in the absence of microglia, $CD45^{high}$, $Cx3Cr1^{+}$, $CD11b^{+}$, $Ly6C^{high}$ monocyte (P5) recruitment is profoundly reduced in microglia depleted, virus infected animals. **d,** $Cx3Cr1^{+/GFP}$ microglia are markedly reduced in the brain after 3 weeks of PLX5622 diet. **e,** In response to virus infection, monocyte numbers increase significantly in control brain, but are reduced in microglia depleted mice. All data expressed as mean ± s.e.m **b,** ****p<0.0001 unpaired t-test n=12 animals per group; **d,** control vs depleted ****p<0.0001, control inf. vs depleted inf. ****p<0.0001 One-Way ANOVA; **e,** control vs control inf. **p<0.01, control inf. vs depleted inf. **p<0.01 One-Way ANOVA. Scale bar: a, h, 50 μm (Fekete et al. 2018).

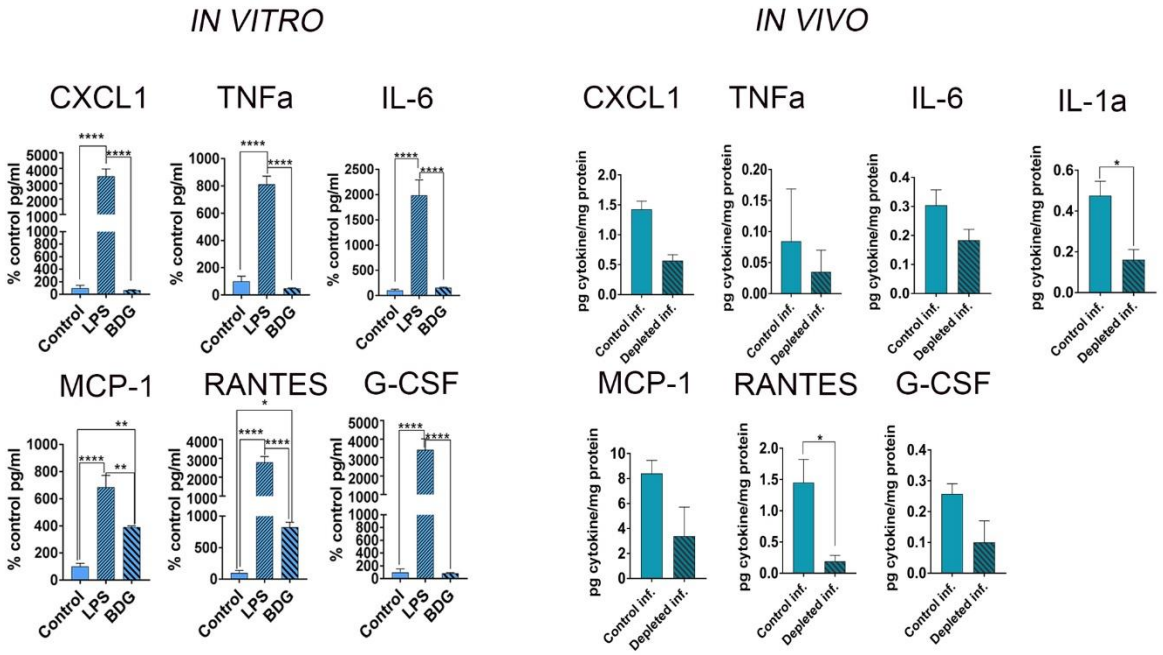

Figure 18. Changes in inflammatory cytokines and chemokines in response to virus infection and selective elimination of microglia. Left, *in vitro* data: Cytokine and chemokine levels were measured in the conditioned medium of microglial cell cultures by cytometric bead array after LPS treatment or exposure to PRV. Samples were collected 24 hours after infection. Right, *in vivo* data: Cytokine and chemokine levels were measured from homogenates of hypothalamic brain tissues of control and microglia-depleted mice infected with PRV in a retrograde transneuronal manner, 5 days prior to sample collection. All measurements have been performed by cytometric bead array. Data are expressed as mean ± s.e.m. One-way ANOVA, n=5 animals and cell cultures per group (Fekete et al. 2018).

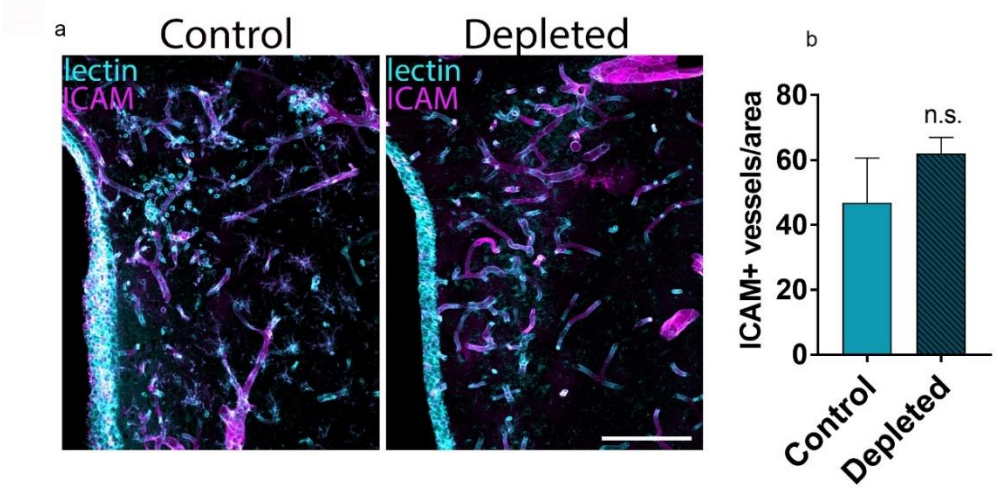

Figure 19. Depletion of microglia does not influence blood-brain barrier injury during virus infection. a, Number of ICAM positive activated blood vessels did not show significant difference in control infected and microglia depleted infected PVN asreas. **b, ,** ICAM positive vessels were not significant in control infected and depleted infected PVNs. n.s.= not significant (unpublished).

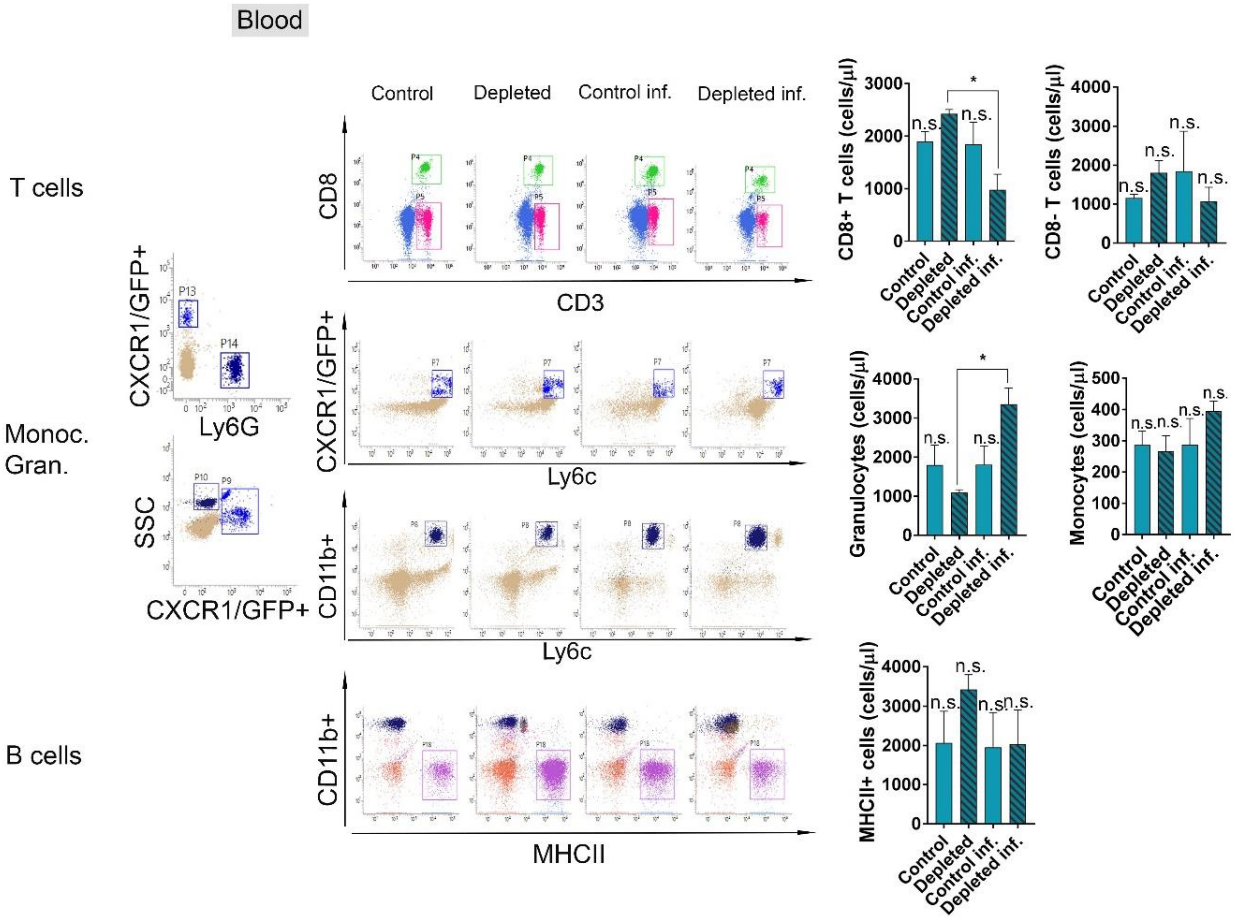

Figure 20. Selective depletion of microglia does interfere with main blood cell populations. Cx3Cr1$^{+/gfp}$ mice were fed a PLX5622 chow diet for 21 days to deplete microglia. On the 16th day of the diet, a group of mice were injected with Bartha-DupGreen (BDG). Blood samples were collected from control mice and from mice 5 days after virus infection with or without microglia depletion, and labelled with mixtures of specific antibodies against leukocyte markers followed by flow cytometric analysis. Total blood cell counts were calculated by using 15 µm polystyrene microbeads (Polybead Microspheres, 18328-5). The number of CD8^{-} (P5 gate) T lymphocytes, CD11b^{+} Ly6c^{+} SSC^{high} Ly6G^{+} granulocytes (P8 gate), CD11b^{+} Ly6c^{high} Cx3Cr1^{+} (Ly6G^{-}) monocytes (P7 gate) and MHCII^{+} CD11b^{-} B cells (P18 gate) were no different between control, depleted, control infected and depleted infected animals. In association with the profoundly increased CNS infection in microglia depleted mice, numbers of CD3^{+} CD8^{+} T lymphocytes (P4 gate) and CD11b^{+} Ly6c^{+} SSC^{high} Ly6G^{+} granulocytes (P8 gate) showed significant difference between depleted and depleted virus infected animals. Data are expressed as mean ± s.e.m. one-way ANOVA, n=4 animals per group. n.s. - not significant (Fekete et al. 2018).

4.7. Recruitment of P2Y12-positive microglia and leukocytes in human herpes simplex encephalitis

To investigate microglia recruitment and neuroinflammatory changes in the human brain, we analysed temporal lobe samples from patients with herpes simplex type 1 virus (HSV-1) encephalitis, in which infection had been confirmed both by PCR and immunohistochemistry, as reported earlier (Csonka et al., 2013). Similarly, to what we have seen in PRV infected mice brain tissue, in human samples both HSV-1 and HSV-2 infected neurons were surrounded by P2Y12-positive microglia cells (Fig21.a, Table 2.). We confirmed this further with another specific microglial marker, Tmem119 (Fig.21.b,). Infected cells were, contacted by 1-3 microglia (on average 1.5 microglia/ HSV-1+ cell (Fig21.c,). CD68 labelling in recruited amoeboid cells indicated active phagocytosis at sites of virus infected neurons (Fig.21.d,). Microglia showed negative results for HSV antigens suggesting that viral infection does not develop in these cells. With CD45-immunohistochemistry and Giemsa staining, we identified recruited leukocytes in close proximity to HSV1-positive neurons. Leukocytes were also negative to Tmem119 and P2Y12, so they could be clearly discriminated from recruited microglial cells (Fig.21.e-g,). Interestingly, we observed strong correlation between the number of recruited leukocytes and the amount of HSV-1 infected neurons (Fig.21.h,). At areas of HSV-1 infection we detected low amount of CD3-positive lymphocytes, CD20-positive B cells and CD15-positive myeloid cells (Fig.21.i,).). In the absence of HSV1 infection, the vast majority of Iba1-positive microglia was found to be P2Y12 positive (96%) and numbers of Tmem119-positive and P2Y12-positive microglia were similar in the brain parenchyma (Fig.22). We also noticed that moderate HSV infection (less than 50 HSV-1-positive cells/mm^2) was associated mostly with the activation of local microglia, which were positive for P2Y12 and Tmem119. In the same areas, amoeboid or ramified CD68-positive cells were also observed. In advanced HSV-1 infected (50-500 HSV-1-positive cells/mm^2) brain tissue, increased number of CD45-positive cells were recognised in the brain parenchyma, which was associated with markedly increased numbers of CD68-positive macrophages. In line with this, the number of ramified microglia, and the total number of P2Y12-positive or Tmem119-positive cells was reduced (Fig.21.j, k, and Fig. 23.).

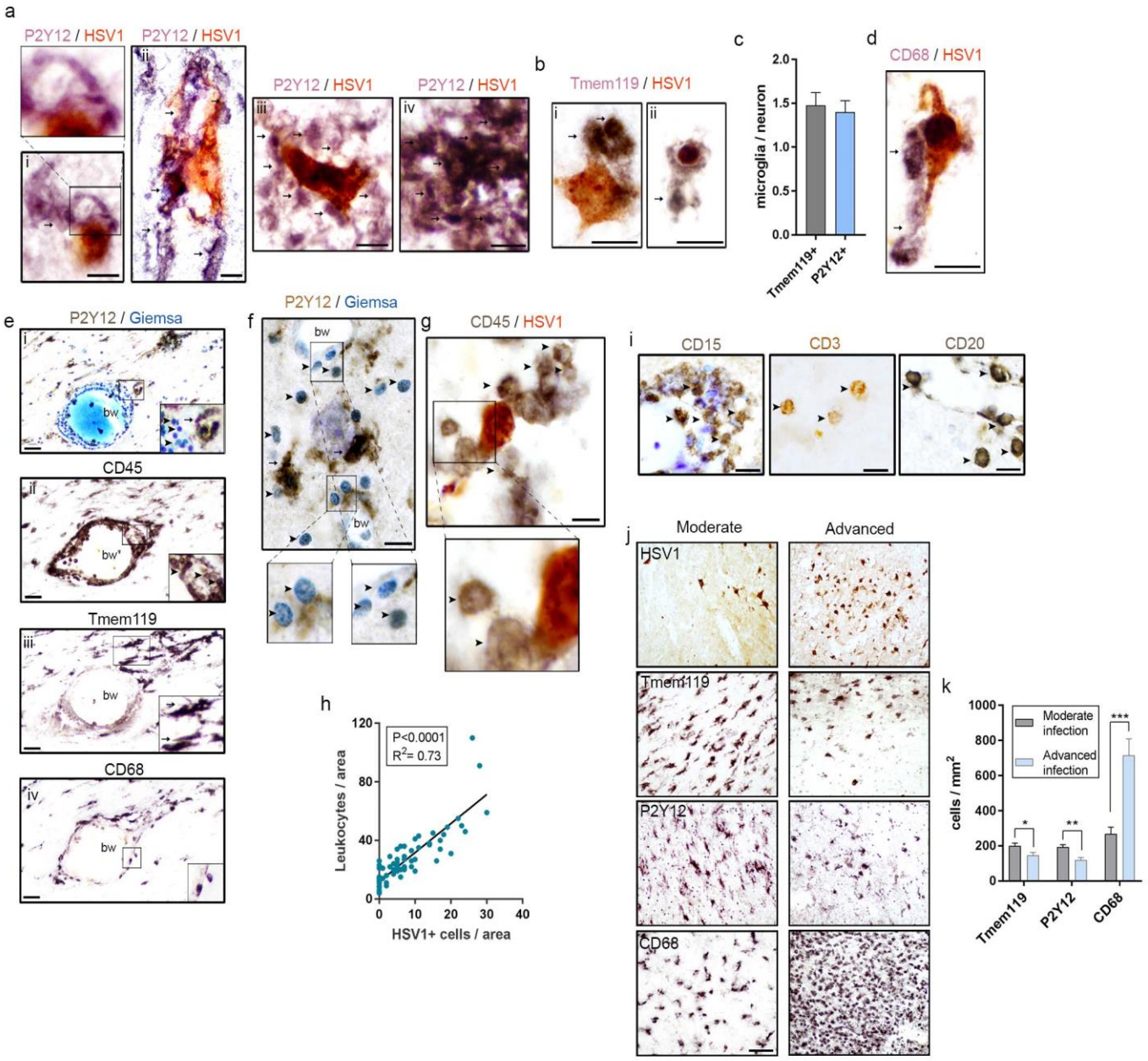

Figure 21. Microglia and leukocytes are recruited to HSV-1 infected neurons in the human brain. a, P2Y12-positive microglia recruited to HSV-1 infected neurons (brown, visualized by NovaRED HRP substrate). Recruitment of microglia to neurons in different stages of infection are visualized (arrows, visualized by DAB-Ni) in the human cerebral cortex. P2Y12-positive microglial processes contact HSV-1 positive neurons (i-iii). In the absence of detectable HSV antigens microglia are displaying amoeboid, phagocytic morphology (iv). **b,** Tmem119 expressing microglia are recruited around HSV-1 infected neurons (i) and phagocytose HSV-positive cells (ii). **c,** Average number of P2Y12-positive and Tmem119-positive microglia contacting infected neurons. **d,** CD68 expressing brain macrophages (DAB-Ni) surround HSV-1 infected neurons (NovaRED). **e,** Virus infection is associated with leukocyte infiltration (arrowheads) visualised by Giemsa staining (i) and CD45 immunostaining (ii) parallel with activated microglia (arrows) labelled with P2Y12 (i) or Tmem119 (iii). CD68-positive macrophages and CD68-positive cells with microglia-like

morphology near blood vessels suggests both blood-borne and resident origin of brain phagocytes. **f,** In infected areas, neurons surrounded by P2Y12-positive microglia are associated with recruited CD45-positive leukocytes **(g). h,** Leukocyte numbers in infected areas show correlation with the number of HSV-1 infected neurons. $p<0.0001$, linear regression, n=64 FOV, from 5 patients. **i,** CD15-positive myeloid cells, low amount of CD3-positive lymphocytes and CD20-positive B cells could be observed at infected brain areas. **j,** Moderate HSV-1 infection is associated with the presence of P2Y12-positive, Tmem119-positive microglia and CD68-positive microglia/macrophages, whereas the number of P2Y12-positive and Tmem119-positive microglia is decreased during advanced infection, while the number of CD68-positive macrophages significantly increases in the parenchyma. **k,** Quantitative representation of P2Y12-positive, Tmem119-positive microglia and CD68-positive brain macrophages in moderate and advanced HSV-1 infection. bv – blood vessel. Scale bars: a, b, d, f, g, h, i - 10μm; e and j - 50μm. **k,** *p<0.05, **p<0.01, ***p<0.001 (Fekete et al. 2018).

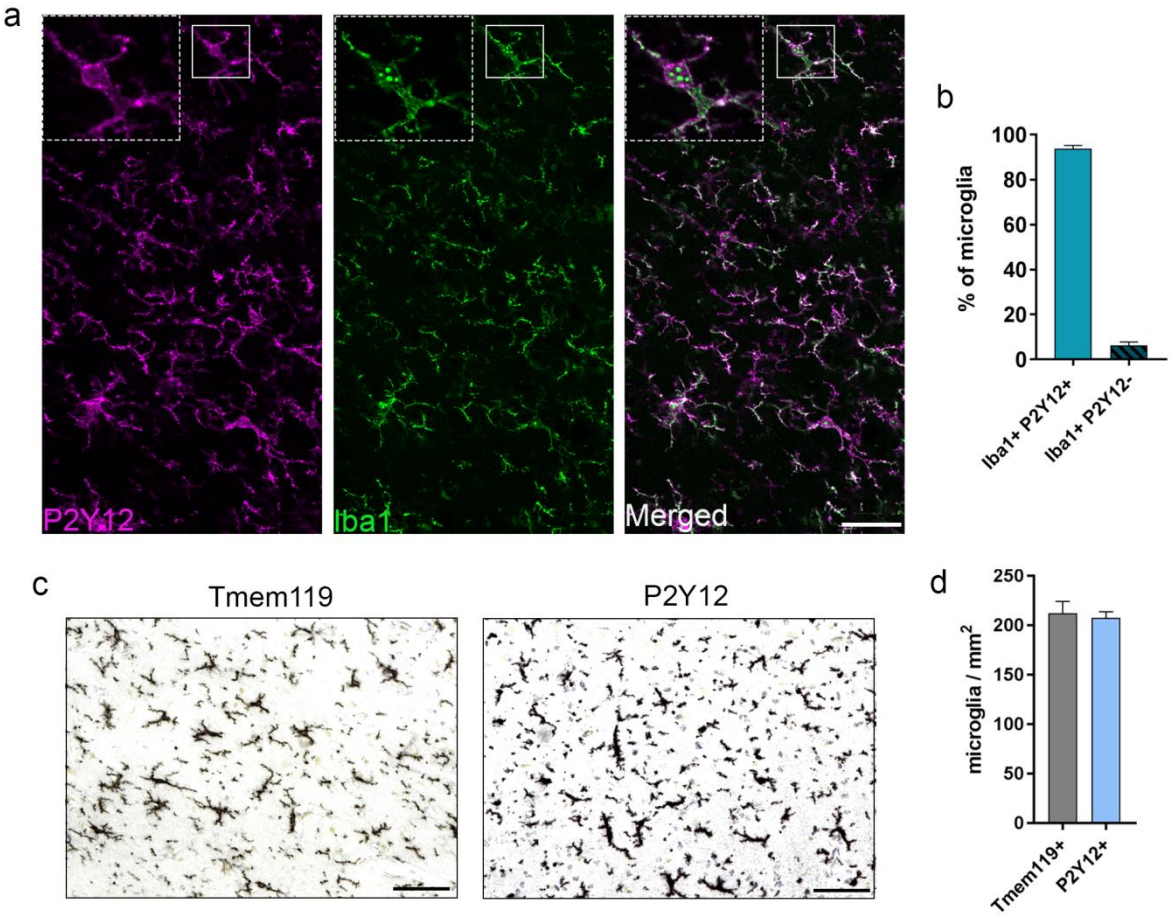

Figure 22. Microglia express P2Y12 in the human brain. a, Co-localization of microglial P2Y12 and Iba1 on perfusion-fixed, free-floating brain sections (frontal cortex). **b,** Proportion of P2Y12-positive microglia among Iba1+ cells. **c,** Immunohistochemistry showing Tmem119-positive and P2Y12-positive microglia in paraffin-embedded brain sections (frontal cortex). **d,** Quantification of Tmem119-positive and P2Y12-positive microglia in the brain. All samples are derived from patients with no known neurological disease (Fekete et al. 2018).

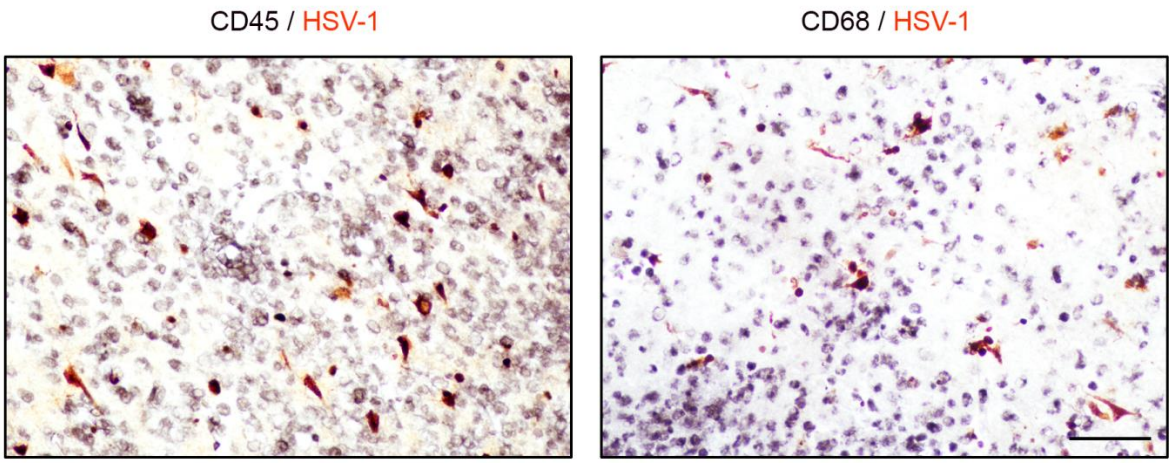

Figure 23. Advanced HSV-1 infection is associated with marked neuroinflammatory responses in the human brain. Recruitment of numerous CD45-positive cells and CD68-positive brain macrophages is seen at sites of advanced virus infection characterized by large number of HSV-1-positive cells. Scale bar: 50μm (Fekete et al. 2018).

5. Discussion

My studies have demonstrated that microglial P2Y12-mediated responses are essential for the recognition and effective elimination of compromised neurons after virus infection that reaches the brain exclusively via retrograde transsynaptic spread. Microglia recruitment occurs within a few hours in vivo and leads to the phagocytosis of infected cells. Marked increases in the number of disintegrated cells and leakage of viral antigens into the extracellular space are seen in the absence of functional microglia, which are associated with exaggerated infection and the development of neurological symptoms. These results also show that P2Y12 receptors are key drivers of microglial phagocytosis both *in vivo* and *in vitro* and that microglial P2Y12 is essential for appropriate responses to nucleotides released by infected neurons in the brain. Furthermore, my research identify microglia as key inducers of monocyte recruitment into the brain in response to neurotropic virus infection and also demonstrate the relevance of these findings in the human brain. We also uncovered that the mechanisms through which microglia contribute to monocyte recruitment are largely independent of the extent of blood-brain barrier injury in this experimental model.

5.1. Regulation of inflammatory responses during neurotropic viral infections

Neurotropic virus infections continue to cause major disease and economic burdens on society, and pose major challange to both human and animal health due to associated morbidity and mortality worldwide. Finding effective treatment opportunities to control infection burden during CNS infections is still an unsolved problem, largely due to the unique and complex features associated with reduced immune surveillance and limited regeneration capacity of the CNS. Infection by neurotropic viruses and immune responses induced by activated microglia and recruited peripheral immune cells can irreversibly disrupt the complex structural and functional architecture of the CNS, often leaving patients or affected animals with various neurological conditions that may contribute to long-term cellular damage or death. Once a pathogen invades the brain, microglia and astrocytes are considered to provide the first line of defense, although evidence from functional studies is presently incomplete. In addition to central immunocompetent cell types, peripherally recruited innate (monocytes, neutrophils) and adaptive ($CD8^+$ T cells, $CD4^+$ T cells, B cells) immune cells are known to be capable of identifying infectious organisms and contribute to central immune responses. As

an inherent confounder to this response upon neurotropic viral infections, infiltrating immune cells are also known to contribute to immune-mediated pathologies, mainly via the production of multiple inflammatory mediators, such as pro-inflammatory cytokines and chemokines (Getts et al., 2013)

Neutrophils are among the first blood-borne immune cells to infiltrate into the parenchyma upon virus infection. Similarly to that seen in non-communicable diseases such as in the case of stroke (Planas, 2018) or TBI (Donat et al., 2017) neutrophils start to appear in the brain parenchyma within hours upon infection. Impaired trafficking or depletion of neutrophils is capable of reducing the size of the lesion after stroke or TBI, especially when acute brain injury is combined with systemic inflammation (McColl et al., 2006), Similar effect of neutrophil depletion on reduced brain injury has been described during West-Nile virus infection. In these studies, impaired neutrophil responses resulted in limited immune cell crossing through blood-brain barrier and neuropathology was diminished, however, the spread of viral infection was not inhibited (Wang et al. 2012).

Different monocyte subsets are also known to be recruited into the infected brain within hours or days and contribute to central inflammatory responses, although their functional role in limiting viral infections is presently not well defined. According to studies, which have used HSV-2 (Iijima, Mattei, & Iwasaki, 2011), coronavirus (Becker et al., 2008) or MHV (Chen BP et al. 2001) infection models, Ly6C^{hi} monocytes appear to play paradoxical role. In case of encephalitic disease, such as TMEV infection, it was shown that recruited Ly6C^{hi} monocytes contribute to the immunopathogenesis of disease. Inhibition of inflammatory monocyte migration resulted in TMEV-infected brain significantly reduced morbidity and mortality (Ajami, Bennett, Krieger, Tetzlaff, & Rossi, 2007). Chemokines produced by resident immune cells or early infiltrating blood-borne myeloid cell types in the infected brain are known to be major contributors to mounting inflammatory responses via promoting the recruitment of T cells and B cells into the CNS. For example, the production of CXCL10 and CCL5 promotes the migration and accumulation of CD4$^+$ and CD8$^+$ T cells in the brain that control viral replication via secretion of IFN-γ (Miller et al., 2016). In line with this, it was shown in a model of HSV-1 infection that CD8$^+$ T cells become activated and contribute to the restriction of HSV-1 replication 8 days after infection in mice. In cytomegalovirus (CMV) infected patients, acyclovir treatment, which is an anti-viral drug with activity against a range of herpes viruses and is used as long term treatment to suppress reactivation of HSV, resulted in reduced T cell response (mainly CD4$^+$ T cell reaction) to viral antigens, however immune response of other cells were only modestly decreased (Pachnio, Begum, Fox, & Moss, 2015).

In a mouse hepatitis virus (MHV) model, delayed depletion of $CD4^+$ T cells did not alter $CD8^+$ T cell recruitment into the brain, but impaired their IFN-γ production, resulting in impaired cell survival and uncontrolled increase of viral titers. Thus, while peripheral immune cells contribute to immune responses in the CNS, it is assumed that the main coordinators of these processes are resident microglia. However, due to the trafficking of massive amounts of macrophages and monocytes into the infected brain, studies to selectively investigate the potential role of microglia regulating responses in anti-viral immunity could not come to clear conclusions due to the absence of selective approaches to influence microglial responses until very recently (Elmore et al., 2014). In addition, most models of CNS infection or injury that require direct manipulation of the CNS microenvironment inherently include non-specific microglial activation, which makes studying microglial responses to infection-related signals difficult.

5.2. Pseudorabies virus infection as an ideal model for studying microglia-mediated inflammatory responses

Transsynaptic spread, self-amplification and borad host range made pseudorabies virus an ideal tool in an extensive number of neuroanatomical studies (Strack AM 1994; Card et al. 2014) seeking to define the architecture of multisynaptic pathways. In order to control the speed and virulence of the virus, attenuated derivatives of PRV-Barthta were developed. Further genetical manipulation, by inserting various fluorophores (GFP, DSRed) inside the genome of the virus made possible to precisely follow the infection in time (Boldogkői et al. 2003). To establish a model of neuronal injury in which microglial responses to local signals can be studied within a realistic time frame and without in situ manipulation of the brain microenvironment, we have used genetically modified PRV-Bartha derivatives, which exhibit precisely controlled, retrograde transneuronal spread but do not infect microglia (Boldogkői et al. 2003; Dénes et al. 2006). These recombinant PRV strains also allowed precise time-mapping of the spread of infection due to the expression of reporter proteins with different kinetics (Taylor, Kobiler, & Enquist, 2012). At the same time, we could investigate the functional contribution of microglia to neurotropic herpesvirus infection, which has not been previously investigated using selective elimination of microglia.

Since immune surveillance by circulating immune cells is restricted in the brain parenchyma (Prinz & Priller, 2014a), early recognition of infection by microglia is likely to be critical to mount an appropriate immune response. The central inflammatory response induced by

neurotropic herpesviruses including microglial activation and recruitment of blood-borne immune cells has been previously characterized by excellent earlier studies. Our former data has also shown that microglia surround infected neurons in the brain (Dénes et al., 2006). Recent reports highlighted the importance of central type I interferon responses against vesicular stomatitis virus and herpes simplex virus type 1 implicating microglia as a source of inflammatory mediators in anti-viral immunity in the brain (Chen, Zhong, & Li, 2019). However, the kinetics and the mechanisms of microglia recruitment to infected cells have remained unexplored to date, similarly to the need for understanding phagocytic activity by microglia to control the spread of infection.

5.3. Microglia sense various danger signals coming from compromised neurons

During neurotropic virus infection, compromised neurons release various danger signals into the extracellular space, which trigger inflammatory processes. Danger signals released by injured neurons such as DNA, heat shock proteins or ATP act as potent activators of microglia and also contribute to the outcome in different brain pathologies (Stevens & Schafer, 2018). However, the exact signals mediating early recognition of injured cells and those inducing phagocytosis of compromised neurons by microglia are poorly defined. In addition, the mechanisms of microglial decision-making regarding the fate of injured neurons is unclear.

A number of studies have demonstrated that purinergic signaling plays an important role in CNS injury responses (Davalos et al., 2005b). Intravital microscopy (IVM) studies revealed that focal laser injury in the brain induces purinergic receptor-dependent projections of microglia toward the injury site, which help the clearance of cellular debris, and facilitate lesion containment. Similarly, nucleotides are released following TBI, that trigger a robust microglial response dependent on purinergic receptor (P2X4, P2Y6, P2Y12) signalling (Fields & Burnstock, 2006). However, due to the complexity of these pathways and the immediate response of microglia to any tissue disturbance, it is difficult to dissect the mechanisms through which microglia recognize stressed neurons in most known experimental models of brain injury. Our PRV model combined with selective microglia depletion and P2Y12R specific KO lines allowed us to study the involvelement of purinergic signaling in the context of virus mediated brain pathology.

5.4. Nucleotides released from compromised neurons cause immediate response from microglia and sensed via microglial P2Y12 receptor

Infected cells, including neurons and microglia were reported to sense HSV-1 via cytoplasmic DNA sensors, namely the adaptor protein stimulator of type I IFN genes (STING) (Reinert et al. 2016; McCarthy, Tank, and Enquist 2009) However, the signals initiating microglia recruitment to infected neurons in the absence of microglial infection had remained unclear. Our *in vivo* and *in vitro* data suggest that soon after the development of productive infection, purinergic mediators released from neurons recruit the processes of uninfected microglia in their vicinity, followed by the displacement of the cells, leading to the formation of tight membrane to membrane interactions with the infected neurons. Since PRV infection alters neuronal activity (McCarthy et al., 2009) we hypothesised that the earliest signals from infected neurons to microglia are more likely to include mediators regulating rapid microglia-neuron interactions *in vivo* than *de novo* production of inflammatory chemokines. Specifically, noxious stimuli in neurons can trigger a sustained increase of extracellular ATP, which results in microglial activation and recruitment within minutes to hours (Fields & Burnstock, 2006). In fact, our data show that purine nucleotides released from affected neurons contribute to microglial process extension, cell migration to infected neurons and subsequent phagocytic activity via microglial P2Y12 receptors. ATP released from injured cells leads to the activation of P2-type and adenosine receptors upon extracellular ATP catabolism by ecto-nucleotidases (Rodrigues, Tomé, & Cunha, 2015). In line with this, we observed increased ecto-ATPase levels and NTDPase1 activity in infected cells and microglia. ATP is a strong chemotactic signal for microglia *in vivo* and hydrolysis of ATP to ADP, which is the main ligand for P2Y12 takes place by ecto-nucleotidases within minute (Sperlágh & Illes, 2007) In turn, increased P2Y12 receptor levels were found on microglial processes contacting infected neurons, as assessed by super-resolution microscopy. Since infected neurons at the stage of immediate-early reporter protein expression are viable and electrophysiologically active (re(McCarthy et al., 2009)f), these results also imply that microglia are well-equipped to identify injured neurons way earlier than the integrity of the cell membranes is compromised. Our ultrastructural analysis and *in vitro* data also confirm this, showing normal cell membrane integrity until late stages of virus infection. Thus, in spite that P2Y12 has been implicated earlier in the recruitment of microglia to sites of tissue injury in the brain (Haynes et al., 2006), the present *in vivo* and *in vitro* studies have identified the

cell-autonomous effect of P2Y12 on microglia to rapidly recognize and eliminate infected neurons for the first time. We also show that P2X7, which plays a major role in microglial inflammatory responses and cytokine production (Sperlágh & Illes, 2014) is dispensable for anti-viral immunity in this experimental model.

5.5. Microglia are essential to limit neurotropic virus infection in the brain

To understand better the specific role of microglia in response to viral infections has been challenging due to the presence of non-microglial myeloid cells with potentially overlapping functions in the healthy brain and by the rapid infiltration of hematopoietic myeloid cells into the parenchyma during inflammation. Although many studies have described microglial functions such as the production of proinflammatory mediators or phagocytosing dying or injured cells, none of them could determine the exact contribution of microglial responses to neurotropic virus infection. In line with this, using *in vitro* and *in vivo* models of P2Y12 -/- mice, our results showed that this purinergic receptor play crucial role in microglial phagocytosis of infected cells, however the question whether microglia participate actively in controlling viral infection have remained unclear. In order to investigate this question we made use of selective microglia depleting tool, the CSF1-R inhibitor drug, called PLX5622. In line with other recent studies using the same microglia elimination model in other neurotropic virus infection models, such as mouse hepatitis virus (MHV) (Wheeler et al. 2018) and West-Nile virus (Seitz et al. 2019) have made the same conclusions, that absence of microglia would result in increased mortality and depletion in a later phase of infection had no influence on survival (Chen et al., 2019). These data indicate, that microglia play an important role in controlling viral replication and reducing mortality in the early stage of infection (Fig. 24.). Similarly what we have confirmed earlier with PRV infection (Dénes et al. 2006; Fekete et al. 2018) another study, using intranasal somatitis virus (VSV) infection, have found activated microglia accumulating around infected olfactoy bulb neurons formed an immune barrier, which plays an important role in limiting the spread of VSV in the CNS and preventing lethal encephalitis (Steel et al., 2014). In our model, the absence of microglia, also resulted in non-synaptic spread of pseudorabies, resulting advanced infection in higher cortical areas. This also indicates, that microglial barrier formation is essential in controlling viral escape from already compromsied cells. In conclusion, our data obtained both *in vivo* in real time and *in vitro* shows that the rapid and precisely controlled migration of functional microglia is critical not only to limit the spread of infection in the brain, but timely

elimination of infected neurons is essential to prevent contact infection and to control the leakage of viral particles and antigens into the brain parenchyma.

5.6. Selective microglia elimination, but not P2Y12 deficiency leads to adverse neurological symptoms in PRV infected mice

We found that although P2Y12 is essential for the recognition and elimination of infected neurons by microglia, microglia depletion, but not P2Y12 deficiency led to characteristic neurological symptoms in virus infected mice. In line with this, microglia-depleted mice had higher numbers of infected / dying neurons than that seen in $P2Y12^{-/-}$ mice, while the levels of extracellular virus proteins were not different, although significantly increased in both groups compared to control mice. Thus, the rapidly deteriorating neurological outcome seen in microglia-depleted animals may be partially due to the markedly increased neuronal infection and to the absence of potentially neuroprotective microglial mediators, such as interleukin-10 (Garcia et al., 2017). While our data show that P2Y12-dependent mechanisms are instrumental to limit neurotropic virus infection in the brain, additional microglial receptors could also contribute to this process. The rapidly worsening neurological symptoms of mice in the absence of microglia, but not in P2Y12-deficient mice, may be due to both exaggerated infection and the lack of microglial factors that control neuronal activity in the injured brain (Stevenson, Austyn, & Hawke, 2002), which should be investigated in further studies. Since the PRV Bartha-Dup strains show highly specific neurotropism in vivo (Szpara, Kobiler, & Enquist, 2010) and we did not find any sign of hematogenous dissemination of infection or immunopositivity to viral antigens in the liver or the spleen even after PLX5622 treatment, a major role of peripheral immune mechanisms in the markedly increased spread of infection in microglia-depleted mice is unlikely.

5.7. Leukocyte infiltration in virus infected brains is influenced by microglia, but is independent from P2Y12 receptor mediated processes

We also identify microglia as key contributors to monocyte recruitment to the brain during virus infection. Previous studies have implicated activated microglia in leukocyte recruitment into the brain upon virus infection, and showed that antibodies to CXCL10 and CCL2 (MCP-1) reduce the migration of murine splenocytes toward HSV-infected microglia *in vitro* (Marques, Hu, Sheng, & Lokensgard, 2006). In our experimental model, elimination of microglia by CSF1R blockade was highly selective, as it did not have a significant impact on circulating and splenic leukocytes (including myeloid cell types) and infection-induced increases in circulating granulocytes was preserved in PLX5622-treated mice. In contrast, recruitment of monocytes to the brain was almost completely abolished in microglia-depleted mice. In these studies, we made use of both CD45 and Cx3Cr1 as markers to reliably discriminate microglia ($CD45^{low}$, $Cx3Cr1^{high}$, $Ly6c^{-}$ cells) from monocytes ($CD45^{high}$, $Cx3Cr1^{+}$, $Ly6c^{high}$ cells) without the need of complex BM chimeric studies that inherently include changes in BBB function and may cause microglia activation (Wilkinson et al., 2013). Importantly, microglial P2Y12 was essential to mediate microglia recruitment and phagocytosis, but was dispensable for monocyte recruitment to the brain. These data suggest that other microglial chemotactic factors (such as MCP-1 or RANTES) could be responsible for driving leukocyte migration to sites of infection and injury in the brain, which should be investigated in further studies. Since monocyte recruitment in $P2Y12^{-/-}$ mice was identical to that seen in control animals, but both an absence of microglia and P2Y12 deficiency resulted in markedly enhanced spread of infection, blood-borne monocytes may not significantly limit viral spread in the current experimental model. A similar conclusion was presented in a model of corona virus infection induced by direct injection of the virus into the brain, in spite that reduction of microglia numbers was associated with higher number of blood-borne macrophages in this study (Wheeler, Sariol, Meyerholz, & Perlman, 2018b). Since $P2Y12^{-/-}$ mice showed comparable leukocyte infiltration to control animals, while microglia depletion markedly influenced leukocyte responses, a role for blood-borne cells in shaping neurobehavioral symptoms seen in this experimental model cannot be fully excluded. In contrast, other studies using PLX5622, CSF-1 antagonist combined with various neurotrop viral infection models did not come to the same conclusion as our results show, regarding the complete absence of leukocyte infiltration. In a mouse model of MVH infection, the effect of

microglia depletion via CSF1R inhibitor treatment only affected the number of infiltrated CD45-positive cells 3 days after post infection, but no differences were observed 7 days after infection, indicating that recruitment of blood-derived cells was not exclusively microglia dependent (Wheeler et al., 2018b). However, in a model of WNH infection it was shown that depletion of microglia alters, but not abolish the numbers of CD4+ T cells to viral infection (Bergmann, Ramakrishna, Kornacki, & Stohlman, 2014). Depletion of microglia in the same infection model can also result in the loss of major MHCII-expressing cell type, which also result in decreased expression of MHC II in incoming monocytes and macrophages. In line with those data, our results indicate that loss of microglia affect adaptive immune response, resulting in a reduced virus-specific reaction of infiltrating immune cells.

5.8. BBB injury is not markedly affected by the absence of microglia during viral infection

Since we found that microglial responses are involved in leukocyte recruitment during virus infection, we examined whether this may be due to differences in BBB permeability that may also be influenced by microglial actions. Blood-brain barrier is a complex structure, which separates the brain microenviroment from the systemic circulation and regulates homeostasis. The neurovascular unit is an essential functional part of the BBB, which is composed from different cell types, including astrocytes, pericytes, perivascular macrophages, endothelial cells and microglia as well (Thurgur & Pinteaux, 2018). A large pool of brain resident microglia, also known as perivascular microglia, are located at the proximal region surrounding the cerebrovasculature, allowing close contact with endothelial cells (ECM). Others have already demonstrated that endothelial-microglia interactions are essential for angiogenesis and other vascular processes and that the microglia-vascular interface acts as a sensor of central or peripheral disturbance and inflammation, constituting the first line of defence of the CNS against injury.

Microglia adjacent to the cerebral blood vessels are in a constant bi-directional communication with endothelial cells to exert their surveying functions on the intergrity of the BBB, as well as the influx of blood derived molecules into the brain. Several studies have described that in response of inflammation or injury microglia produce a large array of inflammatory mediators, including cytokines (interleukin (IL)-1, IL-6, tumor necrosis factor-alpha (TNFA)), chemokines (CCL, CX3CL1, MIP-1) and proteases (matrix metalloproteases, MMPs), which may impact on BBB integrity and contribute to plasma leakage into the brain

parenchyma (Benakis et al., 2015). In diseased states, the vascular endothelium in the brain and the surrounding ECM undergo profound changes, including the breakdown of TJs, remodelling the ECM and enzymatic degradation of ECM proteins by MMPs contributing to a leaky BBB that facilitates the infiltration of systemic circulating blood-derived molecules and immune cells. Vascular endothelial cells (ECMs) also produce a large array of inflammatory mediators (CX3CL1, CCL2) which contributes to tight junction (TJs) breakdown, enzymatic degradation of ECM proteins by MMPs and reactive oxygen species (ROS) resulting in a 'leaky' BBB. Inflammatory cytokine measurements from microglia depleted, virus infected paraventricular nucleus of the hypothalamus (PVN) homogenates have already implicated marked changes in cytokine levels, which promted us to investigate the extent of BBB disruption in these animals (Lopes Pinheiro et al., 2016). Although our data showed that selective microglia elimination, by CSF-1 antagonist, PLX5622 diminished monocyte recruitment into the brain parenchyma during viral infection, an absence of microglia did not alter the extent of BBB injury based on IgG staining. Immunofluorescent detection of intercellular adhesion molecule-1 (ICAM) on activated endothelial surface has also shown that an absence of microglia during viral infection does not influence vascular activation. This is interesting since the number of virus infected neurons and also extracellular virus particles were increased in the infected brain of microglia depleted animals, which could in theory also alter BBB injury or vascular activation by shaping vascular inflammatory responses. Thus, our results suggest that an absence of microglia does not markedly influence BBB injury in this experimental model. Therefore, the mechanisms behind diminished monocyte infiltration are currently unclear, although decreased levels of certain cytokines, including Il-1α, IL-1ß, CX3CL1, MCP-1 or RANTES in the absence of microglia further implicate the involvement of microglia and possibly other cell types of the NVU in this process (Thurgur & Pinteaux, 2018).

5.9. P2Y12-positive microglia interact with infected neurons in human HSV-1 encephalitis

In addition to that seen in mice, we found that P2Y12-positive microglia were found recruited to HSV-1 infected neurons in human post-mortem brain tissues and phagocytosis of these cells by microglia was also observed, which was associated with increased numbers of CD68-positive brain macrophages in infected areas. As seen in mice, histological characterization of these post-mortem samples suggests that P2Y12-positive microglia isolate infected neurons, while decreased numbers of microglia and a marked increase in leukocyte recruitment was associated with more severe infection. The implications of these data for neurological diseases are far-reaching. The findings that microglia control neurotropic virus infection via P2Y12 in mice and the recruitment of P2Y12-positive microglia to HSV-1 cells was observed in the human brain suggest that microglial P2Y12 could play in general an important role in anti-viral immunity in the CNS

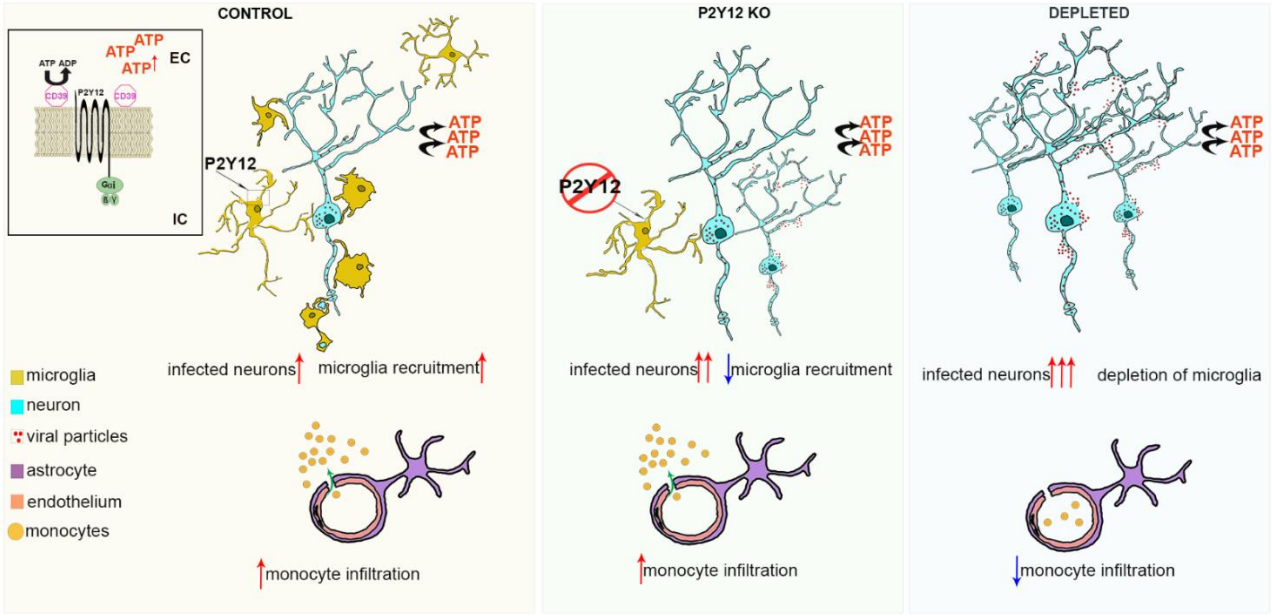

Figure 24. Summary of neuroinflammatory changes in the brain after virus infection. In wild type mice, microglia recruitment around PRV infected neurons are observed, which is associated with monocyte recruitment at sites of virus infection. ATP released by infected neurons are cleaved by CD39 leading to stimulation of P2Y12 receptors and act as a trigger for microglia recruitment and phagocytosis. Lack of microglia lead to significant increase of infected neurons and result the complete absence of monocyte recruitment. The absence of P2Y12 receptors on microglia, lead to reduced recruitment of microglial cells compared to control animals, suggesting pivotal role of P2Y12 receptor in this process, whilst monocyte infiltration is not affected by the absence of this receptor (Fekete et al. 2018).

Beyond infectious diseases caused by alphaherpesviruses such as PRV in swine or HSV-1 in humans, other viruses such as rabies, Zika virus, Alphaviruses, West-Nile virus, Epstein Barr virus, Influenza A viruses, and Enteroviruses can exhibit neurotropism and cause diverse neuropathologies in both humans and rodents (Koyanagi et al. 2017; Vermillion et al. 2017). Recent studies have also identified several links between the presence of latent neurotropic virus infections and their contribution to neurodegenerative disorders. Human herpes viruses, such as Herpes simplex 1 has the ability to disseminate in the CNS and enter a stage of latency, that allows long-term persistence. Latent neurotropic viral infections are known to alter several molecular mechanisms in the host cell, including DNA methylation, RNA synthesis, as well as levels of inflammatory and cell death-associated caspases and other enzymes in the cytosol (Zhou, Miranda-Saksena, & Saksena, 2013). These processes may interfere with several processes involved in aging and neurodegeneration such as production of misfolded proteins, lysosomal and mitochondrial function or autophagy. In case of HSV-1, there is strong evidence, that the virus alters the production and degradation of amyloid inside compromised neurons, eventually contributing to the progression of Alzheimer's disease (Fraser, Pisalyaput, & Tenner, 2010). The emerging role of neurotropic viruses in many forms of neurodegeneration (Kierdorf & Prinz, 2017) and the common molecular fingerprints of cellular injury sensed by microglia in different brain patholgies suggest that understanding the mechanisms through which microglia control the elimination of injured neurons in the brain could facilitate the development of targeted therapies in several common brain diseases.

6. Conclusion

Microgial cells are the resident immune cells of the CNS, comprising 5–10% of the total cell number in the brain. Their dynamic processes are constantly surveying the parenchyma and detect changes in neuronal activity via sensing purines, cytokines, chemokines, amino acids, and inorganic compounds. Microglia are not only important in maintaining the homeostasis of the brain but also respond to injury, infection and neurodegenerative processes through proliferation, morphological changes and secretion of a variety of pro/anti-inflammatory factors - depending on the nature of the damage (Salter & Stevens, 2017). One of the common challenges targeting the brain's defense system is viral infection, which can either be latent persistsing for the life of the host or virulent, resulting in encephalitis causing high morbidity and mortality. The mechanisms, however, through which the brain's immune system recognizes and controls viral infections propagating across synaptically linked neuronal circuits have remained unclear. In line with previous studies (Card et al., 1994; Dénes et al., 2006) using a well-established model of neurotropic alphaherpesvirus infection that reaches the brain exclusively via retrograde transsynaptic spread from the periphery, we have shown that microglia are recruited to and isolate infected neurons within hours. Our data, obtained from *in vitro* and *in vivo* studies show that microglia recruitment and clearance of infected cells require cell-autonomous P2Y12 signaling in microglia, triggered by nucleotides released from affected neurons. We also demonstrate that selective elimination of microglia by CSF1R blockade results in a marked increase in the spread of infection and egress of viral particles into the brain parenchyma. In line with this, we report, that microglia depletion, but not P2Y12 deficiency leads to characteristic neurological symptoms in virus-infected animals. We show, that loss of microglia results in the absence of recruitment of blood-borne leukocytes indicating that microglial cells contribute directly to leukocyte recruitment to the brain during virus infection. We demonstrate that this happens in a P2Y12 receptor independent way. We also identify P2Y12 mediated microglial recruitment in human HSV-1 encephalitis infected brain tissue and reveal that both microglial responses and leukocyte numbers correlate with the severity of infection. Taken together, our data reveal a key role for microglial P2Y12 in defence against neurotropic viruses, whilst P2Y12-independent actions of microglia may contribute to neuroinflammation by facilitating monocyte recruitment to the sites of infection. Understanding the mechanisms of microglial control of the fate of infected neurons could facilitate the development of targeted therapies in several common brain diseases, where the action of neurotropic viruses have been considered.

7. Summary

Neurotropic herpesviruses can establish lifelong infection in humans and contribute to severe diseases including encephalitis and neurodegeneration. Understanding immune mechanisms that are initiated in response to viral infection in the CNS is essential to develop appropriate therapies. As the main immune cell type of the brain parenchyma, microglial cells are known to be rapidly recruited to the sites of injury or infection. In previous studies, we have demonstrated that microglia form barriers around virus-infected cells in the brain. However, the functional role of microglia in defense against neurotrophic viral infection and mechanisms controlling microglia recruitment to infected neurons remained unclear.

Using a well-established model of alphaherpesvirus infection that reaches the CNS exclusively via retrograde transsynaptic spread from the periphery we have investigated the propagation of viral infection and the inflammatory responses of microglial cells without mechanical manipulation of the brain. Selective elimination of microglia resulted in a marked increase in the spread of viral infection and egress of virus particles into the brain parenchyma, which was associated with multiple neurological symptoms. We show that microglia recruitment already occurred in the early stage of virus infection, when compromised neuronal membranes are still intact, indicating that release of chemoattractant molecules, such as ATP, may act as an early signal of injury. By using various *in vitro* and *in vivo* techniques we showed that microglial recruitment and clearance of infected cells require P2Y12 signaling, which is triggered by ATP and other nucleotides released by compromised neurons. We also identify microglia, as key contributors to inflammatory monocyte recruitment into the infected brain, which process is largely independent of the presence of the P2Y12 receptor. In HSV-1 infected human brain tissue we show that microglia express the P2Y12 receptor and are recruited to infected neurons in the human brain during viral encephalitis. We demonstrate further that microglial responses and leukocyte numbers correlate with the severity of infection both in mouse and the human brain. Our data indicate that microglia play a pivotal role in controlling viral infections in the brain. Furthermore, the emerging role for neurotropic viruses in various forms of neurodegeneration suggests that understanding the mechanisms through which microglia control neurotropic viral infections could facilitate the development of more effective therapies in common CNS diseases.

8. Összefoglalás

A neurotróp vírusfertőzések súlyos problémát okoznak világszerte, mivel képesek akár évekig lappangó, látens fertőzést kialakítani, valamint olyan súlyos betegségeket okozni, mint az agyvelő- vagy agyhártyagyulladás. Emellett számos neurodegeneratív betegség kialakulásához járulhatnak hozzá. A neurodegenerációs folyamatokhoz a gyulladás következtében aktiválódó mikroglia sejtek, és a perifériáról toborzódó immunsejtek által kiváltott különböző immunmechanizmusok nagyban hozzájárulnak. Ezért is fontos megértenünk, hogy hogyan is vezérli a mikroglia a sérülés, vagy fertőzés hatására kialakuló immunfolyamatokat a központi idegrendszerben. Korábbi kutatásunk során megmutattuk, hogy a mikroglia képes izolálni a vírussal fertőzött neuronokat. Habár az alapvető antivirális immunfolyamatok részben ismertek az agyban, a mikroglia toborzódás pontos mechanizmusai továbbra sincsenek feltérképezve. Kutatásunk során a herpeszvírusok családjába tartozó neurotróp Pseudorabies vírust (PRV) használtunk, amely kizárólag retrográd, transszinaptikus úton terjed a perifériás ganglionokból a központi idegrendszerbe, így az agy mechanikus manipulációja nélkül tudjuk a fertőzés következtében kialakuló mikrogliális immunválaszt vizsgálni. Kimutattuk, hogy szelektív mikroglia depléciót követően a vírusfertőzés mértéke szignifikánsan megnő, valamint a fagocitózis hiányában a vírus partikulumok az extracelluláris térbe kerülnek, amely súlyos neuropatológiás tüneteket eredményez. Megállapítottuk, hogy a mikroglia toborzódás már a fertőzés korai szakaszában megkezdődik, amikor a fertőzött neuronok membránja még inktakt, azaz a fertőzött neuronok már ebben a stádiumban kibocsáthatnak kemotaktikus molekulákat. I*n vitro* és *in vivo* módszerek segítségével megmutattuk, hogy a mikroglia toborzódás és fagocitózis P2Y12 receptor függő, amit a fertőzött neuronokból felszabaduló ATP és más nukleotidok aktiválnak. Kimutattuk, hogy a mikroglia kulcsfontosságú szerepet játszik a gyulladás következtében kialakuló leukocita infiltráció koordinálásában is. Ezen folyamat független a P2Y12 receptor jelenlététől. Megfigyeltük, hogy mikroglia depletált, vírusfertőzött állatokban a vér-agy gát sérülés ellenére sem történik leukocita infiltráció, amelyből arra következtettünk, hogy a mikrogliának ebben a folyamatban kiemelten fontos szerepe lehet. Kimutattuk, hogy humán HSV-1 enkefalitiszt követően a P2Y12 pozitív mikroglia toborzódik a fertőzött neuronokhoz. A mikroglia toborzódás és az infiltrálódott leukocita szám korrelál a fertőzés súlyosságával mind egér, mind emberi agyban. Eredményeink ezúton hozzájárulhatnak célzott terápiás módszerek kifejlesztéséhez a központi idegrendszert érintő neurotróp vírusfertőzések és neurodegeneratív kórképek kezelésében.

9. References

Abbott N. J., Rönnbäck L., Hansson E. (2006) Astrocyte-endothelial interactions at the blood-brain barrier. Nature Reviews Neuroscience. 7(1):41–53.

Ajami B., Bennett J. L., Krieger C., Tetzlaff W., Rossi F. M. V. (2007) Local self-renewal can sustain CNS microglia maintenance and function throughout adult life. Nature Neuroscience. 10(12): 1538-43.

Archer R. G. E., Pitelka V., Hammond J. R. (2004) Nucleoside transporter subtype expression and function in rat skeletal muscle microvascular endothelial cells. British Journal of Pharmacology. 143(1):202–214.

Arcuri C., Mecca C., Bianchi R., Giambanco I., Donato R. (2017) The Pathophysiological Role of Microglia in Dynamic Surveillance, Phagocytosis and Structural Remodeling of the Developing CNS. Frontiers in Molecular Neuroscience. 19(10):191.

Aspelund A., Antila S., Proulx S. T., Karlsen T. V., Karaman S., Detmar M., Wiig H., Alitalo K. (2015) A dural lymphatic vascular system that drains brain interstitial fluid and macromolecules. The Journal of Experimental Medicine. 212(7):991–999.

Bardina S. V, Michlmayr D., Hoffman K. W., Obara C. J., Sum J., Charo I. F., Lu W., Pletnev A. G., Lim J. K. (2015) Differential Roles of Chemokines CCL2 and CCL7 in Monocytosis and Leukocyte Migration during West Nile Virus Infection. The Journal of Immunology. 195(9):4306– 4318.

Bauer H.-C., Krizbai I. A., Bauer H., Traweger A. (2014) “You Shall Not Pass”-tight junctions of the blood brain barrier. Frontiers in Neuroscience. 3(8):392.

Becker M. M., Graham R. L., Donaldson E. F., Rockx B., Sims A. C., Sheahan T., Pickles R. J., Corti D., Johnston R. E., Baric R. S., Denison M.R. (2008) Synthetic recombinant bat SARS-like coronavirus is infectious in cultured cells and in mice. Proceedings of the National Academy of Sciences of the United States of America. 105(50):19944–19949.

Benakis C., Garcia-Bonilla L., Iadecola C., Anrather J. (2015) The role of microglia and myeloid immune cells in acute cerebral ischemia. Frontiers in Cellular Neuroscience. 14(8):461

Bergmann C. C., Ramakrishna C., Kornacki M., Stohlman S. A. (2014) Impaired T Cell Immunity in B Cell-Deficient Mice Following Viral Central Nervous System Infection. The Journal of Immunology. 167(3):1575–1583.

Boldogkői Z., Balint K., Awatramani G. B., Balya D., Busskamp V., Viney T. J., Lagali P. S., Duebel J., Pásti E., Tombácz D., Tóth J., Takács F. I., Gross Scherf B., Roska B. (2009) Genetically timed, activity-sensor and rainbow transsynaptic viral tools. Nature Methods. 6(2):127-30.

Boldogköi Z., Reichart A., Tóth I. E., Sik A., Erdélyi F., Medveczky I., Llorens-Cortes C., Palkovits M., Lenkei Z. (2002) Construction of recombinant pseudorabies viruses optimized for labeling and neurochemical characterization of neural circuitry. Molecular Brain Research. 109(1–2):105–118.

Boldogköi Z., Sík A., Dénes Á., Reichart A., Toldi J., Gerendai I., Kovács K. J., Palkovits M. (2004) Novel tracing paradigms - Genetically engineered herpesviruses as tools for mapping functional circuits within the CNS: Present status and future prospects. Progress in Neurobiology. 72(6):417–445.

Brittle E. E., Reynolds A. E., Enquist L. W. (2004) Two Modes of Pseudorabies Virus Neuroinvasion and Lethality in Mice. Journal of Virology. 78(23):12951–12963.

Bruttger J., Karram K., Wörtge S., Regen T., Marini F., Hoppmann N., Klein M., Blank T., Yona S., Wolf Y., Mack M., pinteaux E., Müller W., Zipp F., Binder H., Bopp t., Prinz M., Jung S., Waisman A. (2015) Genetic Cell Ablation Reveals Clusters of Local Self-Renewing Microglia in the Mammalian Central Nervous System. Immunity. 43(1):92–106.

Buiting A. M. J., Rooijen N. Van. (1994) Liposome Mediated Depletion of Macrophages: An Approach for Fundamental Studies. Journal of Drug Targeting. 2(5):357–362.

Card J. P. (1998) Exploring brain circuitry with neurotropic viruses: New horizons in neuroanatomy. The Anatomical Record. 253(6):176–185.

Card J. P. (2001) Neurovirology Viruses and the Brain. In Advances in Virus Research.

Card J., Rinaman L., Lynn R., Lee B., Meade R., Miselis R., Enquist L. (2018) Pseudorabies virus infection of the rat central nervous system: ultrastructural characterization of viral replication, transport, and pathogenesis. The Journal of Neuroscience. 13(6):2515–2539.

Chen Z., Zhong D., Li G. (2019) The role of microglia in viral encephalitis: A review. Journal of Neuroinflammation. 16(1):1–12.

Chiovini B., Turi G. F., Katona G., Kaszás A., Pálfi D., Maák P., Szalay G., Szabó M. F., Szabó G., Szadai Z., Káli S., Rózsa B. (2014) Dendritic Spikes Induce Ripples in Parvalbumin Interneurons during Hippocampal Sharp Waves. Neuron. 82(4):908–924.

Csonka T., Szepesi R., Bidiga L., Péter M., Klekner A., Hutóczky G., Csiba L., Méhes G., Hortobágyi T. (2013) The diagnosis of herpes encephalitis--a case-based update. Ideggyogyaszati Szemle. 66(9–10):337–342.

Czöndör K., Ellwanger K., Fuchs Y. F., Lutz S., Gulyás M., Mansuy I. M., Hausser A., Pfizenmaier K., Schlett K. (2009) Protein Kinase D Controls the Integrity of Golgi Apparatus and the Maintenance of Dendritic Arborization in Hippocampal Neurons. Molecular Biology of the Cell. 20(7):2108–2120.

Daneman R. (2012) The blood-brain barrier in health and disease. Annals of Neurology. 72(5):648–672.

Davalos D., Grutzendler J., Yang G., Kim J. V, Zuo Y., Jung S., Littman D. R., Dustin M. L., Gan W.-B. (2005). ATP mediates rapid microglial response to local brain injury in vivo. Nature Neuroscience. 8(6):752–758.

Dénes A., Boldogkoi Z., Hornyák A., Palkovits M., Kovács K. J. (2006). Attenuated pseudorabies virus-evoked rapid innate immune response in the rat brain. Journal of Neuroimmunology. 180(1–2):88–103.

Dissing-Olesen L., LeDue J. M., Rungta R. L., Hefendehl J. K., Choi H. B., MacVicar B. A. (2014) Activation of Neuronal NMDA Receptors Triggers Transient ATP-Mediated Microglial Process Outgrowth. The Journal of Neuroscience. 34(32):10511 – 10527.

Donat C. K., Scott G., Gentleman S. M., Sastre M. (2017) Microglial activation in traumatic brain injury. Frontiers in Aging Neuroscience. 28(9):208.

Elmore M. R. P., Najafi A. R., Koike M. A., Dagher N. N., Spangenberg E. E., Rice R. A., Kitazawa M., Matusow B., Nguyen H., West B. L., Green K. N. (2014) Colony-Stimulating Factor 1 Receptor Signaling Is Necessary for Microglia Viability, Unmasking a Microglia Progenitor Cell in the Adult Brain. Neuron. 82(2):380–397.

Engelhardt B. (2008) Immune cell entry into the central nervous system: Involvement of adhesion molecules and chemokines. Journal of the Neurological Sciences. 274(1–2): 23–26.

Engelhardt B., Liebner S. (2014) Novel insights into the development and maintenance of the blood-brain barrier. Cell and Tissue Research. 355(3):687–699.

Engelhardt B., Sorokin L. (2009) The blood-brain and the blood-cerebrospinal fluid barriers: Function and dysfunction. Seminars in Immunopathology. 31(4):497–511.

Enquist L. W., Leib D. A. (2016) Intrinsic and Innate Defenses of Neurons: Détente with the Herpesviruses. Journal of Virology. 91(1):1–6.

Erblich B., Zhu L., Etgen A. M., Dobrenis K., Pollard J. W. (2011) Absence of colony stimulation factor-1 receptor results in loss of microglia, disrupted brain development and olfactory deficits. PLoS ONE. 6(10):e26317.

Eyo U. B., Gu N., De S., Dong H., Richardson J. R., Wu L.-J. (2015) Modulation of microglial process convergence toward neuronal dendrites by extracellular calcium. The Journal of Neuroscience : The Official Journal of the Society for Neuroscience. 35(6):2417–2422.

Faraco G., Park L., Anrather J., Iadecola C. (2017) Brain perivascular macrophages: characterization and functional roles in health and disease. Journal of Molecular Medicine. 95(11):1143–1152.

Färber K., Kettenmann H. (2006) Purinergic signaling and microglia. Pflugers Archiv European Journal of Physiology. 452(5):615–621.

Fields R. D., Burnstock G. (2006) Purinergic signalling in neuron–glia interactions. Nature Reviews Neuroscience. 7(6):423–436.

Fraser D. A., Pisalyaput K., Tenner A. J. (2010) C1q enhances microglial clearance of apoptotic neurons and neuronal blebs, and modulates subsequent inflammatory cytokine production. Journal of Neurochemistry. 112(3):733–743.

Frieler R. A., Nadimpalli S., Boland L. K., Xie A., Kooistra L. J., Song J., Chung Y., Cho K. W., Lumeng C. N., Wang M. M., Mortensen R. M. (2015) Depletion of macrophages in CD11b diphtheria toxin receptor mice induces brain inflammation and enhances inflammatory signaling during traumatic brain injury. Brain Research. 22(1624):103–112.

Garcia J. M., Stillings S. A., Leclerc J. L., Phillips H., Edwards N. J., Robicsek S. A., Hoh B. L., Blackburn S., Doré S. (2017) Role of Interleukin-10 in Acute Brain Injuries. Frontiers in Neurology. 12(8):244.

Getts D. R., Chastain E. M. L., Terry R. L., Mille, S. D. (2013) Virus infection, antiviral immunity, and autoimmunity. Immunological Reviews. 255(1):197–209.

Ginhoux F., Greter M., Leboeuf M., Nandi S., See P., Mehler M. F., Conway S. J., Ng L. G., Stanley E. R., Igor M., Merad M. (2010) Fate map analysis reveals that adult mice derive from primitive macrophages. Science. 330(6005):841–845.

Goldmann T., Wieghofer P., Jordão M. J. C., Prutek F., Hagemeyer N., Frenzel K., Amann L., Staszewski O., Kierdorf K., Krueger M., Locatelli G., Hochgerner H., Zeiser R., Epelman S., Geissmann F., Priller J., Rossi F. M., Bechmann I., Kerschensteiner M., Linnarsson S., Jung S., Prinz M. (2016) Origin, fate and dynamics of macrophages at central nervous system interfaces. Nature Immunology. 17(7):797–805.

Gönci B., Németh V., Balogh E., Szabó B., Dénes Á., Környei Z., Vicsek T. (2010) Viral epidemics in a cell culture: novel high resolution data and their interpretation by a percolation theory based model. PloS One. 5(12):e15571.

Han X., Li Q., Lan X., EL-Mufti L., Ren H., Wang J. (2019) Microglial Depletion with Clodronate Liposomes Increases Proinflammatory Cytokine Levels, Induces Astrocyte Activation, and Damages Blood Vessel Integrity. Molecular Neurobiology. 56(9):6184-6196

Hanisch U. K., Kettenmann H. (2007) Microglia: Active sensor and versatile effector cells in the normal and pathologic brain. Nature Neuroscience. 10(11):1387–1394.

Haynes S. E., Hollopeter G., Yang G., Kurpius D., Dailey M. E., Gan W.-B., Julius D. (2006) The P2Y12 receptor regulates microglial activation by extracellular nucleotides. Nature Neuroscience. 9(12):1512–1519.

Heppner F. L., Greter M., Marino D., Falsig J., Raivich G., Hövelmeyer N., Waisman A., Rülicke T., Prinz M., Priller J., Becher B., Aguzzi A. (2005) Experimental autoimmune encephalomyelitis repressed by microglial paralysis. Nature Medicine. 11(2):146–152.

Iijima N., Mattei L. M., Iwasaki A. (2011) Recruited inflammatory monocytes stimulate antiviral Th1 immunity in infected tissue. Proceedings of the National Academy of Sciences of the United States of America. 108(1):284–289.

Jansen A. S. P., Van Nguyen X., Karpitskiy V., Mettenleiter T. C., Loewy A. D. (1995) Central Command Neurons of the Sympathetic Nervous System: Basis of the Fight-or-Flight Response. Science. 270(5236):644 – 646.

Kaneko M., Sano K., Nakayama J., Amano N. (2010) Nasu-Hakola disease: The first case reported by Nasu and review. Neuropathology. 30(5):463–470.

Katona G., Szalay G., Maák P., Kaszás A., Veress M., Hillier D., Chiovini B., Vizi E. S., Roska B., Rózsa B. (2012) Fast two-photon in vivo imaging with three-dimensional random-access scanning in large tissue volumes. Nature Methods. 9(2):201-8.

Kettenmann H., Kirchhoff F., Verkhratsky A. (2013) Microglia: New Roles for the Synaptic Stripper. Neuron. 77(1):10–18.

Kierdorf K., Prinz M. (2017) Microglia in steady state Find the latest version : Microglia in steady state. J Clin Invest. 127(9):3201–3209.

Kipnis J., Alitalo K., Louveau A., Nedergaard M., Plog B. A., Antila S. (2017) Understanding the functions and relationships of the glymphatic system and meningeal lymphatics. Journal of Clinical Investigation. 127(9):3210–3219.

Kittel A. (1999) Lipopolysaccharide Treatment Modifies pH- and Cation-dependent Ecto-ATPase Activity of Endothelial Cells. Journal of Histochemistry & Cytochemistry. 47(3):393–399.

Klein, R. S., Garber, C., Funk, K. E., Salimi, H., Soung, A., Kanmogne, M., Manivasagam, S., Agner, S., Cain, M. (n.d.). Neuroinflammation During RNA Viral Infections. 26(37):73–95.

Klein R. S., Hunter C. A. (2017) Protective and Pathological Immunity during Central Nervous System Infections. Immunity. 46(6):891–909.

Kleinberger G., Brendel M., Mracsko E., Wefers B., Groeneweg L., Xiang,X., Focke C., Deußing M., Suárez-Calvet M., Mazaheri F., Parhizkar S., Pettkus N., Wurst W., Feederle R., Bartenstein P., Mueggler t., Knussel I., Rominger A., Haass C. (2017) The FTD-like syndrome causing TREM2 T66M mutation impairs microglia function, brain perfusion, and glucose metabolism. The EMBO Journal. 36(13):1837–1853.

Koizumi S., Ohsawa K., Inoue K., Kohsaka S. (2013) Purinergic receptors in microglia: Functional modal shifts of microglia mediated by P2 and P1 receptors. Glia. 61(1):47–54.

Környei Z., Szlávik V., Szabó B., Gócza E., Czirók A., Madarász E. (2005) Humoral and contact interactions in astroglia/stem cell co-cultures in the course of glia-induced neurogenesis. Glia. 49(3):430–444.

Koyanagi N., Imai T., Shindo K., Sato A., Fujii W., Ichinohe T., Takemura N., Kakuta S., Uematsu S., Kiyono H., Maruzuru Y., Arii Y., Kato A., Kawaguchi Y. (2017) Herpes simplex virus-1 evasion of CD8+ T cell accumulation contributes to viral encephalitis. Journal of Clinical Investigation. 127(10):3784–3795.

Koyuncu O. O., Hogue I. B., Enquist L. W. (2013) Virus infections in the nervous system. Cell Host and Microbe. 13(4):379–393.

Kramer T., Enquist L. W. (2013) Directional spread of alphaherpesviruses in the nervous system. Viruses. 5(2):678–707.

Kyle Austin S., Dowd K. A. (2014) B cell response and mechanisms of antibody protection to west nile virus. Viruses. 6(3):1015–1036.

Lanteri M. C., O'Brien K. M., Purtha W. E., Cameron M. J., Lund J. M., Owen R. E., Heitman J. W., Custer B., Hirschkorn D. F., Tobler L. H., Kiely N., Prince H. E., Ndhlovu L. C., nicon D. F., Kamel H. T., Kelvin D. J., Busch M. P., Rudensky A. Y., Diamond M. S., Norris P. J. (2009) Tregs control the development of symptomatic West Nile virus infection in humans and mice. The Journal of Clinical Investigation. 119(11):3266–3277.

Li Q., Barres B. A. (2018) Microglia and macrophages in brain homeostasis and disease. Nature Reviews. Immunology. 18(4):225–242.

Lokensgard J. R., Cheeran M. C.-J., Hu S., Gekker G., Peterson P. K. (2002) Glial Cell Responses to Herpesvirus Infections: Role in Defense and Immunopathogenesis. The Journal of Infectious Diseases. 1(186):171–179.

London A., Cohen M., Schwartz M. (2013) Microglia and monocyte-derived macrophages: functionally distinct populations that act in concert in CNS plasticity and repair. Frontiers in Cellular Neuroscience. 8(7):34.

Lopes Pinheiro M. A., Kooij G., Mizee M. R., Kamermans A., Enzmann G., Lyck R., Schwaninger M., Engelhardt B., de Vries H. E. (2016) Immune cell trafficking across the barriers of the central nervous system in multiple sclerosis and stroke. Biochimica et Biophysica Acta - Molecular Basis of Disease. 1862(3):461–471.

Lund H., Pieber M., Harris R. A. (2017) Lessons learned about neurodegeneration from microglia and monocyte depletion studies. Frontiers in Aging Neuroscience. 28(9):234.

Madry C., Kyrargyri V., Arancibia-Cárcamo I. L., Jolivet R., Kohsaka S., Bryan R. M., Attwell D. (2018) Microglial Ramification, Surveillance, and Interleukin-1β Release Are Regulated by the Two-Pore Domain K(+) Channel THIK-1. Neuron. 97(2):299-312.

Marques C. P., Hu S., Sheng W., Lokensgard J. R. (2006) Microglial cells initiate vigorous yet non-protective immune responses during HSV-1 brain infection. Virus Research. 121(1):1–10.

McCarthy K. M., Tank D. W., Enquist L. W. (2009) Pseudorabies Virus Infection Alters Neuronal Activity and Connectivity In Vitro. PLOS Pathogens. 5(10):e1000640.

McColl B. W., McGregor A. L., Wong A., Harris J. D., Amalfitano A., Magnoni S., Baker A. H., Dickson G., Horsburgh K. (2006) APOE ε3 Gene Transfer Attenuates Brain Damage after Experimental Stroke. Journal of Cerebral Blood Flow & Metabolism. 27(3):477–487.

McFarland M. D., Hill H. T., Tabatabai L. B. (1987) Characterization of virulent and attenuated strains of pseudorabies virus for thymidine kinase activity, virulence and restriction patterns. Canadian Journal of Veterinary Research = Revue Canadienne de Recherche Veterinaire. 51(3):334–339.

McGavern D. B., Kang S. S. (2011) Illuminating viral infections in the nervous system. Nature Reviews Immunology. 11(5):318–329.

Miller K. D., Schnell M. J., Rall G. F. (2016) Keeping it in check: chronic viral infection and antiviral immunity in the brain. Nature Reviews Neuroscience.17(12):766-776.

Miranda-Saksena M., Boadle R. A., Armati P., Cunningham A. L. (2002) In rat dorsal root ganglion neurons, herpes simplex virus type 1 tegument forms in the cytoplasm of the cell body. Journal of Virology. 76(19):9934–9951.

Muoio V., Persson P. B., Sendeski M. M. (2014) The neurovascular unit - concept review. Acta Physiologica. 210(4):790–798.

Najafi A. R., Crapser J., Jiang S., Ng, W., Mortazavi A., West B. L., Green K. N. (2018) A limited capacity for microglial repopulation in the adult brain. Glia. 66(11):2385–2396.

Nikodemova M., Kimyon R. S., De I., Small A. L., Collier L. S., Watters J. J. (2015) Microglial numbers attain adult levels after undergoing a rapid decrease in cell number in the third postnatal week. Journal of Neuroimmunology. 15(278):280–288.

Ousman S. S., Kubes P. (2012) Immune surveillance in the central nervous system. Nature Neuroscience. 15(8):1096–1101.

Pachnio A., Begum J., Fox A., Moss P. (2015) Acyclovir Therapy Reduces the CD4+ T Cell Response against the Immunodominant pp65 Protein from Cytomegalovirus in Immune Competent Individuals. PLoS ONE. 10(4):1–10.

Paloneva J., Manninen T., Christman G., Hovanes K., Mandelin J., Adolfsson R., Bianchin M., Bird T., Miranda R., Salmaggi A., Tranebjaerg L., Konttinen Y., Peltonen L. (2002) Mutations in two genes encoding different subunits of a receptor signaling complex result in an identical disease phenotype. American Journal of Human Genetics. 71(3): 656–662.

Paolicelli R. C., Ferretti M. T. (2017) Function and dysfunction of microglia during brain development: Consequences for synapses and neural circuits. Frontiers in Synaptic Neuroscience. 9(9):1-17.

Parkhurst C. N., Yang G., Ninan I., Savas J. N., Yates J. R., Lafaille J. J., Hempstead B. L., Littman D. R., Gan W. B. (2013) Microglia promote learning-dependent synapse formation through brain-derived neurotrophic factor. Cell. 155(7):1596–1609.

Peri F., Nüsslein-Volhard C. (2008) Live Imaging of Neuronal Degradation by Microglia Reveals a Role for v0-ATPase a1 in Phagosomal Fusion In Vivo. Cell. 133(5):916–927.

Phares T. W., Marques C. P., Stohlman S. A., Hinton D. R., Bergmann C. C. (2011) Factors supporting intrathecal humoral responses following viral encephalomyelitis. Journal of Virology. 85(6):2589–2598.

Planas A. M. (2018) Role of Immune Cells Migrating to the Ischemic Brain. Stroke. 49(9):2261–2267.

Pomeranz L. E., Reynolds A. E., Hengartner C. J. (2005) Molecular Biology of Pseudorabies Virus: Impact on Neurovirology and Veterinary Medicine. Microbiology and Molecular Biology Reviews. 69(3):462–500.

Pósfai B., Cserép C., Orsolits B., Dénes Á. (2018) New Insights into Microglia–Neuron Interactions: A Neuron's Perspective. Neuroscience. 1(405):103-117.

Prinz M., Erny D., Hagemeyer N. (2017) Ontogeny and homeostasis of CNS myeloid cells. Nature Immunology. 18(4):385–392.

Prinz M., Mildner A. (2011) Microglia in the CNS: Immigrants from another world. Glia. 59(2):177–187.

Prinz M., Priller J. (2014) Microglia and brain macrophages in the molecular age: from origin to neuropsychiatric disease. Nature Reviews Neuroscience. 15(5):300-312.

Prinz M., Priller J. (2017) The role of peripheral immune cells in the CNS in steady state and disease. Nature Neuroscience. 20(2):136-144.

Prinz M., Priller J., Sisodia S. S., Ransohoff R. M. (2011) Heterogeneity of CNS myeloid cells and their roles in neurodegeneration. Nature Neuroscience. 14(10):1227–1235.

Ransohoff R. M. (2016) How neuroinflammation contributes to neurodegeneration. Science. 353(6301):777-783.

Ransohoff R. M., Engelhardt B. (2012) The anatomical and cellular basis of immune surveillance in the central nervous system. Nature Reviews Immunology. 12(9):623–635.

Rassnick S., Enquist L. W., Sved A. F., Card J. P. (1998) Pseudorabies Virus-Induced Leukocyte Trafficking into the Rat Central Nervous System. Journal of Virology. 72(11):9181 – 9191.

Reinert L. S., Harder L., Holm C. K., Iversen M. B., Horan K. A., Dagnæs-Hansen F., Ulhøi B. P., Holm T. H., Mogensen T. H., Owens T., Nyengaard J. R., Thomsen A. R., Paludan S. R. (2012) TLR3 deficiency renders astrocytes permissive to herpes simplex virus infection and facilitates establishment of CNS infection in mice. The Journal of Clinical Investigation. 122(4):1368–1376.

Reinert L. S., Lopušná K., Winther H., Sun C., Thomsen M. K., Nandakumar R., Mogensen T. H., Meyer M., Vægter C., Nyengaard J. R., Fitzgerald K. A., Paludan S. R. (2016) Sensing of HSV-1 by the cGAS–STING pathway in microglia orchestrates antiviral defence in the CNS. Nature Communications. 10(7):13348.

Rinaman L., Card J. P., Enquist L. W. (1993) Spatiotemporal responses of astrocytes, ramified microglia, and brain macrophages to central neuronal infection with pseudorabies virus. Journal of Neuroscience. 13(2):685–702.

Rodrigues R. J., Tomé A. R., Cunha R. A. (2015) ATP as a multi-target danger signal in the brain. Frontiers in Neuroscience. 28(9):148.

Rojas O. L., Narváez C. F., Greenberg H. B., Angel J., Franco, M. A. (2008) Characterization of rotavirus specific B cells and their relation with serological memory. Virology. 380(2):234–242.

Rubino S. J., Mayo L., Wimmer I., Siedler V., Brunner F., Hametner S., Madi A., Lanser A., Moreira T., Donnelly D., Cox L., Rezende R. M., Butovsky O., Lassmann H., Weiner H. L. (2018) Acute microglia ablation induces neurodegeneration in the somatosensory system. Nature Communications. 9(1):4578.

Russo M. V., McGavern D. B. (2015) Immune Surveillance of the CNS following Infection and Injury. Trends in Immunology. 36(10):637–650.

Rustenhoven J., Jansson D., Smyth L. C., Dragunow M. (2017) Brain Pericytes As Mediators of Neuroinflammation. Trends in Pharmacological Sciences. 38(3):291–304.

Salter M. W., Stevens B. (2017) Microglia emerge as central players in brain disease. Nature Medicine. 23(9):1018–1027.

Saura J., Tusell J. M., Serratosa J. (2003) High-yield isolation of murine microglia by mild trypsinization. Glia. 44(3):183–189.

Schafer D. P., Lehrman E. K., Kautzman A. G., Koyama R., Mardinly A. R., Yamasaki R., Ransohoff R. M., Greenberg M. E., Barres B. A., Stevens B. (2012) Microglia Sculpt Postnatal Neural Circuits in an Activity and Complement-Dependent Manner. Neuron.74(4):691–705.

Schmidt S. P., Hagemoser W. A., Kluge J. P. (1992) The Anatomical Location of Neural Structures Most Optimally Sampled for Pseudorabies (Aujeszky's Disease) in Sheep. Journal of Veterinary Diagnostic Investigation. 4(2):206–208.

Shemer A., Erny D., Jung S., Prinz M. (2015) Microglia Plasticity During Health and Disease: An Immunological Perspective. Trends in Immunology. 36(10):614–624.

Sperlágh B., Illes P. (2007) Purinergic modulation of microglial cell activation. Purinergic Signalling. 3(1–2):117–127.

Sperlágh B., Illes P. (2014) P2X7 receptor: an emerging target in central nervous system diseases. Trends in Pharmacological Sciences. 35(10):537–547.

Squarzoni P., Oller G., Hoeffel G., Pont-Lezica L., Rostaing P., Low, D., Bessis A., Ginhoux F., Garel S. (2014) Microglia Modulate Wiring of the Embryonic Forebrain. Cell Reports. 8(5):1271–1279.

Steel C. D., Breving K., Tavakoli S., Kim W.-K., Sanford L. D., Ciavarra R. P. (2014) Role of peripheral immune response in microglia activation and regulation of brain chemokine and proinflammatory cytokine responses induced during VSV encephalitis. Journal of Neuroimmunology. 267(1–2):50–60.

Stevens B., Schafer D. P. (2018) Roles of microglia in nervous system development, plasticity, and disease. Developmental Neurobiology. 78(6):559–560.

Stevenson P. G., Austyn J. M., Hawke S. (2002) Uncoupling of virus-induced inflammation and anti-viral immunity in the brain parenchyma. Journal of General Virology. 83(7):1735–1743.

Szalay G., Martinecz B., Lénárt N., Környei Z., Orsolits B., Judák L., Császár,E., Fekete R., West B. L., Katona G., Rózsa B., Dénes Á. (2016) Microglia protect against brain injury and their selective elimination dysregulates neuronal network activity after stroke. Nature Communications. 3(7):11499.

Szpara M. L., Kobiler O., Enquist L. W. (2010) A common neuronal response to alphaherpesvirus infection. Journal of Neuroimmune Pharmacology. 5(3):418–427.

Taylor M. P., Kobiler O., Enquist L. W. (2012) Alphaherpesvirus axon-to-cell spread involves limited virion transmission. Proceedings of the National Academy of Sciences. 109(42):17046–17051.

Terry R. L., Getts D. R., Deffrasnes C., van Vreden C., Campbell I. L., King N. J. C. (2012) Inflammatory monocytes and the pathogenesis of viral encephalitis. Journal of Neuroinflammation. 9(1):1.

Thurgur H., Pinteaux E. (2018) Microglia in the Neurovascular Unit: Blood–Brain Barrier–microglia Interactions After Central Nervous System Disorders. Neuroscience. 1(405):55-67.

Tietz S., Engelhardt B. (2015) Brain barriers: Crosstalk between complex tight junctions and adherens junctions. Journal of Cell Biology. 209(4):493–506.

Tremblay M.-È., Stevens B., Sierra A., Wake H., Bessis A., Nimmerjahn A. (2011) The role of microglia in the healthy brain. The Journal of Neuroscience : The Official Journal of the Society for Neuroscience. 31(45):16064–16069.

Tsai T. T., Chen, C. L., Lin Y. S., Chang C. P., Tsai C. C., Cheng Y. L., Huang C. C., Ho C. J., Lee Y. C., Lin L. T., Jhan M. K., Lin C. F. (2016) Microglia retard dengue virus-induced acute viral encephalitis. Scientific Reports. 9(6):27670.

Varvel N. H., Grathwohl S. A., Baumann F., Liebig C., Bosch A., Brawek B., Thal D. R., Charo I. F., Heppner F. L., Aguzzi A., Garaschuk O., Ransohoff R. M., Jucker M. (2012) Microglial repopulation model reveals a robust homeostatic process for replacing CNS myeloid cells. Proceedings of the National Academy of Sciences. 109(44):18150–18155.

Vermillion M. S., Lei J., Shabi Y., Baxter V. K., Crilly N. P., McLane M., Griffin D. E., Pekosz A., Klein S. L., Burd I. (2017) Intrauterine Zika virus infection of pregnant immunocompetent mice models transplacental transmission and adverse perinatal outcomes. Nature Communications. 21(8):14575.

Waisman A., Ginhoux F., Greter M., Bruttger J. (2015) Homeostasis of Microglia in the Adult Brain: Review of Novel Microglia Depletion Systems. Trends in Immunology.36(10):625–636.

Wheeler D. L., Sariol A., Meyerholz D. K., Perlman S. (2018) Microglia are required for protection against lethal coronavirus encephalitis in mice. Journal of Clinical Investigation. 128(3):931–943.

Wilkinson F. L., Sergijenko A., Langford-Smith K. J., Malinowska M., Wynn R. F., Bigger B. W. (2013) Busulfan Conditioning Enhances Engraftment of Hematopoietic Donor-derived Cells in the Brain Compared With Irradiation. Molecular Therapy. 21(4):868–876.

Wolf S. A., Boddeke H. W. G. M., Kettenmann H. (2017) Microglia in Physiology and Disease. Annual Review of Physiology. 79(1):619–643.

Wong A. D., Ye M., Levy A. F., Rothstein J. D., Bergles D. E., Searson P. C. (2013) The blood-brain barrier: an engineering perspective. Frontiers in Neuroengineering. 6(7):1-22.

Yamazaki Y., Kanekiyo T. (2017) Blood-brain barrier dysfunction and the pathogenesis of Alzheimer's disease. International Journal of Molecular Sciences. 18(9):1965.

Zhang J., Liu H., Wei B. (2017) Immune response of T cells during herpes simplex virus type 1 (HSV-1) infection. Journal of Zhejiang University-SCIENCE B. 18(4):277–288.

Zhou L., Miranda-Saksena M., Saksena N. K. (2013) Viruses and neurodegeneration. Virology Journal. 10(1):172.

10. List of publications

Publications related to this thesis

Fekete R, Cserép C, Lénárt N, Tóth K, Orsolits B, Martinecz B, Méhes E, Szabó B, Németh V, Gönci B, Sperlágh B, Boldogkői Z, Kittel Á, Baranyi M, Ferenczi S, Kovács K, Szalay G, Rózsa B, Webb C, Kovacs GG, Hortobágyi T, West BL, Környei Z, Dénes Á (2018) *Microglia control the spread of neurotropic virus infection vira P2Y12 signalling and recruit monocytes through P2Y12-independent mechanisms*. **Acta Neuropahtologica** 136(3):461-482. doi: 10.1007/s00401-018-1885-0.

Szalay G, Martinecz B, Lénárt N, Környei Z, Orsolits B, Judák L, Császár E, **Fekete R**, West BL, Katona G, Rózsa B, Dénes Á (2016) *Microglia protect against brain injury and their selective elimination dysregulates neuronal network activity after stroke*. **Nature Communications** 7:11499. doi: 10.1038/ncomms11499.

Other publications

Singel KL, Grzankowski KS, Khan ANMNH, Grimm MJ, D'Auria AC, Morrell K, Eng KH, Hylander B, Mayor PC, Emmons TR, Lénárt N, **Fekete R**, Környei Z, Muthukrishnan U, Gilthorpe JD, Urban CF, Itagaki K, Hauser CJ, Leifer C, Moysich KB, Odunsi K, Dénes Á, Segal BH (2019) *Mitochondrial DNA int he tumour microencironment activates neutrophils and is associated with worse outcomes in patients with advanced epithelial ovarian cancer.* **Br J Cancer** 120(2):207-217. doi: 10.1038/s41416-018-0339-8

Nagy AM, **Fekete R**, Horvath G, Koncsos G, Kriston C, Sebestyen A, Giricz Z, Kornyei Z, Madarasz E, Tretter L (2018) *Versatility of microglial bioenergetic machinery under starving conditions.* **Biochim Biophys Acta Bioenerg.** 1859(3):201-214. doi:10.1016/j.bbabio.2017.12.002.

Hegyi B, Környei Z, Ferenczi S, **Fekete R**, Kudlik G, Kovács KJ, Madarász E, Uher F (2014) *Regulation of mouse microglia activation and effector functions by bone marrow-derived mesenchymal stem cells.* **Stem Cells Dev.** 23(21):2600-12. doi: 10.1089/scd.2014.0088.

11. Acknowledgements

I am most grateful to my two supervisors Ádám Dénes and Zsuzsanna Környei who have been supervising my development with infinite patience and devotion since my very first day as PhD student. Especially I want to thank Ádám, who took the major part of my supervision. Thank you all those insipirng scientific discussions and sometimes arguments. Thank you all the opportunities I got during these years.

I would like to thank all of our past and present lab members, of the Laboratory of Neuroimmunology. I'm glad that I have the opportunity to work in such a great lab with inspiring athmosphere both scientifically and personally.